Investigation on Some Aspects of Charge Trapping in Dielectrics used in High Voltage Systems

Thesis Submitted by
Nasirul Haque

Doctor of Philosophy (Engineering)

Electrical Engineering Department,
Faculty Council of Engineering & Technology
Jadavpur University
Kolkata, India

2018

JADAVPUR UNIVERSITY
KOLKATA - 700032, INDIA

INDEX NO. 246/16/E

1. Title of the Thesis:

Investigation on Some Aspects of Charge Trapping in Dielectrics used in High Voltage Systems

2. Name, Designation and Institution of the Supervisors:

Dr. Sivaji Chakravorti
Professor,
Electrical Engineering Department
Jadavpur University
Kolkata 700032

Dr. Sovan Dalai
Associate Professor,
Electrical Engineering Department
Jadavpur University
Kolkata 700032

.

3. List of Publications:

- N. Haque, B. Chatterjee, S. Chakravorti and S. Dalai, "Investigations on Charge Trapping and De-trapping Properties of Polymeric Insulators through Discharge Current Measurements", ***IEEE Transactions on Dielectrics and Electrical Insulation***, Vol. 24, No. 1, pp. 583-591,2017.

- N. Haque, B. Chatterjee, S. Chakravorti and S. Dalai, "Studies on the Effect of Temperature on the Charge Trapping and De-trapping Processes of Polymeric Insulators through Depolarization Current Measurements", ***IEEE Transactions on Dielectrics and Electrical Insulation***, Vol. 24, No. 3, pp. 1896-1904, 2017.

- N. Haque, B. Chatterjee, S. Chakravorti and S. Dalai, "Study on Charge De-trapping and Dipolar Relaxation Properties of Epoxy Resin from Discharging Current Measurements", ***IEEE Transactions on Dielectrics and Electrical Insulation***, Vol. 24, No. 6, pp. 3811-3820,2017.

- N. Haque, B. Chatterjee, S. Chakravorti and S. Dalai, "Studies on the Effects of Moisture and Aging on Charge De-trapping Properties of Oil Impregnated Pressboard based on Isothermal Relaxation Current Measurement", *A*ccepted for Publication,***IET High Voltage***,Paper No. HVE-2018-5095.

.

4. List of Presentations in National/International Conferences:

- N Haque, S Dalai, S Chakravorti and B Chatterjee, "Investigation of Charge Trapping Behavior of LDPE using De-trapping Characteristics", ***Proceedings of IEEE Seventh POWER INDIA International Conference (PIICON)***, Bikaner, India, 2013.
- N Haque, S Dalai, S Chakravorti and B Chatterjee, "Identification of Charge Injection and Conduction Properties of Epoxy Resin from Polarization Current Measurements", ***Proceedings of of International Conference on Condition Assessment Techniques in Electrical Systems (CATCON)***, Ropar,Punjab, India, 2017.

Certificate from the Supervisors

This is to certify that the thesis entitled "**Investigation on Some Aspects of Charge Trapping in Dielectrics used in High Voltage Systems**", submitted by **Shri Nasirul Haque**, who got his name registered on 21^{st} April 2016 for the award of Ph.D. (Engg.) degree of Jadavpur University is absolutely based upon his own work under the supervision of **Prof. Sivaji Chakravorti** and **Dr. Sovan Dalai** and that neither his thesis nor any part of the thesis has been submitted for any degree/diploma or any other academic award anywhere before.

.

1. – – – – – – – – – – – – – – – –
Signature of the Supervisor
and date with Official Seal

2. – – – – – – – – – – – – – – – –
Signature of the Supervisor
and date with Official Seal

Acknowledgement

The author would like to take this opportunity, to humbly, express his gratitude for the innumerable gesture of help, cooperation and inspiration that he have received from his supervisors *Prof. Sivaji Chakravorti* and *Dr. Sovan Dalai* of Electrical Engineering Department, Jadavpur University, in carrying out the research. The author was allowed to enjoy all the necessary freedom in carrying out the research work and at the same time the intense supervision by the supervisors helped in enhancing the quality of the research. This work is by far one among the most significant accomplishments in the author's life and it could not have reached this stage without profiting from their expertise, encouragement and valuable criticisms. The author is particularly grateful to his supervisors for their confidence in his work during difficult times. The author also expresses his sincere gratitude towards his supervisors for their invaluable guidance not only towards his research, but also for their active role in helping him with his overall professional development.

The author expresses his sincere gratitude to Dr. Biswendu Chatterjee,Associate Professor, Department of Electrical Engineering, Jadavpur University for his active involvement, assistance, advice and useful suggestions in carrying out the research work.

The author is grateful to the Head of Electrical Engineering Department, Jadavpur University, for providing the laboratory facilities required for carrying out this work.

The author acknowledges his respected teachers Prof. Kesab Bhattacharya and Prof. Abhijit Mukherjee for their advice and encouragement in completing the research.

The author is thankful towards his colleagues Dr. Arpan Kumar Pradhan, Dr. Riddhi Ghosh, Mr. Soumya Chatterjee and Mr. Suhas Deb for providing their continuous emotional support and also providing the much needed relief from the daily stress associated with the research work.for making the laboratory an interesting place to work.The author would also like to acknowledge Mr. Amrendra Kumar, Mr. Prodipta Das, Mr. K.Yashaswi Raj and Mr. Biswajit Chakraborty for their support and for making the laboratory an interesting place to work.

The author would also like to express his heart-felt gratitude to his parents Sri Nazirul Haque and Smt. Yeasmin Haque for their never ending support, love and blessing without which it would have been impossible to complete the work.

Finally as it is impossible to mention everybody by name, the author would like to convey his thanks to all who have contributed in one way or another, in making this work reach the present stage.

.

Dedicated to–
My Parents
&
the loving memory of Dadu

Abstract

Research experience gathered over several years indicates that formation of trapped space charge is vital for the reliability of the insulation used in the high voltage equipment. This accumulation is mainly due to charge injected from electrodes, whose low mobility allows it to be trapped because of impurities, insulation defects and the inhomogeneous and non-crystalline nature of polymer dielectrics. Therefore, measurement and analysis of trapped charge in polymeric dielectrics is a matter of paramount importance. However, space charge measurement techniques suffer from limitations of high complexity and are also not suitable for complex geometries. The present thesis comprises studies on the measurement of discharging current on a previously stressed dielectric. A mathematical model has been developed that can evaluate trapping parameters directly from the measured discharging current. In this context, it may be noted that the presented method does not depend on the use of transfer function or signal processing tools and can be applied to electrical insulation of any geometry. The developed methodology was applied to three common materials: LDPE, epoxy resin and oil impregnated pressboard.

Chapter 1 of this thesis introduces the research topic and gives a comprehensive overview of charge trapping/de-trapping phenomena and space charge measurement techniques.

Chapter 2 describes a methodology to extract information about charge trapping behaviour in a dielectric specimen from discharging current measurements. The developed methodology facilitates a direct estimation of trapped charge distribution along trap energy level and is independent of the insulation geometry.

In Chapter 3, studies were performed to characterize the behaviour of dipoles and space charge in epoxy resin from discharge current measurements. An attempt was made to separate the space charge effect from discharge current by correlating frequency domain to time domain measurements using Hammon approximation.

In Chapter 4, investigations were performed to understand the effect of aging and moisture on charge trapping in oil-impregnated pressboard. At the same time, charge transport in oil-impregnated pressboard was studied using the hopping charge model.

The concluding Chapter 5 summarizes the present work and gives ideas about possible extension of the research work.

List of symbols and abbreviations

A	–	Richardson's constant
a	–	Distance between a filled trap and nearby unfilled trap
A_c	–	Coefficient in Curie Von Schneidler's law.
A_{eq}	–	Equilibrium constant of A_c for irreversible thermal aging.
A^*_{eq}	–	Threshold level of A_c for thermal aging
c	–	centroid of space charge distribution in a specimen
C_0	–	Geometric capacitance
c_1	–	Concentration of unaged moieties in thermal aging reaction
c_2	–	Concentration of aged moieties in thermal aging reaction
χ	–	Change in total harmonic distortion of leakage
χ	–	Electrical susceptibility
$\circ$	–	Temperature (degree) sign
d	–	Thickness of a dielectric
Δ_m	–	Modified energy difference between unaged and aged state of polymer molecules under the influence of space charge
ΔE_H	–	Number of power frequency cycles recorded
ΔG	–	Energy difference between unaged and aged state of polymer molecules
ΔI_d	–	Current in a time interval
Δt	–	time interval
E	–	Electric field
E_{mt}	–	Mean trap depth
E_{trap}	–	Trap depth or trap energy
EA_{ref}	–	Electron affinity of the bulk dielectric material under study
EA_{trap}	–	Electron affinity of trap
ϵ_0	–	Vacuum permittivity

ϵ_r	–	Relative permittivity
ϵ_∞	–	High frequency relative permittivity
ϵ"	–	Imaginary component of relative permittivity
$f(t)$	–	Dielectric response function
G_1	–	Gibb's free energy of unaged polymeric moiety
G_2	–	Gibb's free energy of aged polymeric moiety
Γ	–	Thermal de-trapping rate constant
h	–	Planck's constant
H_b	–	Trap density
i_c	–	Conduction current
i_{charge}	–	Charging current
i_d	–	Dipolar polarization current
i_{depol}	–	Depolarization current
$i_{de-trap}$	–	De-trapping current
i_{dis}	–	Discharging current
i_{inj}	–	Injection current
i_{pol}	–	Polarization current
J	–	Current density
J_0	–	Initial current density
J_{Child}	–	Space Charge Limited Current density
J_H	–	Hopping Current density
$J_{measured}$	–	Measured current density
J_{Ohm}	–	y-Ohmic current density
J_{TFL}	–	Trap filling limited current density
k	–	Boltzmann's constant
k_{aging}	–	Rate of thermal aging reaction in polymers
μ	–	Charge mobility
N_c	–	Charge carrier density in conduction band

ν	–	Escape frequency of a trapped career during hopping process
ν_{th}	–	Thermal velocity of a trapped career
ω	–	n^{th} Frequency (in radian per second)
q	–	Charge of an electron
$r0$	–	Radius around a space charge centre
ρ	–	Volume charge density
$\rho_{de-trapped}$	–	Volume charge density of de-trapped charge
σ	–	Surface charge density
$\sigma^{'}$	–	Surface charge density on the electrode
σ_0	–	DC conductivity
σ_B	–	Potential barrier at metal-dielectric interface
σ_c	–	Cross section of trap
σ_H	–	Hopping conductivity
σ_i	–	Image charge density
t	–	Time
T	–	Temperature (Kelvin)
T_{th}	–	Temperature threshold for thermal aging
T	–	Temperature (Kelvin)
θ	–	Ratio of trapped carrier and free carrier
U_c	–	Step voltage
V	–	Voltage
W	–	Work function
W_{em}	–	Electromechanical energy stored in a region because of space charge
W_H	–	Hopping probability of a carrier
Y	–	Young's modulus

Contents

List of Figures

List of Tables

Chapter 1

Charge Trapping and De-trapping

1.1 Introduction

Dielectric materials are essential to the proper operation of all electrical equipment as it provide necessary insulation. These are used in a wide range of applications, e.g. transformers, bushings,cables,wires etc. Over the past few decades, there has been strong emphasis on bulk power transmission over long distances across the globe. This approach of power transmission has been boosted by the development and growth of HVDC systems and high voltage power equipment. The reliability and maintenance of these components is largely related to the performance of the dielectric materials used for insulation under high electric fields.

The performance of polymeric materials as electrical insulation in High Voltage Direct Current (HVDC) systems is intricately related to the formation of space charge and its dynamics in the insulation [1]. Accumulation of space charge leads to over-stressing of part of the insulation, and may cause premature failure [2]. The space charge accumulation phenomenon is closely related to the charge trapping and de-trapping processes in the polymeric dielectric. These processes are very complicated as they are related to the nature of polymers. Due to thermal and electrical aging, the nature of the polymer is further modified, which further affects the trapping and de-trapping processes [3]-[4]. It has been demonstrated that charge trapping and de-trapping

processes parameters, i.e. trap distribution, trap depth, are very sensitive to aging of insulation. Therefore evaluation of these parameters becomes very important for diagnostics of high voltage insulation.

1.1.1 HVDC Technology

A major challenge to power transmission technology is to deliver large amount of power over long distances with very minimum losses. Moreover, the power transmission system must be able to interconnect different incompatible AC networks and add stability to the grid. High Voltage Direct Current (HVDC) transmission fulfill these requirements with high efficacy. The major advantages for HVDC systems are,[5]-[8]
(i) Asynchronous interconnections
(ii) Low losses
(iii) Long distance sea crossings
(iv) Improved Controllability
(v) Environmental concerns
A typical HVDC transmission system comprises of three essential components: (A) Rectifier Station to convert AC power to DC, (B) Transmission of DC power through cables and overhead lines and (C) Inverter Station to convert the DC power back to AC . When DC power is transmitted through cables, the insulation behavior is primarily governed by the field distribution and conductivity. Surface and space charges play a vital role in the field distribution under dc fields. Moreover, temperature of the insulation also affects the conductivity significantly. Because of these reasons, the insulation behavior in HVDC systems becomes complicated.[9]

1.1.2 Insulating Materials for HVDC Technology

Before 1990s , mass impregnated paper and oil filled cable were the only type of insulation used in HVDC systems. Mass impregnated paper cable was mainly used in power transmission over long sea routes. This type of cable insulation requires no oil filling and has demonstrated high realibility in practice. On the other hand, oil filled cables have oil impregnated insulation and need oil feeding at every 10 to 20 kilometers. However, they have higher power transmission capacity and operating temperature. They have also proven their reliability over several years of operation.

In the past two decades, there has been considerable interest in the application of polymeric materials as insulating materials in HVDC cables. Polyethylene based materials (i.e. LDPE, HDPE, XLPE) offer excellent insulating properties and have been successfully used in High Voltage AC (HVAC) transmission systems for several years. However, it should be remembered that higher resistivity does not always ensure improved performance under DC conditions. Different aspects of electrical, thermal and mechanical behavior need to be thoroughly investigated regarding the application of polyethylene based materials for HVDC applications[9]-[11]. Another significant polymeric material for HVDC insulation is epoxy resin[12]. Although not used in cables, epoxy resin based insulation is being frequently used in cable joints, dry type transformers, switchgear insulation.

In this thesis work, the focus has been concentrated on three cases of insulation- (A) LDPE, for Polyethylene based insulation (B) Epoxy Resin (C) Oil-paper insulation.

1.2 Background of the work

1.2.1 Charge trapping and De-trapping Phenomena

Charge trapping and de-trapping processes are related to the microstructural properties of insulators. Further discussion on this topic will be incomplete without mentioning the atomic model theory proposed by Niels Bohr[13]. According to this model, electrons move in separate orbits around the nucleus of an atom having discrete energy levels. An electron may leap from one orbit to another, and in this process it gains or looses energy. This introduces the concept of forbidden energy gap, valence band and conduction band. Valence band refers to the highest occupied energy band, which is occupied by valence electrons. On the other hand, conduction band refers to the lowest unfilled energy band. If electrons occupy this band, they can move freely and cause electrical conduction. In metals the conduction band is partially filled. In insulators and semiconductors the filled valence band is separated from an empty conduction band by a band gap. A band gap is an energy range in a solid where no electron states can exist due to the quantization of energy. In an insulating material, the band gap is very large, greater than 2 eV. Such a large energy gap makes it impossible for an electron

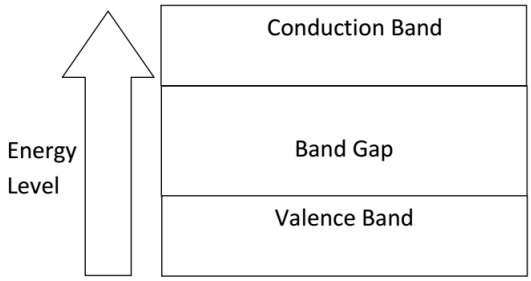

Figure 1.1: Illustration of energy bandgap in a dielectric.

to jump from valence band to conduction band, therefore giving rise to the insulating behavior of the material. For semiconductors it is between 0.2 and 1 eV and for conductors it is less than 0.1 eV. Figure 1.1 gives a representation of energy band model.

Now, the molecular structure of polymeric insulating materials are often characterized by the presence of amorphous regions.These amorphous regions are produced mainly by conformational disorders, presence of impurities and chemical defects. Conformational disorders exist primarily because long polymer chains often form intercrystalline links while going from one lamella to another. The chemical impurities and defects found in polymeric insulating materials mainly consist of hydroxile and ketone functions and certain byproducts of crosslinking process. All these factors give rise to specific locations in the insulation where local electron affinity is different from the overall material. If these sites have larger electron affinity than the host material[14]-[16] then during high voltage application the injected carriers get trapped, and this process is referred as charge trapping. These trapping sites have energy level between the conduction band and valence band. The trap energy or trap depth (E_{trap}) is defined as the difference of electron affinity of the trap site (EA_{trap}) and electron affinity of the overall material (EA_{ref}). This can be expressed as,[16]

$$E_{trap} = EA_{trap} - EA_{ref} \tag{1.1}$$

If trap energy is positive for a defect site, then an electron will

prefer to stay in that trapping site and will not contribute to the conduction process. Thus, overall, the trapping process can be understood as a process of energy storage in which charges are confined to specific sites preventing them to contribute to electrical conduction. The trapping sites vary in material according to its trap depth and capture cross section. Depending upon trap depth, the traps can be classified as shallow traps or deep traps. Shallow traps correspond to mainly physical defects in the material, and have trap depth less than 0.5 eV. Deep traps are mainly caused by chemical impurities, and have values higher than 0.5 eV. In this thesis work, the focus has been given on deep traps.

Once, the charged carrier is trapped, it can also de-trap or escape from the trapping site in the presence or absence of electric field provided it gains sufficient energy. The trapped carrier can gain energy through a number of mechanisms [17], i.e. photon assisted de-trapping, phonon assisted de-trapping or thermal de-trapping, electron tunnelling and impact ionization In thermal de-trapping process, the trapped carrier receives energy from lattice vibrations, thereby causing it to de-trap. The released carrier can be further re-trapped by another trapping site. The process is repeated continuously and the charged carriers hop from one site to another in the direction determined by the electric field. This forms the basis of hopping mechanism of charge conduction in polymers, which will be discussed later in this chapter. The time t taken by a trapped carrier to thermally de-trap is given by,

$$t = \frac{1}{\Gamma} \tag{1.2}$$

where, Γ is the thermal de-trapping rate constant , which can be given as,[18]

$$\Gamma = N_c \sigma_c \nu_{th} \exp(\frac{-E_t}{kT}) \tag{1.3}$$

$$or\ \Gamma = \nu exp(\frac{-E_t}{kT}) \tag{1.4}$$

where,

$$\nu = N_c \sigma_c \nu_{th} \tag{1.5}$$

ν is the attempt to escape frequency ,σ_c is the capture cross-section of

the trap, k is Boltzmann's constant, and T is temperature and N_c is the effective density of states in the conduction band given by

$$N_c = 2(\frac{2\pi m_e kT}{h^2})^{\frac{3}{2}} \tag{1.6}$$

m_e is electron mass, ν_{th} is the thermal velocity of carriers, given by

$$\nu_{th} = (\frac{3kT}{m_e})^{\frac{1}{2}} \tag{1.7}$$

From equations (1.2) and (1.3) it is observed that the trap releasing time t is highly dependent on the capture cross section σ_c and trap energy E_t.

1.2.2 Charge injection and transport

As discussed in earlier section, metals have abundant free electrons in valence band. These electrons are free to move anywhere in the metal. However, when a metal-dielectric contact is made, electrons cannot easily enter in the dielectric from metal.In order to do so, the electron needs to pass a potential barrier, σ_B, which can be expressed by,

$$\sigma_B = W - \chi \tag{1.8}$$

where W is the work function of the metal and χ is the electron affinity of the dielectric. The conduction process in dielectric is therefore, is dependent on both the nature of dielectric as well as nature of metal(electrode)-dielectric contact. There are several mechanisms of conduction in dielectrics, and in many cases, multiple mechanisms may be collectively responsible for conduction. For the ease of understanding, the mechanisms can be broadly classified in two categories,[19]-[21]: (a)Electrode limited conduction mechanisms and (b)Bulk limited or transport limited conduction mechanisms

Electrode limited conduction mechanisms

In this category, the conduction mechanisms are primarily controlled by the nature of electrode-dielectric contact. The most important controlling factor is the barrier height at metal-dielectric interface. This category includes (i) Schottkey or thermionic emission, (ii) Fowler Nodheim tunneling, (iii) direct tunneling and (iv) thermionic field emission.

Schottky or thermionic emission

In this mechanism, electrons are thermally excited to obtain sufficient energy to overcome the metal-dielectric potential barrier. At the same time, the application of external electric field also reduces the height of the potential barrier to some extent, thereby allowing more electrons to be injected. The Schottky injection law is valid for electric fields upto around 100 kV/mm. Ambient temperature also affects the charge injection current , which is given by the following equation,[22]

$$J = AT^2 exp(\frac{-q(\sigma_B - \sqrt{\frac{qE}{4\pi\epsilon_0\epsilon_r}}}{kT}) \tag{1.9}$$

where, J is the current density, A is effective Richardson's constant, σ_B is the Schottky barrier height, E is the electric field across the dielectric, k is Boltzmann's constant and T is absolute temperature.

Fowler-Nodheim (F-N)tunneling

At very high fields, i.e. above 100 kV/mm, the potential barrier is further decreased. This makes the width of the potential barrier very thin at some particular locations. Electrons exhibit paticle wave duality, and the wave nature does not vanish at the dielectric-metal interface. There is a finite probability of electrons appearing on the other side of the barrier, especially if the barrier is very thin. This mechanism is called Fowler0-Nodheim tunneling mechanism, where the electrons does not obtain sufficient energy to overcome the potential barrier, rather they tunnel out and appear in the conduction band of the dielectric. This conduction mechanism is independent of temperature. The current is given by following equation,[23]-[24]

$$J = \frac{q^3E^2}{8\pi hq\sigma_b} exp(\frac{-8\pi K^{\frac{1}{2}}\sigma_B^{\frac{3}{2}}}{3hE}) \tag{1.10}$$

where h is Planck's constant, K is a constant with a value equal to $2qm_t$, m_t being the effective electron mass and other terms as aforesaid mentioned.

Bulk limited Conduction mechanisms

The bulk limited conduction mechanisms mainly depend on the material properties of the dielectric. It is not affected by the metal-dielectric contact. The main controlling parameters are, trap depth, trap density, mean trap separation distance , electronic drift mobility etc. The bulk limited conduction mechanisms include :(i) Poole Frenkel emission, (ii) hopping conduction, (iii)Space charge limited conduction and (iv) Ionic conduction.

Poole Frenkel (P-F)mechanism

Poole Frenkel emission process is quite similar to Schottky emission process. The main difference is, in Schottky emission, the applied field reduces the metal-dielectric potential barrier to facilitate electron injection and in this case, applied field reduces the potential barrier around a trapping centre, where the electron is confined. The emission of electron from the trapping centre is mainly aided by thermal excitation. Since this conduction mechanism is due to thermal activation under high electric field, it is noticed only at high temperature and electric fields. the conduction current density is given by equation.[25]-[27]

$$J = q\mu N_c E exp[\frac{-q(E_{trap} - \sqrt{\frac{qE}{4\pi\epsilon_0\epsilon_r}})}{kT}] \tag{1.11}$$

where μ is the electronic drift mobility, N_c is the density of states in conduction band, E_{trap} is the trap energy level and other notations are the same as defined before.

Hopping conduction

This conduction process is related to the tunneling effect of trapped electrons. In P-F mechanism, the trapped electrons obtain sufficient energy to overcome the trap depth through thermal activation. However, in hopping mechanism the trapped electron does not obtain sufficient energy to overcome the trap potential barrier. Rather, the trapped electron travel from one trap to another trap through tunnel mechanism, similar to F-H tunneling observed at metal dielectric interface. However, this mechanism is valid only when the inter trap distance is very small.

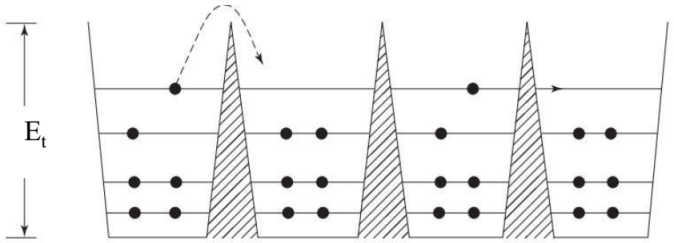

Figure 1.2: Illustration of hopping conduction in a dielectric.

Figure 1.2 shows the schematic of hopping conduction. The conduction current is given by the following equation.[28]-[31]

$$J = qaN_c\nu exp(\frac{qaE}{kT} - \frac{E_{trap}}{kT}) \tag{1.12}$$

where, a is the mean spacing between trap sites,ν is the frequency of thermal vibration in trapsites and other notations are the same as defined before.

Space charge limited conduction (SCLC)

Space charge limited conduction (SCLC) occurs when the conduction is the result of the injection of excess carriers from an Ohmic contact into a material of very low mobility. A typical current voltage characteristics regarding SCLC is depicted in Figure 1.3. It comprises of three separate curves, viz. Ohms law , traps-filled limited (TFL) current, and the current obeying Childs law.

At very low fields, the current density linearly increases with applied voltage. This implies that the number of injected carriers is far less than the number of thermally activated free careers inside the dielectric. This signifies ohmic behavior and negligible charge injection at such stress levels. The ohmic current is characterized by equation 1.13. However, as electric stress level increases, after a particular threshold V_{TR}, electrode injection increases considerably. Because of the presence of traps some of the carriers become trapped and do not contribute to the conduction. As a result, only a proportion of the charges contribute

to the conduction. This stage is known as traps-filled limit conduction (TFL) and the current density is proportional to the square of applied voltage. This current is represented by equation 1.14. At further higher fields, the injection is so high that all traps are filled and conduction is carried by excess carriers. This reflects a rapid rise in current density after a threshold voltage V_{TFL}. For the voltage above V_{TFL}, the current is fully controlled by the space charge, which limits the further injection of free carriers in the dielectric.The three distinct currents, namely ohmic, trap filled and space charge limited currents can be given through the following equations,[32]-[34]

$$J_{Ohm} = qn_0\mu\frac{V}{d} \tag{1.13}$$

$$J_{TFL} = \frac{9}{8}\mu\epsilon_0\epsilon_r\theta\frac{V^2}{d^3} \tag{1.14}$$

$$J_{Child} = \frac{9}{8}\mu\epsilon_0\epsilon_r\frac{V^2}{d^3} \tag{1.15}$$

where, J_{Ohm}, J_{TFL} and J_{Child} are ohmic, trap filled and space charge limited current respectively, V is the applied voltage, d is the thickness of thin films, n_0 is the concentration of free charges in thermal equilibrium and θ is the ratio of free career density to total (free and trapped) career density.

Ionic conduction

The ionic conduction mechanism is caused by the movement of ions under the effect of electric fields. These ions originate from defects in the lattice structure of the dielectric material. Due to the presence of external electric field, ions may jump across a potential barrier from one defect site to another defect site. The ionic conduction current can be expressed through the following equation,

$$J = J_0 exp[-(\frac{q\sigma_b}{kT} - \frac{Eqa}{2kT})] \tag{1.16}$$

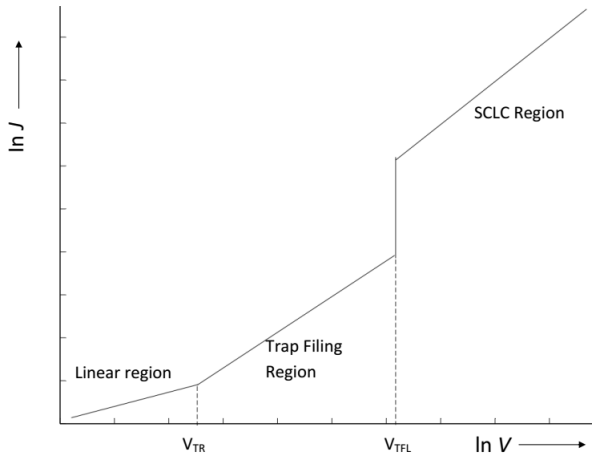

Figure 1.3: Typical Space Charge Controlled Current (SCLC) characteristics.

where J_0 is the initial current density, $q\sigma_b$ is the potential barrier height, E is the applied electric field, a is the spacing of nearby two trapping sites and other terms are as defined above.

1.3 Charge Trapping Investigations:An Overview

So far from the discussion, it can be understood that the trapping and de-trapping processes play a vital role in conduction and space charge accumulation phenomena in solid dielectric materials. Therefore, over the past few decades, there has been growing interest on the investigation of charge trapping behavior in polymeric insulating materials. Before 1970s, space charge measurement in charged dielectric specimens were performed through destructive techniques. These techniques included Dust figure method and probe method [35]-[36]. In 1975, R.E. Collins proposed a non destructive method of space charge measure-

ment by perturbing the space charges in a dielectric specimen through a thermal wave[37]. This method was further improved in the following years leading to the development of quite a few non invasive space charge measurement techniques. Among them,Pulse Electro Acoustic (PEA) technique and Pressure Wave Propagation (PWP) technique are most important. Consequently, these methods were applied to study the trapping behavior in polymeric materials. In such studies, typically, a thin dielectric specimen is electrically stressed and then kept in short circuit condition over a period of time. By measuring the net charge at different time instants of voltage stressing and discharging, the collected information was used to model the trapping and de-trapping behavior of the dielectric. Besides space charge mapping techniques, surface potential decay method, charging-discharging current and some other methods were also applied to study trapping behavior of dielectrics.

1.3.1 Space Charge Distribution Techniques

In this section, a brief review is presented of different methods for extracting space charge distribution information in a stressed dielectric.

Thermal pulse and step method

The specimen containing space charges are disturbed through a thermal wave penetrating the sample. The space charge produces an image charge in the electrodes. The thermal wave displaces the charge, thereby the values of image charge will go through a change, thereby producing an electric signal. By applying de-convolution techniques, information regarding space charge distribution can be deciphered from the measured electrical signal[37]. A corollary of this method is thermal step method, where the thermal pulse is replaced by a thermal step[38].

Laser intensity modulation method (LIMM)

In LIMM method, the metalized surfaces of a specimen is heated through a sinusoidally modulated laser beam. As a result a temperature wave is diffused in the sample, which is attenuated and delayed during its propagation throughout the sample. The interaction of this non-uniformly distributed thermal wave and space charges present in

the sample produces a pyro electric current, from which space charge information is extracted.[39]

Optical methods

A polarized light passes through the test object, which must be transparent. The space charge distribution interacts with the optical wave, modifying its optical phase and other polarization properties. By measuring these changes in polarization properties, information regarding space charge is obtained[40]-[41].

Pressure Wave Propagation(PWP) method

The space charge distribution is perturbed by applying a pressure wave. This pressure wave is produced through piezoelectric crystal or laser shots. The pressure wave disrupts the space charge distribution, producing an electrical signal in the electrodes, similar to thermal pulse/step method. From the measured signal, by empolying suitable signal de-convolution methods, information about the spatial distribution of space charge is extracted[42]-[45].

Pulse electro acoustic method

A strong pulsating electrical field is applied in a specimen containing space charge. The interaction between externally applied electric field and space charge will produce a mechanical force. As a result an acoustic wave will be generated , which will be detected by a piezoelectric transducer placed after the earth electrode. Consequently, the piezoelectric transducer will produce a voltage signal, from which space charge information is extracted[46]-[51].

1.3.2 Surface potential decay method

Isothermal surface potential decay method (ISPD) is another popular method for investigation of trapping behavior in solid dielectrics. In this method, the dielectric specimen is charged through corona charging.

During the corona charging process, ions accumulate on the surface of the dielectric specimen.This leads to electron transfer in the surface, to neutralise the ions. As a result, the surface potential slowly decreases with time. This whole process of charge transfer leads to electron (or hole, depending on the charging polarity) trapping on the surface region.Theoretical models have been developed to interlink the energy distribution of traps with the surface potential decay. However, it should be remembered that the potential decay is also influenced by dipolar polarization, neutralization through atmospheric ions and conduction through the surface of the sample under study. Therefore, these factors need to be carefully checked before making comments on the trapping behavior. There had been quite extensive research on this surface potential decay over the past few decades [52]-[55]However, the conclusions are not unanimous and more research is needed for further improvement in this method.

1.3.3 Other methods

Iso-thermal relaxation current or discharging currents have been used for understanding trapping behavior in some early investigation , most notably by Lindmayer et al.[56] and Simons et al.[57] Similarly, charging and conduction currents have also been analyzed to study charge trapping[58]. However, there has been limited progress in determination of trap energy distribution in a dielectric from such current measurements.

1.4 Limitations of space charge measurement techniques in charge trapping investigation

Among all the methods discussed above, PEA and PWP methods have provided most significant contributions to the knowledge regarding space charge behavior in dielectrics. Normally, to investigate charge trapping and de-trapping processes, the sample is electrically stressed and then kept in short circuit condition over a period of time. During this short circuit period, the net amount of charge stored in the sample is measured using these two methods and from that, charge trapping

parameters, such as trapped charge, trap depth or trap energy , distribution of traps are calculated. However, both methods suffer from similar limitations. In each case, the measured signal does not directly reflect the space charge distribution in the sample. By applying transfer function analysis and de-convolution tools , the space charge distribution is deciphered from measured signal. In all these methods, the measured signal is usually very low and proper de-noising also becomes very important for accurate estimation of space charges. Therefore, although space charge measurement techniques have significantly contributed to charge trapping and de-trapping investigations, as the method of space charge measurement is itself indirect (through acoustic signals) and hence the interpretation and analysis of the obtained signals remain a critical issue.

Another difficulty with these measurement techniques is that they are mostly applicable to thin dielectric samples of planar geometry. Although PEA method has been used for space charge measurements in cables[59]-[60], for complex irregular insulation structures its application becomes very difficult. For example, it is very difficult to perform space charge measurement on an aged polymeric insulator used in transmission line. For such type of insulation structures, trapping and de-trapping analysis remains a challenge. Therefore, a direct method of charge trapping and de-trapping will certainly be more convenient from the prospect of insulation diagnosis as compared to indirect methods.For direct estimation of charge trapping parameters, Isothermal Surface Potential Decay has been another popular choice. In this method, the dielectric specimen is charged through corona charging, and then the surface potential decay of the sample is recorded over a period of time. Charge trapping parameters i.e. trap depth, trap density are estimated from the surface potential decay measurement. However, such method cannot be directly employed in electrical insulation systems of other than planar geometry. It is very difficult to arrange an experimental set-up for corona charging of radial geometry insulation i.e. cables. For these reasons, a simple low complex direct method which can be employed for charge trapping investigations in electrical insulations of arbitrary shape or geometry will be highly beneficial for physicists, engineers and industry professionals.

1.5 Importance of charge trapping investigations

The exact mechanism of aging in solid polymeric dielectrics is a topic of considerable discussion. However, it has been well accepted that trapped charges play a vital role in the accelerated aging of polymeric materials. In this section, the knowledge so far gained particularly in last three decades on fundamental principles of electrical aging and the impact of trapped charges on them is briefly discussed.

The degradation of polymer dielectrics under thermal stress is conventionally explained through a thermodynamic approach followed by the pioneering work done by Daikins[61]. In this theory, the polymer is regarded as a set of chemical and morphological units, called moieties, that are subjected to local reactions. The aging process is assumed to be dominated by one single reaction that involves an initial, or reactant, or unaged state (referred to as state 1), and a final, or product, or degraded state (referred to as state 2). They both have an associated Gibbs free energy per moiety, G_1 and G_2, respectively. This reaction is expected to be partly reversible[62]. Overall, the aging theory described by Daikins consider aging as a thermally controlled process.
Erying described different chemical reactions related to aging in [63]. Most of these reactions are related to chain scission. The reaction rate of this process is related to the energy difference ΔG through the following equation,

$$k_{aging} = \frac{kT}{h} exp(-\frac{\Delta G}{kT}) \tag{1.17}$$

$$\Delta G = G_2 - G_1 \tag{1.18}$$

where, k_{aging} is the reaction rate constant of aging process, G_1 is the free energy of the reactant at unaged state and G_2 is the free energy of the aged state. The creation of the product requires some output energy (either thermal or electrical). As a result, the product state has higher energy than the reactant state implying ΔG having positive value.
It has been already mentioned, that the aging reaction is partly reversible. If a large number of moieties are converted from ground (un-

aged) to product (aged)state, then it can be said that material degradation has been triggered and the lifetime of the insulation is now limited. If c_1 and c_2 are the concentrations of unaged and aged moieties respectively, then a parameter A_{eq} can be evaluated representing the fraction of polymer sites that is converted from ground (unaged) state to reactant state (aged), through the following equation,

$$A_{eq} = c_2/(c_1 + c_2) \tag{1.19}$$

It can be showed that A_{eq} is related to energy difference ΔG through the following equation,

$$A_{eq} = (1 + exp\frac{\Delta G}{kT})^{-1} \tag{1.20}$$

It is observed from equation 1.19 that A_{eq} will increase with increase in temperature. At some temperature T_{th} , A will reach a certain value, say A^*_{eq}, which indicate a rapid degradation in the insulation. Thus for $T > T_{th}$ the insulation life will be shortened. T_{th} is termed as the threshold temperature of aging, which is related to A^*_{eq} through the following equation,

$$A(T_{th}) = (1 + exp\frac{\Delta G}{kT_{th}})^{-1} = A^*_{eq} \tag{1.21}$$

$A^*_{eq}$is the fraction of sites that needs to be converted in order to produce local damage sufficient to initiate a rapid failure.
The effect of charge injection-extraction on tree initiation in XLPE cables was first discussed by Tanaka et al[64]. In [64] a model was developed that correlated the tree inception time with applied electric stress. In 1995 Dissado et al. developed a new model which incorportated the effect of trapped charge on insulation lifetime through thermodynamic modeling[65]. In the subsequent years, this model was further improved by the same authors [66]. The most significant contribution of this new model was that it identified new parameters representing the electromechanical and electrostatic stresses associated with trapped charge.

When trapped charge is present in the insulation, it will produce its own electric field. This will lead to mechanical stress , particularly in the nearby region of space charge (electrostriction effect) . Let Q

amount space charge occupies a spherical region of $r0$ radius with ρ volume density. Then, electromechanical energy W_{em} stored over a spherical region of radius r from the center of the space charge region can be calculated as,

$$W_{em} = \frac{3\alpha^2 q^4}{4480\pi^3 Y \epsilon^4 r_0^5} \tag{1.22}$$

where α is the electrostriction coefficient and Y is Young's Modulus. The electromechanical energy W_{em} will increase the ground state free energy per moiety in the space charge region by an amount of BW_{em}, where B is a proportionality constant. If this mechanical stress finally leads to scission of long polymer chains, then it can be safely assumed that end products after chain scssion will be relieved of this mechanical stress. Therefore, for chain scission reactions, the energy difference between ground state and reactant state is decrfeased by a factor BW_{em}. The modified energy difference is given as,

$$\Delta_m G = \Delta G - BW_{em} \tag{1.23}$$

From equation 1.23 it can be understood as Δ_mG value is decreased, the reaction rate of aging will be accelerated. At the same time, the threshold temperature for aging, T_{th} will decrese, as observed from equation 1.21. Overall, it can be said that the trapped charge will simulate aging reaction that otherwise would have occurred only at elevated temperatures. In this way trapped charge accelerates the thermal aging process. Besides it, there may be also recombination of trapped charges of opposite polarity, which may release sufficient energy to damage the insulation. If the charges are trapped in and around microscopic voids, then the outcome may be more severe. The electromechanical stress associated with trapped charge will elongate the void dimensions with time, thereby finally leading to tree inception.

1.6 Scope of the Thesis

In this thesis, the behavior of trapped charge has been investigated for a few dielectric materials which are very popular for electrical insulation

purpose. The organization of this thesis is as follows,

Chapter 2:
In chapter 2, a methodology is described to extract information about charge trapping behavior in a dielectric specimen from discharge current measurements. The developed methodology facilitates a direct estimation of trapped charge distribution along trap energy level and it is independent of insulation geometry. The method also does not depend on the use of transfer function or any signal processing tool for analysis. By applying this method, the charge trapping behavior of Low Density Polyethylene, a non polar dielectric was investigated at different electric field and temperature.

Chapter 3:
The behavior of a polar dielectric at high electric fields is more complicated compared to a non polar dielectric because of presence of permanent dipoles. Both space charge and permanent dipoles affect the insulation behavior at high electric fields. From the point of insulation diagnostics, it will be highly beneficial if these two are properly identified from material characteristics, as they can reveal a lot about the aging condition of the material. In chapter 3, studies were performed to characterize the behavior of dipoles and space charge in polar dielectric from discharge current measurements. Epoxy resin, a widely used dielectric in high voltage system is chosen as the material of interest in chapter 3. An attempt was made to separate the space charge effect from discharge current by correlating frequency domain to time domain measurements using Hamon approximation.
Chapter 4:
In chapter 4, oil-paper insulation is considered as the material for interest for charge trapping insulation. The focus was given to understand the effect of aging and moisture on charge trapping in oil-paper insulation. Charging- Discharging current measurements were conducted oil-impregnated pressboard specimens having different moisture content and aging condition. The aging of samples were artificially performed through accelerated thermal aging. Using the methodology described in chapter 3 , the effect of moisture and aging on charge trapping parameters of oil impregnated pressboard samples were studied through discharging current measurements. At the same time, charge transport in oil impregnated pressboard was studied using hopping charge trans-

port model.

Chapter 5:
Conclusions and Scope of future work have been detailed in ***Chapter 5***.

1.7 Originality of the thesis

To the best of knowledge of the author, the following are the original contributions of the present work:

1. Presence of trapped charge is a major concern for solid polymeric insulation. Space charge measurement techniques suffer from the limitations of high complexity and are also not suitable to complex geometries. In this thesis, a method has been proposed that can identify the distribution of trapped charge from discharge current measurements. The presented method does not require complicated signal processing tools and can be applied to any insulation geometry. Results presented in this dissertation reflect the effectiveness of the methodology to efficiently identify the charge trapping parameters in different dielectric materials.

2. The insulating behavior in polar dielectric is complicated by the complex interaction between space charge and permanent dipoles. If discharging current of a polar dielectric previously stressed at high electric field is taken under study, then it should be remembered that both space charge and relaxation of permanent dipoles are responsible for this current. Separation of these two components from each other in discharging current has been an uphill task. In this dissertation work, a method is proposed for separation of space charge and dipolar polarization from each other is a difficult issue. For this pupose, Hamon approximation, a well known method for conversion of time domain dielectric spectroscopy to frequency domain spectroscopy has been utilized.

3. Compared to polymeric materials, fewer studies have been performed on charge trapping behavior of oil-impregnated pressboard insulation, which is a vital component of power transformer and other high voltage equipments. In addition to charge trapping, the charge transport mechanism in oil-pressboard insulation is also

poorly understood. In the present thesis work, the effect of moisture and aging on charge transport and charge trapping parameters of oil-pressboard insulation has been studied using charging-discharging current measurements.

Chapter 2

Study on Charge Trapping Behavior in LDPE from Discharging Current Measurements

2.1 Introduction

The study of external charging and discharging currents in any dielectric can reveal a lot of information about the dielectric properties of that material [67]. These currents are attributed to a variety of factors, i.e. dc conductivity, polarization, charge injection etc. There had been several previous investigations involving charging-discharging current measurements in different electrical insulation systems [68]-[73]. Such measurements have been successfully used to interpret insulation condition and moisture ingress in oil-paper insulation used in transformers. However, there has not been much application of such current measurements for investigation of trapping behavior in solid dielectrics.Partly, it may be attributed to the absence of theoretical models directly correlating trapping parameters (such as trap depth, trapped charge distribution) to experimentally measured charging or discharging current.The importance of investigating charge trapping behavior in dielectrics has been already discussed in section 1.5. It has also been discussed, that although advent of space charge mapping techniques have greatly facilitated space charge investigations, they also suffer from certain limitations.In these methods, typically, a signal corresponding to the space

charge distribution is acquired from a charged dielectric specimen. However, the space charge measurement system has its own transfer function, and the data regarding space charge it provides must be treated very carefully. Sophisticated signal processing and de-convolution techniques are needed to extract the relevant information from measured signal[74]-[75]. Another difficulty is that these space charge measurements are difficult to perform on insulations having arbitrary geometry. These techniques are best suited for dielectric specimens with planar geometry and radial geometry.Overall, it can be certainly said that a direct method of measuring charge trapping and de-trapping, which is independent of insulation geometry, will certainly be more convenient from the point of view of insulation diagnosis as compared to indirect methods.

The application of charging-discharging current can help to overcome many of the aforementioned difficulties. These current measurements offer straight forward and direct method to understand dielectric properties. The measurement system is simple and it does not interfere much with the original current signal, keeping its characteristics unchanged. The measurements can be performed on dielectric specimens having any shape or geometry. Considering all these possibilities, external charging-discharging current measurements have been selected for charge trapping investigation in this thesis work.

In this chapter, a theoretical model has been developed to correlate charge trapping parameters with discharging current of a previously stressed dielectric sample. By applying this model,the relative distribution of trapped charge across different trap depths or trap energy levels are directly evaluated. The presented method does not depend on the use of transfer function or signal processing tools and can be applied to electrical insulation of any geometry. In the present chapter, the charge trapping and de-trapping behavior of low density polyethylene (LDPE), a widely used non-polar polymeric material for electrical insulation purpose, have been investigated.LDPE is often used as jacket or insulation material of wires. Some applications of LDPE insulated wires are found in Electronics wiring, Oil and gas industry and Telecommunication industry.From the existing literature[76], it has been observed that the space charge trapping behaviours of LDPE is very much similar with XLPE, which is being increasingly used for high voltage applications. Commercially available samples were stressed at different fields and corresponding discharge currents were recorded and analyzed through the

developed model.To study the effect of temperature on trapping process, depolarization current measurements have been carried out over a wide range of 20° C to 80° C. The results were analyzed and it was observed that the temperature significantly affects the trap formation and de-trapping processes.

2.2 Theory

2.2.1 Basic theory of charging and discharging currents in dielectrics

If initial transients are ignored, then, under the application of high amplitude step DC voltage, the charging current drawn by a dielectric specimen is comprised of three basic components-

(i) Injection current(i_{inj}) that corresponds to charge injection into dielectric from the electrode material.It has been already discussed in section 1.2.1, that in a typical polymer microstructure, there exist amorphous regions with different electron negativity than the host material [14]-[15]. If these regions have higher electron affinity than the host material, then they will capture the injected charge. This represents the charge trapping phenomenon in the dielectric.
(ii) Polarization current (i_{pol}) that corresponds to the alignment of dipoles in the dielectric material.
(iii)DC conduction current (i_c), that represents the steady state conduction current in the material.
Mathematically it can be represented as,

$$i_{charge} = i_{inj} + i_{pol} + i_c \tag{2.1}$$

It should be remembered, that in the above equation, the contribution of very fast polarization processes have been ignored. These polarization processes are known as electron polarization and are completed well before 1s of current measurement.
Now if the applied dc voltage is removed and the charged dielectric specimen is grounded, the relaxation current or discharge current will flow from the specimen to ground. This current, which takes considerable

time to reach near zero values, is caused by two physical process. The first one is the relaxation of erstwhile oriented dipoles, which releases the previosly bound charges in the electrode. The second is the charge de-trapping current. This de-trapping current comes from the trapped charges present in the insulation.The charge de-trapping phenomenon has already been discussed in section 1.2.1. The trapped charge slowly obtains sufficient energy to de-trap by primarily thermal means and a portion of them is finally extracted through the electrodes. As a result, the net discharge current can now be considered as a combination of two different currents, one due to charge de-trapping and the other due to dipolar relaxation. The net discharge current can now be expressed as,

$$i_{dis} = i_d + i_{de-trap} \tag{2.2}$$

where i_{dis} , i_d and $i_{de-trap}$ are net discharge current, dipolar polarization component of discharging current and current due to charge de-trapping, respectively.

2.2.2 Dielectric properties of LDPE

LDPE is a widely used material for high voltage insulation. It also has extremely low water absorption, low dielectric losses and very high resistivity. It has also high immunity against electrical aging [77]. The microstructure of LDPE, is however not very simple one. It is a semicrystalline material with strong presence of amorphous regions. Besides amorphous regions, the long polymer chains often form intercrystalline links. These conformational disorders affect the trapping and accumulation of space charge to a great extent. In a typical dielectric, there should be no energy state other than conduction band and valence band. But due to these conformational disorder, several 'sites' exist in polymer having energy level in between valence band and conduction band. This is illustrated in Fig.2.1. These 'sites' act as traps, where charges get confined.

The reason behind charges getting trapped can be explained through electron affinity. The electron affinity is the energy required to bring an electron from vacuum to the conduction band, as depicted in Fig.2.2. The electron affinity of a trapping site is the energy required to bring a electron to the trap site level. Now, if the trapping sites exhibit higher

electron affinity than the overall material, electron will get trapped in that site. The difference of electron affinity of the trap site (EAtrap) and the overall material (EAref) is expressed as the trap energy. This can be expressed as,[16]

$$E_{trap} = EA_{trap} - EA_{ref} \tag{2.3}$$

Once a charge carrier gets trapped, it will remain there until it obtains the required trap energy of that site. Once it obtains sufficient energy, it will move out of the trap and contribute to the charge conduction process. This process is called "de-trapping" of the carrier. Thus, in a general view the charge trapping process can be regarded as an energy storage process in which charges are confined to specific sites preventing them to contribute to electrical conduction.During de-trapping process, the trapped carrier can gain energy through various processes, e.g. thermally assisted de-trapping, impact ionization electron tunnelling and impact ionization. In the present work, no photon bombardment was performed in the samples. Electron tunnelling and impact ionization are associated with very high electric fields, which were not applied in the present case. Therefore, only thermally assisted de-trapping was considered in present analysis. In thermally assisted de-trapping the trapped carrier obtains necessary energy for de-trapping from thermal lattice vibrations.

2.3 Charge extraction under short circuit conditions

It has been already discussed, that if a dielectric containing space charges is short circuited, then the de-trapped charges and relaxation of dipoles together will produce a discharge current. In the present chapter, discharging current behavior in LDPE is studied. LDPE, which is a non-polar material depicts very weak dielectric relaxation behavior due to absence of polar groups[78]. In [78], a dipolar relaxation process was identified in LDPE having relaxation time of 1.2s at 80°C. Below this temperature, the relaxation was found to be negligible. Therefore, it can be safely assumed, that if the initials transients are discarded, then the discharging current in LDPE is almost entirely due to charge

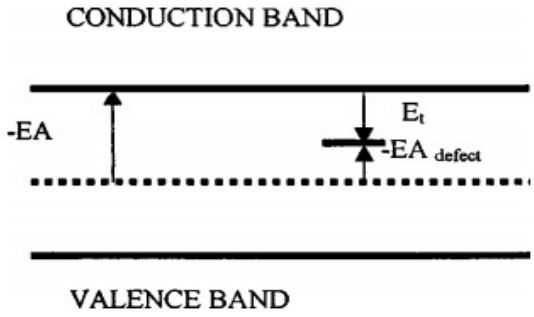

Figure 2.1: Illustration of Electron affinity in a dielectric[15].

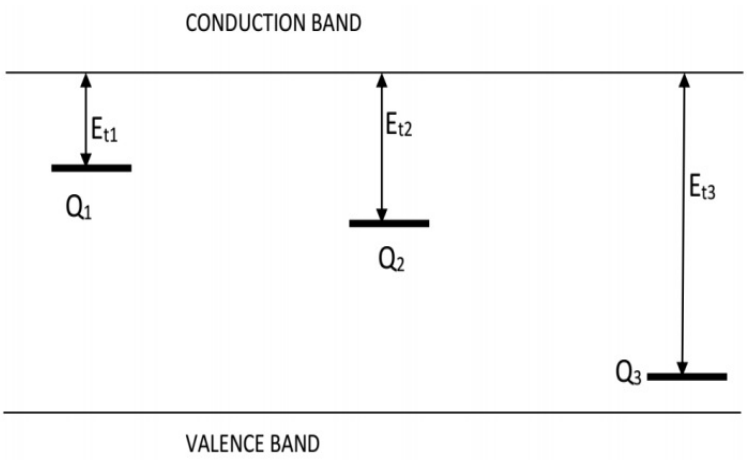

Figure 2.2: Representation of trapping energy states in a dielectric.Q_1,Q_2 and Q_3 charges are trapped at trap depth E_{t1},E_{t2} and E_{t3} trap depth.

de-trapping. On that premise, equation 2.2 becomes,

$$i_{dis} \approx i_{de-trap} \tag{2.4}$$

In this section, a mathematical model is presented to estimate charge trapping parameters, i.e. trap distribution and trap depth from the aforementioned discharge current. The developed model is based on the early investigations by Simmon and Tams [53] and subsequent studies by Mazzanti et al, [79]-[80]and Chen et al [18]. To simplify the understanding of charge trapping and de-trapping process, following assumptions are made,
(i)The injected charges remain very close to the electrode. To satisfy this argument in the experimental study, the samples were stressed for very short duration (typically for 2 minutes).Such approach has also been used in [3].
(ii) On the basis of trap depth, the traps are non-uniformly distributed across the sample.
(iii) For a particular trap depth, the trap density is same across the sample.
(iv)During the depolarization (short circuit) process, the charges de-trapped are not captured again by other traps. The time taken by the de-trapped charge to reach electrode is insignificant compared to the residence time in the trap. It should be remembered that in practical scenario, however re-trapping is very common. However, keeping in mind the previous assumption that the trapped charges remain very close to the electrodes, charge re-trapping is ignored.
(v) Electron-hole recombination is ignored.

During high voltage application, a major part of injected charges get trapped in the trapping sites present in the polymeric insulation. These charges produce their own electric field inside the dielectric specimen. Now, if the charged dielectric specimen is short circuited, the capacitive charges and the charges trapped in shallow traps are quickly discharged. However, because of the presence of deep traps, the mobility of these charges becomes very low and they cannot be easily depleted from the dielectric even under short circuit conditions. The electric field due to these deep trapped charges will continue to exist even in short circuit situation. But the net electric field across the dielectric sample will become zero to satisfy the sort circuit condition. To satisfy this con-

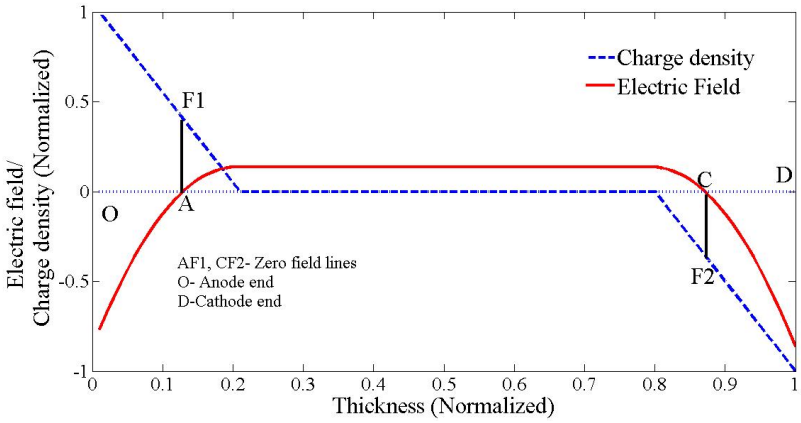

Figure 2.3: Typical space charge distribution and internal Electric field inside the dielectric field due to space charges only.

dition, a negative charge layer appears on the positive electrode, which produces an electric field equal to the mean internal electric field but of opposite polarity, thereby making the net effective field across the sample zero. As a result, there should be one (for unipolar charge injection) or two (for bipolar charge injection) zero field lines inside the sample [56]. This case is depicted in Figures 2.3 and 2.4. Figure 2.3 depicts a typical space charge distribution and the corresponding internal electric field distribution in a dielectric specimen. When this specimen is short circuited, a negative charge layer appears on the positive electrode to make the effective field zero. As a result, the effective electric field across the specimen is redistributed and zero field lines appear. This case is depicted in Figure 2.4, demonstrating two zero field lines (AF1 and CF2). It can be observed from Figure 2.3 and 2.4, that under the effect of electric field the positive charges in the region OA and the negative charges in region CD will quickly move towards the electrodes and will be absorbed. Charges lying outside the zero field planes will move towards the middle of the sample and recombine.

Now, the image charge induced by space charge on the electrode at

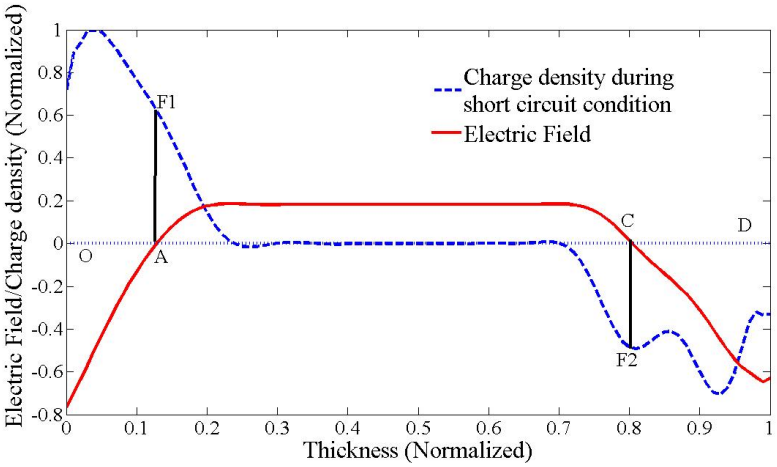

Figure 2.4: Internal Field distribution under short circuit conditions.

any instant under short circuit condition will be calculated. Let, the case of positive charges are considered first. Let $\rho(x)$ is the volume charge density distributed form.
This volume charge distribution can be approximated by an equivalent surface charge density of σ_{eq} . The value of σ_{eq} is given by [68].

$$\sigma_{eq} = \frac{d-r}{d}\sigma \tag{2.5}$$

Where,

$$\sigma = \int_0^d \rho(x)dx \tag{2.6}$$

and r is the centroid of the distributed positive charge. Equation 2.5 can also be written as,

$$\sigma_{eq} = c\sigma dx \tag{2.7}$$

where

$$c = \frac{d-r}{d} \tag{2.8}$$

This σ_{eq} induces σ_i on the electrode surface.[68]

$$\sigma_i = -\sigma_{eq} \tag{2.9}$$

According to equation 2.5, σ_{eq} is obtained by weighting all the charges by their respective ratios (d-x)/d onto the surface x=0. It should be noted that the negative charges located near the negative electrode will also induce a small amount of positive charge on the electrode. However, as the negative charges are very far from the positive electrode compared to the positive charges, their induction effect is negligible and therefore, ignored in the present study.

Now, let the short circuit is removed. The dielectric sample is open circuited now. In this situation, a portion of the trapped charge will be de-trapped in a time interval Δt due to thermal de-trapping processes. Let this de-trapped charge is denoted as $\rho_{de-trapped}$. The zero field planes will continue to exist in the sample under this situation. Most of $\rho_{de-trapped}$ will quickly move towards the disconnected positive electrode under the effect of electric field, but it will not be extracted as the positive electrode is open circuited. Now, if the sample is again short circuited this released charges will quickly disappear from the sample. This portion of $\rho_{de-trapped}$ is termed as $\rho_{released}$. A small fraction of $\rho_{released}$, which lies outside the zero field plane will drift further inside the specimen, and will be finally lost due to recombination with negative charges. Now, if the injected charges are very close to the electrodes, then the zero field lines will also be very close to the electrodes and it can be assumed that nearly all the injected charges are enclosed by the zero field lines(charges in the region OA and CD). Under such assumption, the fraction of released charges which will move inside the dielectric and recombine with oppositr polarity charges can be ignored. At this condition,

$$\rho_{de-trapped} \approx \rho_{released} \tag{2.10}$$

The summation of positive charge density across the thickness of the sample will change from σ to $\sigma^{'}$.

$$\sigma^{'} = \int_0^d (\rho(x) - \rho_{released})dx \tag{2.11}$$

The net de-trapped charge $Q_{de-trapped}$ can be expressed as,

$$Q_{de-trapped} = A(\sigma - \sigma^{'}) \tag{2.12}$$

Similarly, the equivalent charge density projected on the positive electrode surface will change from σ to $\sigma^{'}$. As a result, the image charge

density in the positive electrode will also change to $\sigma_i^{'}$. The change in image charge density $\Delta\sigma_i$ is given by,

$$\Delta\sigma_i = \sigma_i^{'} - \sigma_i = c(\sigma^{'} - \sigma) \tag{2.13}$$

Because of $\Delta\sigma_i$ and $\rho_{released}$, a net current I_{rel} will flow from the positive electrode. By integrating I_{rel} , net extracted charge Q is obtained.

$$Q = \int_0^t I_{rel}(t)dt \tag{2.14}$$

This Q can be expressed as a summation of de-trapped charges and change in image charge,

$$Q = cA(\sigma^{'} - \sigma) + Q_{de-trapped} \tag{2.15}$$

From equation 2.12 and equation 2.15,

$$Q = Q_{de-trapped}(1 - c) \tag{2.16}$$

Because of the change in image charge density and extracted charge , in the interval a net current will flow from the positive electrode to ground. This current, which can be recorded through an electrometer, is termed as depolarization current . Its value can be determined as,

$$\Delta I_d = \frac{\Delta\sigma_i + Q_{de-trapped}}{\Delta t} or \Delta I_d = \frac{Q_{de-trapped(1-c)}}{\Delta t} \tag{2.17}$$

From equation 2.17 it is observed that the depolarization current ΔI_d in a particular time interval Δt is proportional to the actual de-trapped charge $Q_{de-trapped}$ through a proportionality constant $(1 - c)$. The value of charge centroid c depends on the shape of actual space charge distribution, which can be obtained through space charge mapping techniques [39]-[51]. However, in the present work, the focus has been given on obtaining the trapped charge distribution directly from the measured de-polarization current, without performing space charge measurements. Previous experimental investigations have revealed that during charge de-trapping process, the basic shape of the charge distribution in a dielectric specimen remains almost same to a large extent [80]. Therefore, in this work the value of c has been assumed constant to a certain value, from which a relative distribution of trapped charges can be obtained. From the time at which particular amount of charge is extracted, the corresponding trap depth can be evaluated.

2.3.1 Estimation of trapping parameters

Let, the depolarization current is decomposed into several components $\Delta I_1, \Delta I_2, \Delta I_3 ..... \Delta I_n$ at time intervals of Δt_1 (0 to t_1), Δt_2 (t_1 to t_2), Δt_3 (t_2 to t_3).... Δt_n (t_{n-1} to t_n). The charge extracted in these time intervals is proportional to the charge de-trapped in that time period (equation 2.17). At each time interval, charges corresponding to particular trap depth is released. Therefore, the trap depth of the charge released at any time interval can be obtained from the following equation,

$$\Delta t_n = \frac{1}{N_c \nu_{th} \sigma_c exp(\frac{-\Delta E_{tn}}{kT})} or, \Delta E_{tn} = kTln(N_c \nu_{th} \sigma_c \Delta t_n) \qquad (2.18)$$

If the value of capture cross section is kept constant, then, from the values ofΔt_1, Δt_2, Δt_3.... Δt_n different values of trap depth ΔE_{t1},ΔE_{t2}...ΔE_{tn} can be calculated. Charges residing at ΔE_{t1} are depopulated in Δt_1 thereby producing current component ΔI_1, i.e. charges residing in trap energy range ΔE_{t1} produce ΔI_1 and so on. In this way, from equations 2.17 and 2.18, a continuous distribution of charge versus trap depth can be obtained. This can lead to significant understanding of trapping and de-trapping processes. In this work, all values of Δt have been taken as 1s. The value of trap cross section has been taken $10^{-18} m^2$ [18].

2.4 Experimental Arrangement

The experimental set-up in this work consisted of a high voltage DC source, an electrometer (Keithley 6517 A) and LDPE samples with metalized aluminum electrodes. The electrometer Keithley 6517A is capable of measuring currents upto value of 1 fA. The schematic of the experimental set up is shown in Fig. 2.5. The dielectric specimen is charged with the HVDC source (Vdc) for certain duration. Then the sample is short-circuited and the current is measured through an electrometer (A). To perform the experiments at controlled temperature, environment chamber Thermotron is used. The environmental chamber facilitates controllable temperature over a range of -40°C to 198°C.

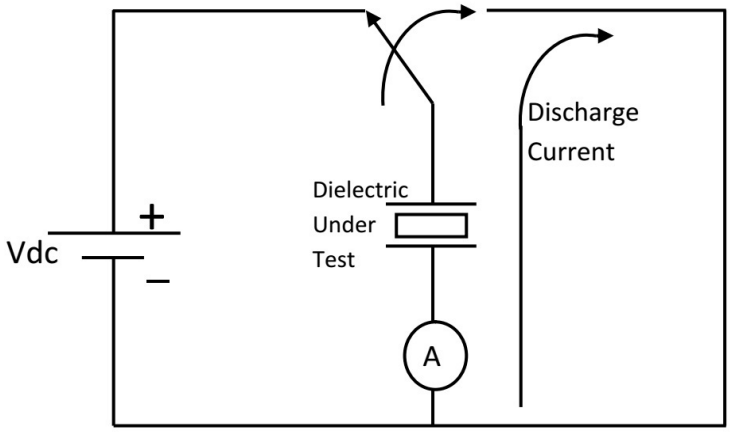

Figure 2.5: Basic experimental arrangement for Current measurement.

2.5 Experimental Results

2.5.1 Effect of Electric Field

Discharge current measurements were performed on commercial LDPE samples of thickness 0.2 mm. The samples were stressed using aluminium electrodes of 50 mm diameter. Prior to discharging, the sample was stressed at 25 kV/mm for two minutes duration. After charging, the discharging current measurements were performed. The initial 1 s part of the discharge current was neglected as it contained transients. From the measured discharge current, the extracted charge at a particular time interval and corresponding trap depth of the extracted charge is calculated according to the methodology described in section 2.3. To study the effect of electric stress, another LDPE sample of same dimension was stressed at a field of 40 kV/mm for duration of two minutes. The extracted charge at different intervals were measured from the discharge current following the same methodology as in section 2.3. Fig. 2.6 depicts the comparison of two discharge current profiles obtained at 25kV/mm and 40 kV/mm stresses.Table 2.1 provides a comparison of extracted charge profiles at these two electric fields. It was observed that

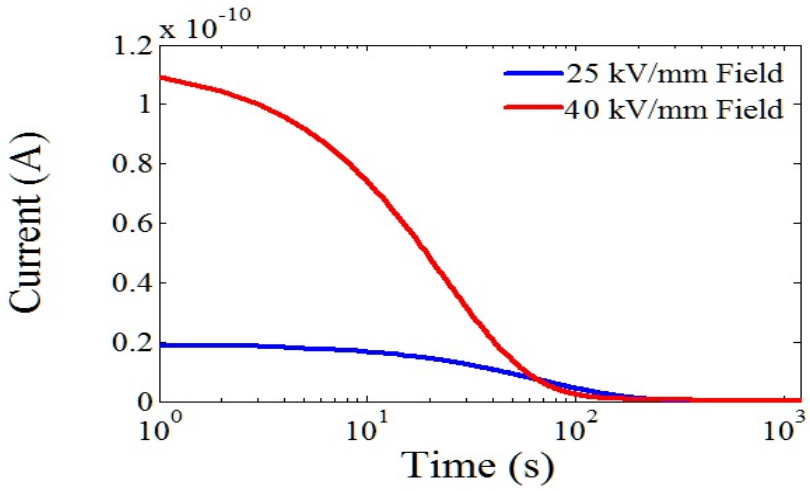

Figure 2.6: Comparison of discharging current measured from LDPE specimens stressed at 25 kV/mm and 40 kV/mm electric fields

the net released charge from the sample stressed at 40 kV/mm was much higher compared to the charge extracted from the sample stressed at 25 kV/mm. However, the difference is mainly in the trap depth region 0.83 eV to 1 eV. For very deep traps, the trapped charge amount was found to be quite similar for both stress levels.

2.5.2 Effect of Temperature

To study the effect of temperature, discharge current measurements were performed on stressed commercial LDPE samples at temperatures of 40°C, 60°C and 80°C, respectively. The samples were stressed at 25 kV/mm for 2 minutes before being subjected to depolarization current measurements. Before charging, the samples were kept at particular temperature for one hour to obtain thermal equilibrium.For each case, the depolarization current data was recorded for 1200 seconds. The trap depth upto which the present method can measure is dependent on the measurement time (1200 s in this case). For obtaining further deeply

Table 2.1: Trap depth and trapped charge distribution at 25 kV/mm and 40 kV/mm fields.

Electric Field	Time interval (s)	Released charge (C)	Trap depth (eV)
25 kV/mm	1-200	1.1110E-9	0.8396-0.9733
	200-400	7.7410E-11	0.9733-0.9908
	400-600	2.5710E-11	0.9908-1.001
	600-800	2.3210E-11	1.001-1.0083
	800-1000	2.2110E-11	1.0083-1.0139
	1000-1200	2.1710E-11	1.0139-1.0185
50kV/mm	1-200	2.7210E-9	0.8396-0.9733
	200-400	110E-10	0.9733-0.9908
	400-600	5.2410E-11	0.9908-1.001
	600-800	2.7610E-11	1.001-1.0083
	800-1000	1.8710E-11	1.0083-1.0139
	1000-1200	1.1610E-11	1.0139-1.0185

trapped charges, the measurement time needs to be enhanced. Fig. 2.7 depicts the depolarization current measurements performed at the four different temperatures.

From Fig.2.7, it was observed that with increase in temperature, discharging current steeply increases. This relates to the fact, that with increase in temperature, the charge injection increases. It should be remembered that with increase in temperature, the polymeric material expands. As a result, the relative distance and separation between polymeric chains increases, giving rise to more amorphous regions in the crystalline structure. As a result, new traps are formed, increasing the trap density. Due to the presence of these two factors, viz. enhanced charge injection and new trap formation, the amount of trapped charge increases with temperature, a portion of which is later de-trapped and absorbed by the electrode during discharging current measurement. As discussed in section 2.3, the obtained discharge current is proportional to the de-trapped charge. Using the methodology described in 2.3, from the time dependent values of discharge current, corresponding trap depths are calculated. From the time dependent nature of discharging current, the relative distribution of trapped charge is also obtained. It was observed, that at every temperature, the trapped charge is non-uniformly distributed in terms of trap energy, with less deep traps capturing much

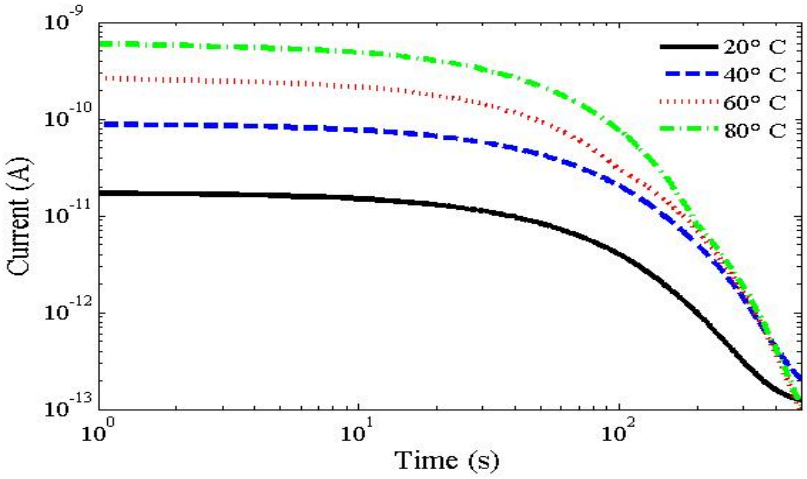

Figure 2.7: Discharging current measured at different temperatures.

more charge than deeper traps. Another important observation was the discharging current decreased more rapidly in higher temperatures compared to lower temperatures. This implies that with increase in temperature, the rate of de-trapping increases. This observation becomes more prominent in Table 2.2. Fig.2.8. depicts relative trap charge distribution at the four different temperatures.

It was observed, that the energy distribution of trapped charge is close to exponential nature, with much less charge in deeper traps. Moreover, with increase in temperature the curve of energy distribution shift towards right, pointing higher trap energy at elevated temperatures.From Table 2.2, it was observed that the proportional representation of charges released in the time period spanning 1 to 200 s, increases with increase in temperature. In 20°C, the proportion of charge released in 1-200 s interval to the total charge released was 86.7 percent, which increased to 92 percent in 40°C, 95.5 percent in 60°C and 98.2 percent in 80°C. It should be remembered, that at higher temperature the trap depth or trap energy required to overcome the trap barrier becomes very high (equations 2.18), as shown in Table 2.2. So it was expected that charges will take more time to de-trap. But, observed results show dif-

Table 2.2: Trap depth, released charge and trapped charge distribution at different temperatures.

Temperature	Time interval (s)	Released charge (C)	Percentage of overall released charge	Trap depth (eV)
20°	1-200	1.1110-9	86.72	0.8396-0.9733
	200-400	7.7410-11	6.05	0.9733-0.9908
	400-600	2.5710-11	2.01	0.9908-1.001
	600-800	2.3210-11	1.81	1.001-1.0083
	800-1000	2.2110-11	1.73	1.0083-1.0139
	1000-1200	2.1710-11	1.7	1.0139-1.0185
40°	1-200	5.6810-9	92.07	0.9004-1.0433
	200-400	3.6010-10	5.84	1.0433-1.0621
	400-600	4.6410-11	0.75	1.0621-1.0729
	600-800	2.8810-11	0.47	1.0729-1.0807
	800-1000	2.8010-11	0.45	1.0807-1.0867
	1000-1200	2.7110-11	0.44	1.0867-1.0916
60°	1-200	1.2410-8	95.48	0.9615-1.1135
	200-400	5.4410-10	4.28	1.1135-1.1334
	400-600	2.4610-11	0.22	1.1334-1.1450
	600-800	2.0110-12	0.02	1.1450-1.1533
	800-1000	—-	——	1.1533-1.1597
	1000-1200	———	—-	1.1597-1.1649
80°	1-200	2.8710-8	98.21	1.0228-1.1839
	200-400	5.2110-10	1.77	11.1839-1.2050
	400-600	2.8810-11	0.01	1.2050-1.2173
	600-800	2.3510-12	0.008	1.2173-1.2261
	800-1000	—-	——	1.2261-1.2329
	1000-1200	——	—-	1.2329-1.2384

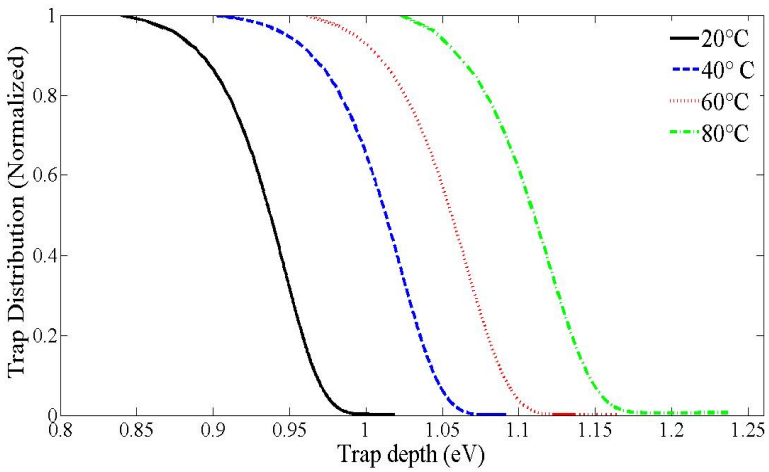

Figure 2.8: Relative trapped charge distribution at different temperatures.

ferent nature. This anomaly can be explained by the fact that in higher temperatures, the charge carriers acquire more energy through lattice vibrations, and hence they easily de-trap and are extracted by the electrodes. Consequently deep traps act as shallow traps, as they quickly liberate the charges. This observation is in accordance with [81]. In all the observations of Fig. 2.7 and Table 2.2, the LDPE samples were stressed for very short periods, typically two minutes. This was done to ensure that the injected charges remain very close to the electrodes. To study the effect of prolonged charging period at elevated temperatures, a specimen was stressed at 25 kV/mm field at 80°C temperature for one hour before subjecting it to depolarization current measurements. The comparison of the depolarization currents observed for two minute stressing and one hour stress is shown in Fig.2.9

It was observed that the two currents were distinctly different from each other. It was observed that initially the discharging current was small in the case of one hour stress compared to the case of two minute stress. However, in the case of one hour stress, the rate of decreasing of discharging current was much slower compared to the case

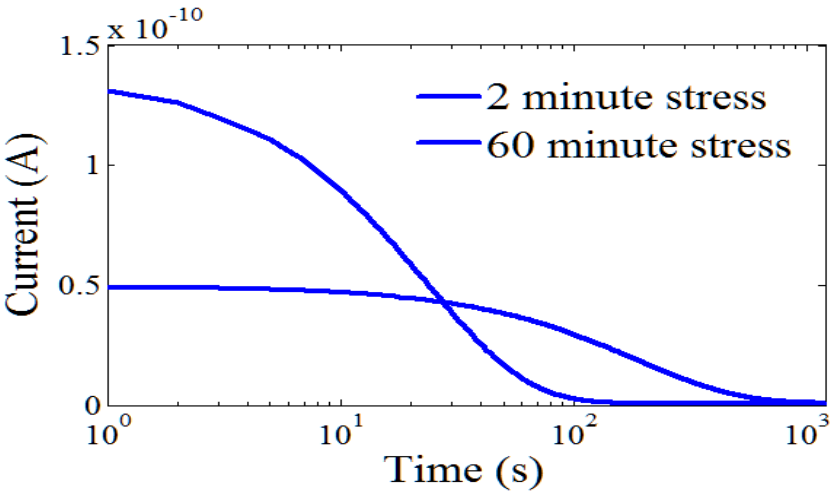

Figure 2.9: Comparison of Depolarization current at 2 minute stress and one hour stress.

of two minute stress. This behavior can be explained through charge dynamics at higher temperatures. At 80°C, one hour stress, the charges penetrate deep in the sample and may possibly reach the opposite electrode. As a result, the charge enclosed by the zero field lines (Figure 2.4) becomes less. So initially, the discharging current is small. However, in such case the zero field lines also penetrate deeper. The de-trapped charges have to cover much more distance and career re-trapping becomes significant. All these factors make the charge extraction process quite slow. On the other hand, in the case of two minute stress, the charges remain very close to the electrodes and have to cover little distance to reach electrode after release, making re-trapping of the carrier insignificant. Consequently, the discharging current quickly decreases.

2.6 Conclusions

Estimation of charge trapping parameters has been proven to be a difficult task to researchers for quite some time. Most of the present

methods are indirect in nature and require sophisticated signal processing tools. In this chapter, a new method for direct estimation of trapped charge distribution without performing space charge measurements is presented. The presented method directly obtains essential parameters related to the trapping process, i.e. trap depth and a relative distribution of trapped charge across different trap depths, from the discharging current measurements of a stressed dielectric specimen. The amount of extracted charge decreases very fast with time, indicating non-uniform trapped charge distribution across different trap depths. Further qualitative analysis revealed the exponential nature of trapped charge distribution, as deeper traps contained much lesser amount of charge than comparatively less deep traps. The amount of trapped charge increases with applied stress. Although the experimental work was performed on LDPE in this chapter, the method is applicable for any solid or composite dielectric insulation, i.e. cables, polymer composite insulators, dry type transformer etc. In the next chapters, application of presented technique on other dielectric materials will be discussed.

The effect of temperature on charge de-trapping is also studied in this chapter. For this purpose, depolarization current measurements were performed over a wide temperature range from 20°C to 80°C. From the obtained results and analysis, following conclusions are drawn.

(i) The amount of trapped charge increases with temperature. This happens due to two factors. One, with increase in temperature, the charge injection increases. Secondly, as the temperature increases, there is thermal expansion in the material, which increases the relative separation between different polymer chains. It modifies the microscopic structure in the material, bringing more non crystalline nature. It results in more trap formation, which captures the injected charges.

(ii) At each temperature, in terms of trap depth or trap energy, the obtained trap charge distribution was nearly exponential in nature. The traps with higher trap energy capture much less amount of charge than the trap with lesser energy.

(iii) At higher temperatures, charges are quickly de-trapped compared to de-trapping at lower temperature. This can be explained due to the fact that at high temperatures, the de-trapped charges are thermally excited and easily obtain the required energy to de-trap through thermal means. From the above analysis, it can be pointed out that in practical cases, e.g. cables, there are often high temperature periods in load cycle. Under such circumstances, there will be significant charge injections, which

will be trapped in the dielectric. If the thermal stress is prolonged then the charges will be able to gain sufficient energy to de-trap. Otherwise it will remain in the insulation giving rise to space charge accumulations.

Chapter 3

A Method to Identify Charge De-trapping and Dipolar Relaxation Properties of Epoxy Resin from Discharging Current Measurements

3.1 Introduction

In ***Chapter 2***, a mathematical model has been developed to correlate trapping parameters from discharging current measurements performed on LDPE samples. As LDPE is a non polar material, it was assumed that the discharging current recorded after 1s of short circuit is mainly due to charge de-trapping, and dipolar relaxation was neglected. However, in the case of polar dielectric material, the effect of dipolar relaxation on discharging current cannot be neglected. Therefore, in that case, it is important to segregate the component of dipolar relaxation from discharging current before estimating charge trapping parameters. Present chapter deals with this issue, as epoxy resin, a polar dielectric is considered for charge trapping investigation in this chapter.

Epoxy resins are very frequently used as electrical insulation in a wide range of equipment i.e. transformers, rotating machines, bus bars etc[82]. With advancement in HVDC technology, epoxy resin is also being frequently used in DC insulation systems. As the DC electric field

distribution is dependent on the resistivity of the material, the role of space charge becomes important.There has been strong experimental evidence of space charge accumulation in epoxy resin at medium and high electrical stresses [83]. The origin of this space charge has already been discussed in chapter 1.
Charging and Discharging current measurements has been an important tool for studying dielectric properties. If epoxy resin is considered, space charge accumulation considerably influences charging-discharging current measurements performed on it, especially when the measurements are performed at high electric fields. There has been some investigations on charging-discharging currents in epoxy resin. In [84]-[85], the effects of temperature and field on charging-discharging currents in epoxy resin were studied. In [85], the threshold field for space charge accumulation in epoxy resins was measured from discharging currents employing the non-ohmic nature of conductivity as evidence of space charge accumulation. However, as epoxy resin is a polar material, dipolar relaxation also affects the charging-discharging currents. Therefore, a simplified model to distinguish space charge behavior from dipolar relaxation might be helpful for a better understanding of dielectric properties of epoxy resin. This may prove beneficial for insulation design as well as condition monitoring of epoxy insulation. The present work makes an attempt in this direction.In this chapter, a method is proposed to separate the effect of dipolar relaxation in discharging current from frequency domain spectroscopy using Hamon approximation.By subtracting this component from discharging current, the current due to charge de-trapping is identified. By conducting experiments at different field and temperature, the changes in both the dipolar component and space charge component in charging-discharging currents are studied.

3.2 Theory of Dielectric relaxation

Dielectric relaxation is a process of polarization/relaxation observed in a dielectric during the application and subsequent removal of external electrical stress. When a dc voltage is applied on a dielectric, the dipoles present in the dielectric start to orient according to the direction of applied electric field. This will bound charges on the electrodes or high voltage DC exciter terminals, causing a polarization current to flow. After a time span, the stressed dielectric is short circuited. As a

result, the dipoles start to disorient and the bound charges on the electrodes become free. This results in the flow of depolarization current. This process is termed as time domain dielectric spectroscopy (TDDS). AC counterpart of this process is observed in frequency domain dielectric spectroscopy (FDDS), where the dielectric is subjected to ac electric field of wide frequency range, typically 10^{-4} Hz to 10^{4} Hz. The theory of dielectric relaxation in solids has been thoroughly discussed in [86]. In TDDS, the polarization current recorded after the application of step voltage U_c is given by [87]-[88],

$$i_{pol}(t) = C_0 U_c[\frac{\sigma_0}{\epsilon_0} + \epsilon_\infty \delta(t) + f(t)] \tag{3.1}$$

where, σ_0 is dc conductivity , ϵ_0 is permittivity of free space,ϵ_∞ is the high frequency permittivity of the dielectric, $\delta(t)$ is a delta function representing very fast polarization processes in the dielectric, C_0 is the geometric capacitance of the investigated test object and $f(t)$ is the response function of the dielectric. If very fast polarization processes are ignored, then, equation 3.1 can be rewritten as,

$$i_{pol} = i_c + i_d \tag{3.2}$$

where, i_c and i_d are dc conduction and polarization component of i_{pol} respectively.

Now if U_c is removed after $t = t_c$ and the charged dielectric specimen is grounded, then the dipoles will tend to relax to their original position. This will release the bound charges, thereby causing a current to flow. This current, also known as depolarization current is given by the following equation:

$$i_{depol}(t) = -C_0 U_c[f(t) - f(t + t_c)] \tag{3.3}$$

For large values of t_c , $f(t) >> f(t + t_c)$, and the second term in equation 3.3 can be neglected. In that case, equation 3.3 can be rewritten as in 3.4, and the depolarization current becomes proportional to the dielectric response function[87].

$$i_{depol(t)} \approx C_0 U_c f(t) \tag{3.4}$$

From equation 3.1 and 3.4, if the dielectric behaves linearly, then

$$i_{depol}(t) \approx i_d \tag{3.5}$$

A similar study can also be conducted in frequency domain. If the dielectric specimen is excited with sinusoidal voltage V then the dipoles will also oscillate according to the applied field. As a result, a current will be produced, which can be described through the following equation [87],

$$I(\omega) = j\omega C_0[\epsilon_\infty + \chi' - j(\frac{\sigma_0}{\epsilon_0\omega + \chi''(\omega)})]U(\omega) \tag{3.6}$$

$$or, I(\omega) = j\omega C_0[\epsilon'(\omega) - j\epsilon''(\omega)]U(\omega) \tag{3.7}$$

where $\epsilon'(\omega) - j\epsilon''(\omega)$ is the complex susceptibility of the dielectric, the frequency domain counterpart of response function . Often, it is more suitable to use complex permittivity instead of complex susceptibility, which is expressed as $\epsilon'(\omega) - j\epsilon''(\omega)$.
The characteristics of imaginary component of permittivity of epoxy resin are discussed in [88]. It was observed that frequency characteristics of epoxy consist of mainly two processes- dc conduction process and dipolar relaxation process. At very low frequencies, the duration of half cycle is long enough to cause ionic charge transport from one electrode to another. This resembles the conduction process in a dielectric under dc voltage. This dc conduction process is dominant in very low frequency range (10^{-3} Hz to 10^{-4} Hz) and is characterized by a slope of -1 in log-log scale. The mid frequency and high frequency responses correspond mainly to dipolar orientation under AC fields.

3.3 Hamon Approximation

If the dielectric behaves linearly with applied field, then by applying Fourier transform techniques the frequency domain response can be calculated from time domain response. An alternative method for calculation of frequency domain dielectric response from time domain

measurements is Hamon approximation [89].Compared to Fourier transform, the computational burden is much less in Hamon approximation, allowing faster calculation. Besides this, Hamon approximation has been proven to be an effective method for calculation of frequency domain data from time domain data particularly in the case of solid dielectric materials, where non-Debye relaxation is prominent [87]-[90]. Hamon approximation is based on a simple relation between imaginary part of complex relative permittivity and depolarization current given by,

$$\epsilon''(\omega) \approx \frac{\sigma_0}{\epsilon_0 \omega} + \frac{-i_{depol}(\frac{0.1}{f}))}{2\pi f C_0 U_0} \tag{3.8}$$

3.4 Relationship between charge de-trapping and discharge current measurements

The accumulation of space charge is highly dependent on the trapping characteristics of the dielectric. In a typical polymer microstructure, there exist amorphous regions with different electron negativity than the host material [14]-[15]. If these regions have higher electron affinity then the host material, then they will capture the injected charge. These amorphous regions are known as traps. At the same time, dipolar polarization and dc conduction will also contribute to the charging current. Quite reasonably, the charging current at high electric fields can be described as the combined effect of three different currents, given by the following equation,

$$i_{charge} = i_c + i_d + i_{inj} \tag{3.9}$$

where i_{charge} and i_{inj} are the total charging current and charge injection current, respectively.

For a polar dielectric like epoxy, the discharge current will also be highly affected by dipolar relaxation, as it will also lead to change in bound charge density at the electrodes. As a result, the net discharge current can now be considered as a combination of two different currents,

one due to charge de-trapping and the other due to dipolar relaxation. The net discharge current can now be expressed as,

$$i_{dis} = i_d + i_{de-trap} \tag{3.10}$$

where i_{dis} , i_d and $i_{de-trap}$ are net discharge current, dipolar polarization component of discharging current and current due to charge de-trapping, respectively.

The frequency domain dielectric spectroscopy measurement is normally carried out at very low field, as the voltage is normally kept less than 200V. At such low alternating fields, charge injection can be safely ignored [91]-[92]. As a result the FDS measurements are solely due to dipolar orientation and dc conduction. From equation 3.8,

$$\epsilon''(\omega) - \frac{\sigma_0}{\epsilon_0 \omega} \approx \frac{i_{depol}(\frac{0.1}{f})}{2\pi f C_0 U_c} \tag{3.11}$$

Again from equation 3.7

$$\epsilon''(\omega) = \frac{\sigma_0}{\epsilon_0 \omega} + \chi''(\omega) \tag{3.12}$$

At very low frequencies, the dc conduction process is dominant over dipolar relaxation process. In equation 3.12, dipolar relaxation process is represented by the term $\chi''(\omega)$. Therefore, at very low frequencies,

$$\epsilon''(\omega) \approx \frac{\sigma_0}{\epsilon_0 \omega} or \epsilon''(\omega) \approx \frac{G_{dc}}{\omega} where G_{dc} = \frac{\sigma_0}{\epsilon_0} \tag{3.13}$$

In the imaginary permittivity vs. frequency characteristics, from the value of imaginary permittivity at very low frequencies, the contribution of dc conduction process in the characteristics, G_{dc} can be calculated. Once G_{dc} is estimated, the contribution of dc conductivity at any frequency can be estimated by $\frac{G_{dc}}{\omega}$.

By separating the DC contribution from the imaginary permittivity characteristics, the contribution of dipoles in ϵ'' can be evaluated. Once this dipolar contribution is evaluated, the depolarization current solely due to dipolar relaxation i_{depol} can be calculated from equation

3.11. As FDS is obtained at discrete frequency levels, therefore, by Hamon approximation, i_{depol} and hence $f(t)$ will be obtained only at discrete time instants. By using curve fitting algorithms, $f(t)$ can be modeled over a continuous time range.
Once $f(t)$ is evaluated, the current due to only dipolar relaxation i_{depol} can be calculated using equation 3.4. Once it is identified, the current component due to charge de-trapping ($i_{de-trap}$) in the discharging current (i_{dis}) can be identified. In this way, the response due to dipolar relaxation and the response due to charge de-trapping can be separated in discharge currents of a polar dielectric like epoxy resin.

3.5 Sample preparation and experimental arrangement

For preparation of experimental samples, epoxy resin used in this study is a non-vinyl polymer made of a Bisphenol-A. After adding hardener, the composite is cured at 100°C for few hours and then post cured at 25°C for 24 hours in a controlled environment. The thickness of the epoxy specimens used is around 300 micron. The glass transition temperature of the epoxy was around 60°C.Metalized aluminum electrodes were attached on both sides of the epoxy samples. The experimental set-up consisted of a high voltage DC source, an electrometer (Keithley 6517 A) and data acquisition system. The electrometer Keithley 6517A is capable of measuring currents upto value of 1 fA. The schematic of the experimental set up is shown in Figure 3.1. The dielectric specimen is charged with the HVDC source (Vdc) for a certain duration. Then the sample is short-circuited and the current is measured through an electrometer (A). To perform the experiments at controlled temperature, environment chamber Thermotron is used. The environmental chamber facilitates controllable temperature over a range of -40°C to 180°C.

3.6 Results and discussions

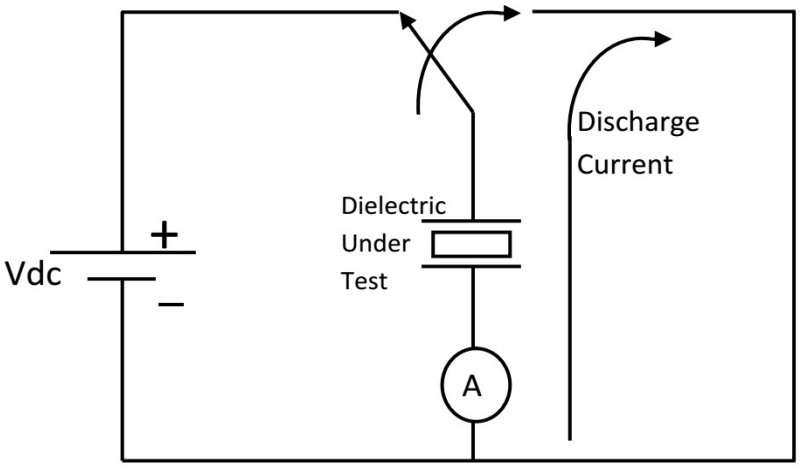

Figure 3.1: Basic experimental arrangement for Charging-Discharging current measurement.

3.6.1 Charging Current Measurements

The recorded charging currents from epoxy resin samples are depicted in Figure 3.2 . The charging currents were at electric field levels of 10kV/mm and 20 kV/mm for a duration of 10000s at 25°C ambient temperature. It can be seen from Figure 3.2, that at 10 kV/mm, the conduction current does not reach steady state value even at 1000s. At 20 kV/mm, the current reaches a quasi steady state at around 10000s. The high value of initial current and the long time taken by the conduction process to achieve steady state illustrates that at these fields, space charge injection and transport processes are dominant in the current response. The final value conduction current at 10000s at10 kV/mm field was 18 pA, which increased to 65pA during charging at 20 kV/mm field. As discussed in chapter 1, in a typical space charge limited current characteristics,the conduction current increases almost in square proportional to the applied voltage. In the present case, as the applied field was increased from 10 kV/mm to 20 kV/mm, the final values of charging current increased by around 3.6 times. However, during application of 10 kV/mm electric field, the charging current was not completely stabilized

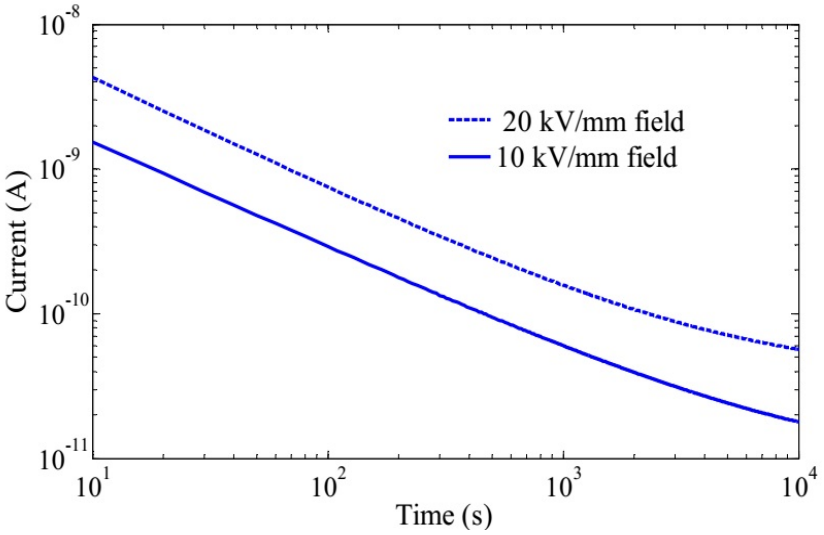

Figure 3.2: Charging current of epoxy resin sample.

and charge injection was possibly active till the end of measurement. Therefore, it is difficult to comment on the exact nature of charge transport in epoxy resin from the measured results.

3.6.2 Discharging Current Measurements

The recorded discharging currents from epoxy resin samples at 25°C and 50°C are depicted in Figure 3.3 and Figure 3.4, respectively. The samples were charged at electric field levels of 2kV/mm, 5 kV/mm, 10kV/mm and 20 kV/mm for duration of two minutes prior to discharging. In all measurements, the initial recorded values of 10 seconds were discarded as it contained transients. Below 1 pA, the measured current was found to be highly affected by noise Therefore, current upto 1 pA only is shown in Figure 3.3 and 3.4. It can be observed from Figure 3.3 and 3.4, the decay of discharging current portrayed almost straight line nature in log-log scale, similar to observations in [84]-[85]. Moreover, the magnitude of the discharging current was highly affected by the applied field during stressing. In the case of 2 kV/mm stressing, the discharging

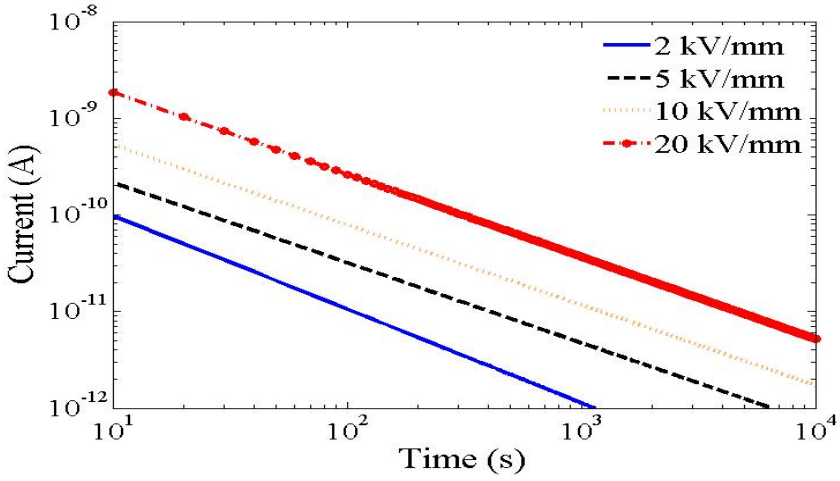

Figure 3.3: Discharging Current of epoxy resin sample at 25°C.

current magnitude around 1000s was only around 1pA, whereas when the sample was stressed at 20 kV/mm, the observed discharging current was around 40 pA. This high non linearity can be attributed to significant charge de-trapping in the latter case. As discussed in section 3.4, in order to separate the dipolar contribution from discharging current, the values of imaginary permittivity of epoxy resin at low frequencies are needed. For this reason, frequency domain spectroscopy measurements were performed on the epoxy resin samples at both 25°C and 50°C by FDS instrument IDAX 300. The obtained values of imaginary permittivity at both the temperatures are depicted in Figure 3.5. Similar to discharging current measurements, here also imaginary permittivity of epoxy resin also portrayed steep increase with temperature, especially at lower frequencies.

The applied voltage during FDS measurements was around 150 V, which results in electric field of around 0.66 kV/mm. At such low fields, charge injection can be ignored. Therefore the response is primarily due to dipolar relaxation and ionic conduction. As shown in Figure 3.5 the imaginary permittivity characteristic closely follows a straight line of slope -1 in the 10^{-4} to 10^{-3} Hz frequency range at both tem-

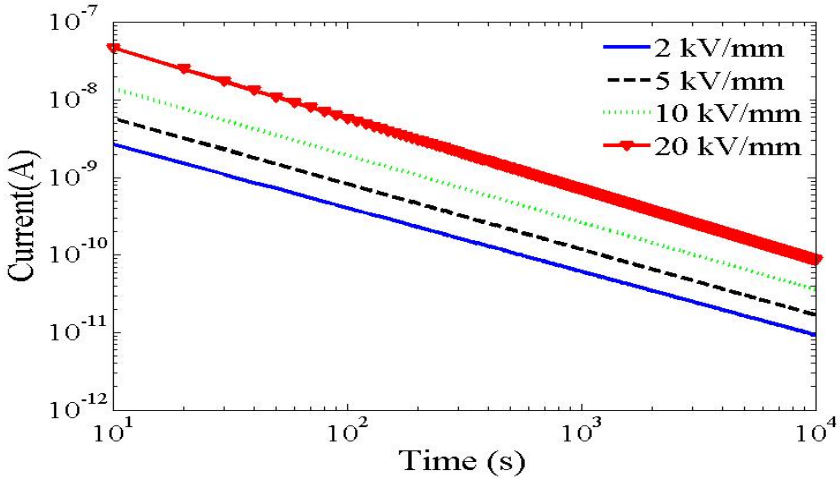

Figure 3.4: Discharging Current of epoxy resin sample at 50°C.

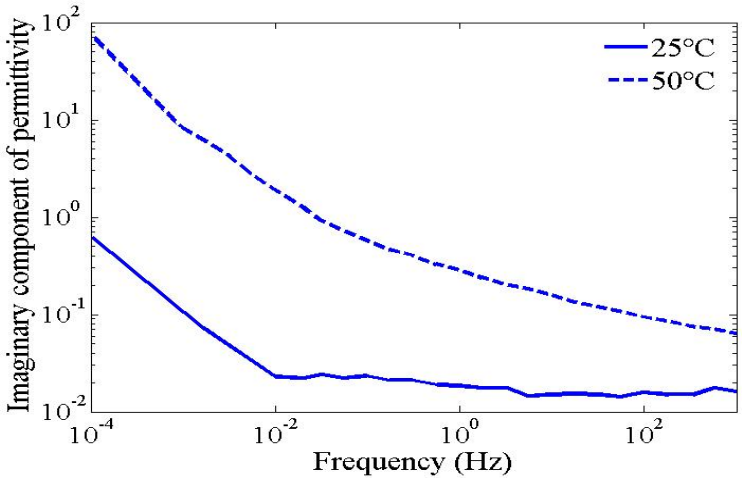

Figure 3.5: Epoxy resin imaginary permittivity as obtained from measurements by IDAX300.

peratures, which represents the conduction process. Therefore, it can be said that at very low frequency (around 10^{-4}) the dipolar relaxation process is negligible to the conduction process. From the value of at 10^{-4}, the value of G_{dc} conductivity and its contribution to $\epsilon''(\omega)$ at frequency ω can be can be estimated using equation 3.12.

Now the dc contribution $G_{dc}(\omega)$ is subtracted from $\epsilon''(\omega)$. From this resultant plot, the dielectric response function $f(t)$ can be estimated using Hamon approximation employing the methodology described in section 3.4. It should be mentioned here, that FDS measurements are performed only at discrete frequencies, and hence i_{depol} can be calculated only at discrete time instants. It has been experimentally observed, that dipolar relaxation in epoxy follows Curie Von Schneidler form of $A_c t^{-n}$, with n having values close to 1 [87]. The calculated values of i_{depol} obtained from Hamon approximation were fitted to the equation form $A_c t^{-n}$ using curve fitting technique in MATLAB software.This will provide the dielectric response function $f(t)$. Once $f(t)$ is determined, the dipolar component of polarization and depolarization current i_d at stress levels of 2,5, 10 and 20 kV/mm are calculated using equation 3.4 and 3.5. It should be mentioned here, that in the present work it is assumed that the dielectric response function $f(t)$ does not change with increase in externally applied electric field, which may not be true always. It has been experimentally observed that at very high electric fields (above 50 kV/mm) the dipolar relaxation process does not remain identical at every stress level [92]. However, investigation of non-linear nature of dipolar relaxation with respect to field is a topic of a separate study. In the present work, the focus is on separation of dipolar relaxation component and charge de-trapping component from discharge current. Therefore in this work, it is assumed that dielectric response function remains same in the electric field range of 2 kV/mm-20 kV/mm and increases linearly with applied field in this region. Once i_d is estimated, then using equation 3.10, the de-trapping current $i_{de-trap}$ is calculated for different samples stressed under different stress levels and temperature. The calculated values and correlation coefficient between the fitted and calculated values of $f(t)$ for 25°C and 50° C at 2 kV/mm field are given in Table 3.1.

It was observed, at both 25°C and 50°C temperatures, for samples stressed at 2kV/mm and 5kV/mm field, the calculated $i_{de-trap}$ was

Table 3.1: Effect of temperature on fitting parameters A_c and n

Temperature	A_c	n	Correlation Coeficient
25°	9.954e-010	-1.018	1
50°	2.165e-008	-0.8302	1

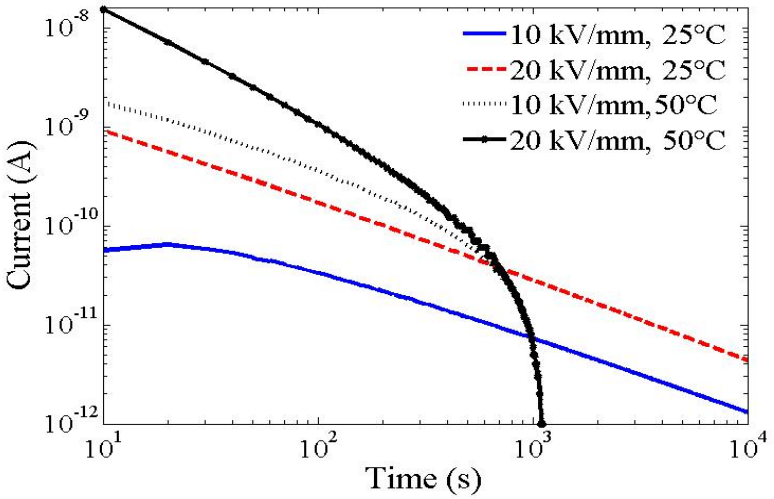

Figure 3.6: Comparison of calculated de-trapping current at different field and temperatures.

negligibly small (around few pico amperes). In [89], it is mentioned that Hamon approximation provides 5% in calculated values. Therefore, an impression is obtained that there is negligible or no charge de-trapping at these measurements. However, for samples stressed at 10 kV/mm and 20kV/mm fields, the calculated de-trapping current was found to be positive and noticeable. The calculated de-trapping currents at 10 kV/mm and 20kV/mm fields and 25°C and 50°C temperatures are depicted in Figure 3.6. From Figure 3.6, it can be observed that with increase in temperature and field, the de-trapping current steeply increases. The de-trapping current for the samples stressed at 20 kV/mm is much higher than the de-trapping current for the sample stressed at 10

kV/mm. This trend is consistent at both 25°C and 50°C temperatures. This relates to the fact that with increase in the electric field, charge injection and trapping increases. At similar stress levels, the de-trapping current observed at 50°C is much higher than the de-trapping current observed at 25°C. This is due to several factors. Firstly charge injection increases with temperature. It has been observed in [84] that, as temperature of epoxy resin approaches towards glass transition temperature (Tg), charge injection and charge mobility is highly enhanced. Present findings in Figure 3.6 are consistent with observations in [84]. The glass transition temperature of the investigated epoxy resin samples is between 60°C and 70°C. Therefore, during stressing at 50°C the charge injection is expected to be much higher compared to measurements performed at 25°C, which is reflected in the high value of de-trapping current at 50°C. Another factor is the expansion of the polymeric material with temperature. As a result, the relative distance and separation between polymeric chains increases. This leads to formation of new traps, increasing the trap density [93]. Due to the presence of these two factors the amount of trapped charge increases with temperature, which is depicted in the calculated de-trapping currents in Figure 3.6. Another interesting observation, which can be made from Figure 3.6 that the de-trapping current decays more rapidly at 50°C compared to 25°C. This implies that the de-trapping process is much faster in 50°C compared to 25°C, which is quite reasonable as it becomes easier for the trapped charges to obtain required energy for de-trapping at high temperature. At the same time, the charge mobility is also much higher at 50°C compared to 25°C, thereby leading to faster charge extraction.

The glass transition temperature of epoxy resin used in this work is between 60°C-70°C. Therefore, during measurements at 50°C, there is a strong possibility of epoxy resin exhibiting liquid-viscous behavior. As stated by Hamon, the Hamon approximation method is for deducing dielectric loss factor in a solid dielectric and the method has not been applied to liquids[89]. Consequently, most research works concerning Hamon approximation has been focused on solid dielectrics. However, it was also stated in [89] that the main criterion of applying this approximation is that the value of n (Curie Von Schneidler form of At^{-n} , mentioned in Table 3.1) should lie between -0.3 and -1.2. Applying this criteria there are many references in literature where Hamon approximation has been applied to polymers near or above glass transition temperature (Tg). For example, in [94],Hamon approximation was applied on polymers at

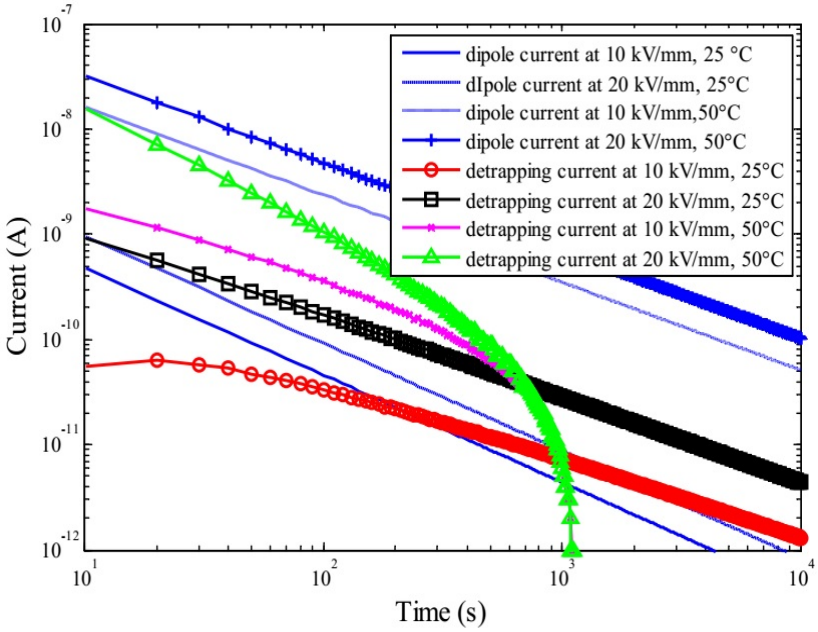

Figure 3.7: Comparison of dipolar and de-trapping contribution in discharging currents.

temperatures considerably higher than their respective Tgs. However, in present work, authors were not sure of the accuracy of Hamon approximation for measurements in epoxy resin above Tg, hence 50°C was chosen as the upper limit of temperature. Moreover, the observed value of n at 50°C was -0.8302, lying nearly midway of the prescribed range, making a strong case of applying Hamon approximation at 50°C measurements. A comparison of separated current components of dipolar contribution and de-trapping contribution from measured discharge currents are given in Figure 3.7.

In Figure 3.7, the dipolar contribution and charge de-trapping contribution in discharging current has been termed as dipole current and de-trapping current respectively. Two distinct behaviors are observed at 25°C and 50°C. In case of discharging current recorded from the sample stressed at 10 kV/mm field 25°C temperature, initially dipole

current is higher than the de-trapping current. Around 200s, a crossover occurs, where de-trapping current surpasses the dipole current. When current regarding 20 kV/mm field, 25°C is considered, the crossover time is much earlier, around 20 s. However, at 50°C measurements, different phenomenon is observed. At both 10 kV/mm and 20 kV/mm fields, the observed de-trapping current is less than the dipole current. The dipolar contribution increases steeply with temperature. Such observation has also been reported in [84]-[85]. This can be attributed to easier relaxation by the dipoles at temperatures close to Tg. The de-trapping current is observed to steeply decline when compared to the dipole current at 50°C measurements. This can be attributed to faster charge extraction at elevated temperatures.

Once the de-trapping current is calculated, trap depth and normalized trapped charge distribution is calculated using the methodology described in section 2. The calculated parameters at 25°C and 50°C are shown in Figure 3.8 and Figure 3.9 respectively. From both figures, it can be observed that the amount of trapped charge is much higher at electric field level of 20 kV/mm compared to 10 kV/mm. However, the increment in trapped charges with field is not uniform at all trap depths. The trap distribution is nearly exponential at 20kV/mm stress at both the temperatures, in the investigated trap depth range. However, in the case of 25°C, at 10 kV/mm, a peak was observed at 0.93 eV in the trapped charge distribution. At deeper trap depths, the trapped charge amount gradually decreases.

3.7 Conclusions

In this chapter, a method for separating the dipolar polarization component and charge de-trapping component from discharge currents has been presented. The presented method incorporates the observation from frequency domain spectroscopy measurements to discharging current measurements. The salient observations of the experimental work performed are listed below.

(1) The discharging current in epoxy resin is highly influenced by applied electric field and temperature.

(2) At fields below 10 kV/mm the response is mainly due to dipolar relaxation. However, at 10 kV/mm and 20 kV/mm the discharging currents are highly influenced by charge de-trapping.

(3) The dipolar polarization-relaxation process is highly affected by tem-

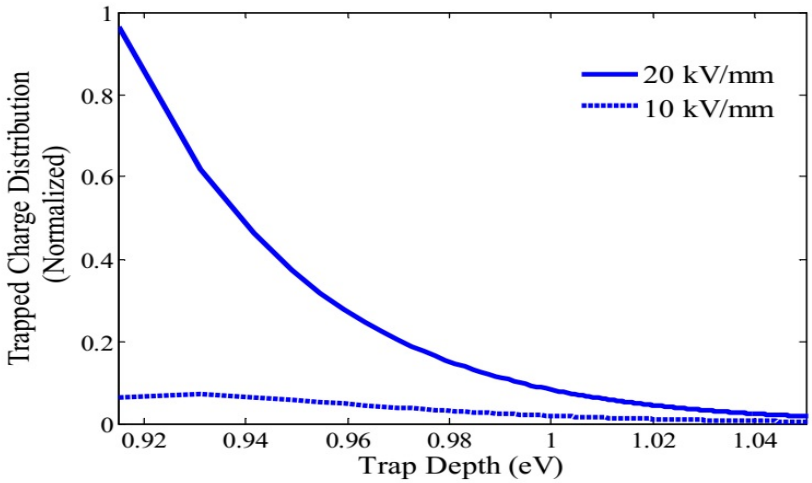

Figure 3.8: Trapped charge distribution of epoxy resin sample under study at 25°C.

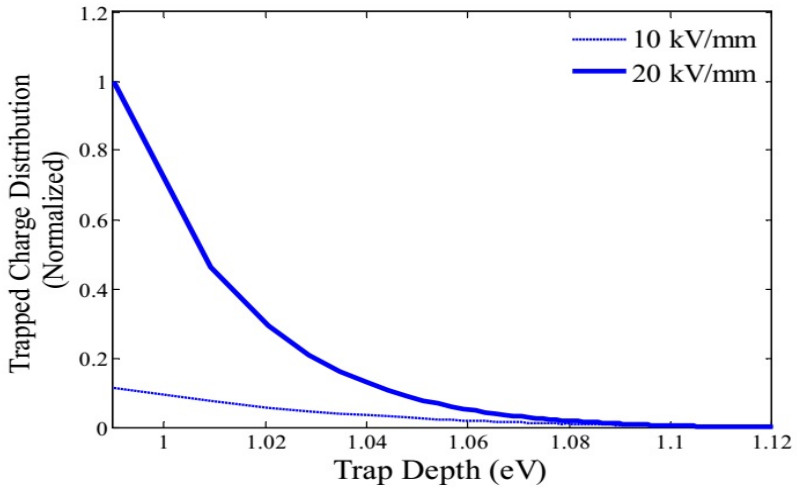

Figure 3.9: Trapped charge distribution of epoxy resin sample under study at 50°C.

perature of the epoxy resin sample.
(4) The distribution of trapped charge is different at 10 kV/mm and 20 kV/mm. However, at the same electric stress level, the nature of distribution was quite similar at both 25°C and 50 °C.
Separation of dipolar response and space charge effect is difficult even with advanced space charge distribution detection method [91]-[92]. This is because the capacitive surface charges are often superimposed on the space charge distribution. The presented method in this work can be useful for this purpose, as it does not rely on space charge measurement techniques. It solely depends on time domain and frequency domain measurements and does not require complicated signal processing tools or transfer function analysis, which are essential for space charge measurements.

Chapter 4

Effect of Moisture and Aging on Charge De-trapping and Transport in Oil-Pressboard Insulation

4.1 Introduction

In ***Chapter 2***, Low-density Polyethylene, a nonpolar material was selected for charge trapping investigation. Charge trapping in epoxy resin, a polar dielectric has been discussed in ***Chapter 3***. In the present chapter, oil impregnated pressboard insulation, another widely used material for HVDC insulation is chosen for charge trapping and de-trapping investigation. In addition, charge de-trapping parameters, the effect of moisture and aging on charge transport in oil-pressboard insulation has also been investigated.

Oil-paper insulation has been extensively used in transformers, power cables and high voltage equipment. Its popularity is driven by mainly two reasons- it possesses strong dielectric and mechanical properties and the cellulosic material is available in abundance from soft wood[96]-[97]. These two factors make oil impregnated cellulosic insulation an attractive choice for insulation purpose in transformers, bushings, cables etc. In particular reference to HVDC systems, oil-paper insulation has been extensively used in HVDC cables and converter transformers. If HVDC system is concerned, Converter transformer is a crucial component of HVDC system. The insulation system in converter transformer is

basically comprised of oil impregnated pressboard. This oil-pressboard insulation used in converter transformer has to withstand significant DC stresses. As a result, the DC conduction properties in oil impregnated cellulosic insulation become an important factor in insulation design and lifetime assessment of converter transformers. A low mobility in the insulation will lead to space charge build-up. The accumulation of space charge will enhance electric field in certain regions inside the insulation and trigger insulation deterioration and aging [59]. On the other hand, a very high value of conductivity may cause localized overheating, leading to winding faults[99]. It is noteworthy that cellulosic insulation is hygroscopic in nature. So far as transformers are considered, after installation of a transformer, the oil-pressboard insulation gradually ages over several years of continuous operation. During this time, the moisture content increases in cellulosic insulation due to the degradation of the molecular chain by oxidation processes which are primarily driven by thermal stresses[100]-[101]. With the reduction in chain length, the mechanical strength decreases, making the insulation brittle. All these factors together may lead to the end of insulation life. For these reasons, a study of conduction properties of oil impregnated pressboard and more importantly, the effect of moisture and aging on these properties may be beneficial to the researchers and Insulation Engineering Community. However, till date there has been little attention paid to the DC conduction mechanisms of oil-cellulosic insulation[102]-[104]. In [103], the DC conduction behavior of oil impregnated kraft paper was investigated at different electric fields. However, the effect of moisture and aging on conduction process was not considered. The effect of moisture conduction mechanism was discussed in[104]. However, in that work the effect of electric field on conduction properties was not studied and the focus was given on moisture assessment from conduction current measurements.

The present work provides an improved approach for understanding the effect of aging and moisture on the conduction properties and charge trapping properties of oil-pressboard insulation. The conduction behavior of oil-pressboard insulation is inherently related to the accumulation of space charge. The factor of space charge accumulation is further related to the charge trapping and de-trapping properties of oil-pressboard. In comparison with polymeric insulations (i.e. LDPE, HDPE,XLPE), there has been significantly less amount of research on charge trapping in oil-paper insulation[105]-[106]. The amount of investigation on the effect of moisture on charge trapping and de-trapping in oil-

paper insulation is even lesser[107]-[108]. In the present work, it is tried to bridge the gap and extract information regarding the effect of moisture and aging on charge trapping and de-trapping in oil-paper insulation from charging-discharging current measurements. For this purpose, two sets of oil impregnated pressboard specimens were prepared- one set was aged with a varying degree through accelerated thermal aging and the other set contained unaged specimens with three different (1%,2% and 3% by weight) moisture contents. The conduction currents at five different electric fields (1 kV/mm, 5kV/mm, 7kV/mm,10 kV/mm and 12kV/mm)of these specimens were recorded and analyzed. A detailed examination of conduction current characteristics revealed that the conduction process in oil-pressboard becomes non-linear above 5kV/mm stress. The experimental findings indicated that carrier Hopping mechanism is mainly responsible for charge conduction in oil-pressboard insulation. Next, the parameters related to charge trapping were extracted from measured discharging current data obtained from a similar set of samples used in conduction current experiments. It was observed, that moisture and aging do not affect charge conduction processes in the same way. The effect of moisture was observed to be far stronger compared to aging. In the previous chapter, a method has been established to separate the effect of dipolar component and charge de-trapping component in discharging current measurements based on frequency domain measurements. Using the same methodology charge de-trapping parameters have been extracted from oil impregnated pressboard insulation samples in this work.

4.2 Sample Preparation and Experimental Set-up

Pressboard specimens having the thickness of 1 mm and other dimensions of 8cm×8cm were used for sample preparation. At first, to desorb the moisture present in pressboard, the specimens were heated at 105°C and its weight was monitored at regular intervals. Once a steady value in weight is obtained, the sample under heating was considered as dry and de-moisturized. Then, for preparing samples having different aging condition, some dry samples were impregnated with transformer oil in vacuum and kept in a sealed container. Prior to impregnation,

the transformer oil was heated and de-gassed. The sealed container was put in a thermal oven, where accelerated thermal aging was performed. The temperature of the thermal oven was kept at 140°C [109]-[110]. The thermal oven used in this experiment can provide heating temperature with an accuracy of 0.5°C. After each 200 hour aging interval, the oven was stopped, followed by cooling of the sealed container for a brief (around 2 hours) period and then two pressboard specimens were taken out from it. One was subjected to charging current measurements at different electric fields and the other was subjected frequency domain spectroscopy measurements and discharging current measurements after stressing it at 10kV/mm field.

For moisture related study, the dry specimens were kept in open air for moisture absorption and their weights were monitored continuously. Due to moisture ingress from open air, the weight of the samples will increase. From this increase, the percentage of moisture (by weight) can be calculated. After the sample obtained the desired moisture percentage, it was impregnated with degassed transformer oil and kept in a sealed container for a few days at 40°C temperature [111]. In this way, oil impregnated pressboard specimens with 1%,2% and 3% were prepared. It should be mentioned that when a pressboard specimen with particular moisture content was impregnated with mineral oil, some amount of moisture will migrate to oil from pressboard. For this reason, prior to current and FDS measurements, the moisture content in oil of sealed containers was measured with an oil-moisture sensor. The moisture sensor used can measure moisture content in oil with an accuracy of 1 ppm. In all containers, the moisture content in oil was observed to be below 50 ppm. From this information, the total weight of moisture in oil is calculated. This moisture has come from pressboard. Therefore, the reduction in pressboard moisture content due to moisture migration can be calculated now. It was observed that the reduction in moisture content in pressboard samples is extremely small and hence, it was ignored in further analysis. The flowchart of the whole experimental work and analysis conducted for the study of charge transport, and identification of charge trapping parameters in oil-paper pressboard are depicted in Figure 4.1 and 4.2, respectively.A schematic of the whole process is given in Figure 4.1.

The schematic of FDS measurement is depicted in Figure 4.3. The frequency range of FDS measurement was 0.1 mHz to 10 Hz. Figure 4.4 depicted the experimental arrangement for charging and discharg-

ing measurements. The experimental set-up consisted of a high voltage DC source, an electrometer (Keithley 6517 A) and data acquisition system. The actual experimental set up has been depicted in Figure 4.5. In both FDS measurements and charging-discharging current measurements, three electrode arrangement was used, to get rid of the influence of surface conduction current in measurements. The electrodes used were made of aluminium and all measurements were performed at room temperature i.e., 25°C.

4.3 Results and Discussions

4.3.1 Charging Current Measurements

Charging current measurements were performed on pressboard specimens with different moisture content and aging conditions at electric fields of 1 kV/mm, 5kV/mm, 7 kV/mm, 10 kV/mm and 12kV/mm, respectively. The charging current profile of the samples having different aging condition and moisture content at 1kV/mm field are depicted in Figure 4.6 and 4.7, respectively. The steady-state conduction current density at different electric fields for all specimens having different aging condition and moisture content are shown in Figure 4.8 and Figure 4.9, respectively. Under Ohmic conduction model, the conductivity is constant with respect to the applied electric field, and the current density is simply proportional to the applied voltage. However, in conduction current measurements, it was observed that all oil-pressboard samples having the different aging conditions and moisture contents deviated from constant conductivity behavior at high electric fields. The final steady-state current density at different aging conditiosn and moisture contents, the predicted current under Ohmic (constant conductivity) behavior and the difference between measured current density and predicted Ohmic current density at different stress levels are shown in Table 4.1 and 4.2 respectively. The difference between measured current density and predicted current density under Ohmic conduction is given below,

$$difference(\%) = ((J_{Ohm} - J_{measured})/J_{Ohm}) \times 100 \qquad (4.1)$$

The graphical representations of the results tabulated in Table 4.1 and 4.2 are depicted Figure 4.8 and 4.9., respectively. From Table 4.1

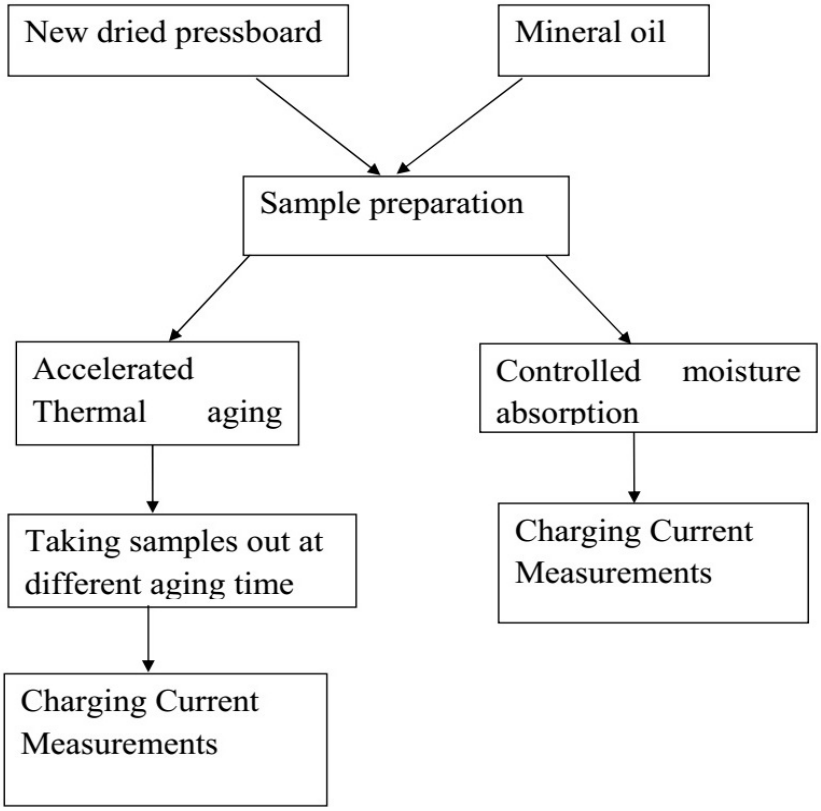

Figure 4.1: Flowchart of the experimental procedure for charge transport study.

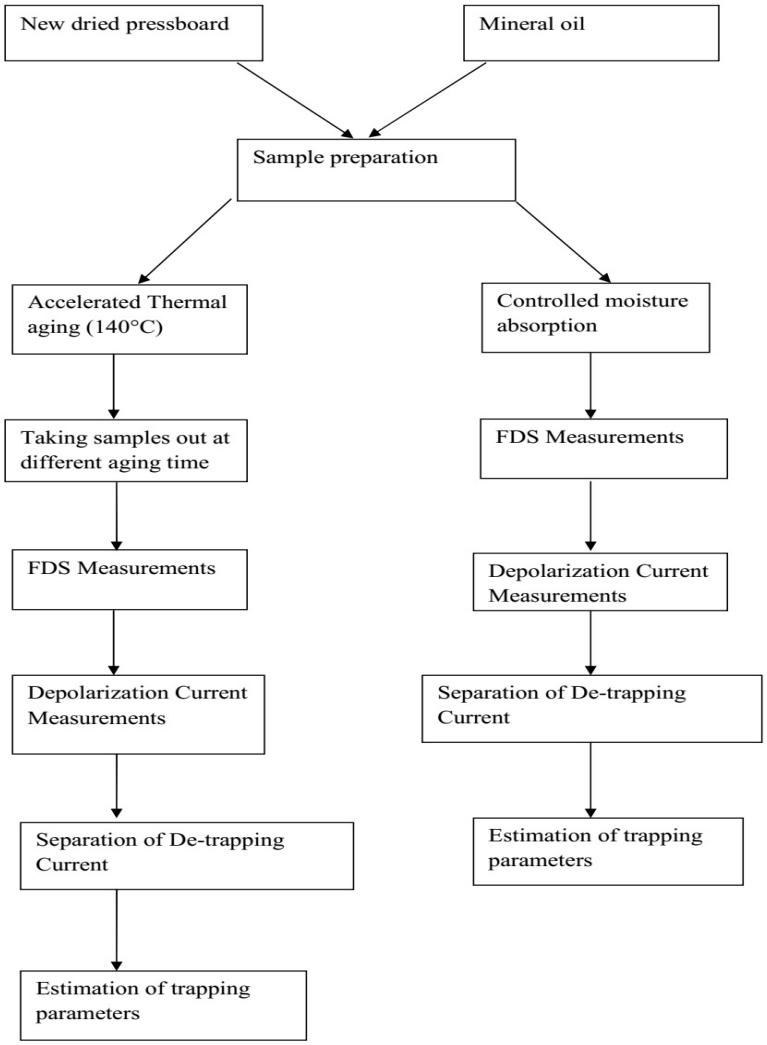

Figure 4.2: Flowchart of the experimental procedure for charge de-trapping study.

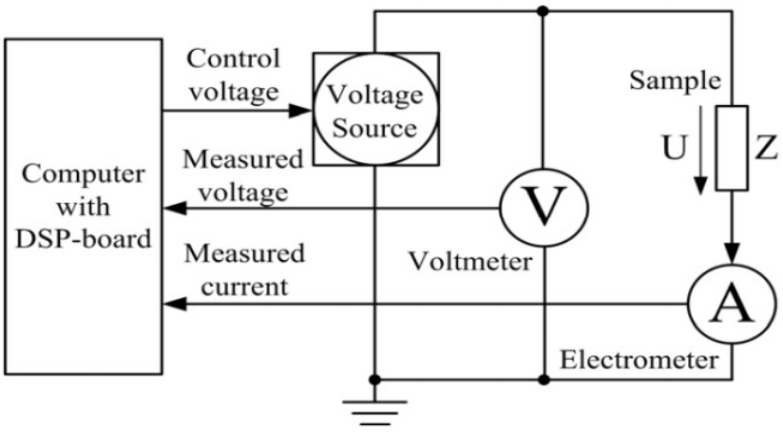

Figure 4.3: Schematic of the experimental set-up for FDS measurements.

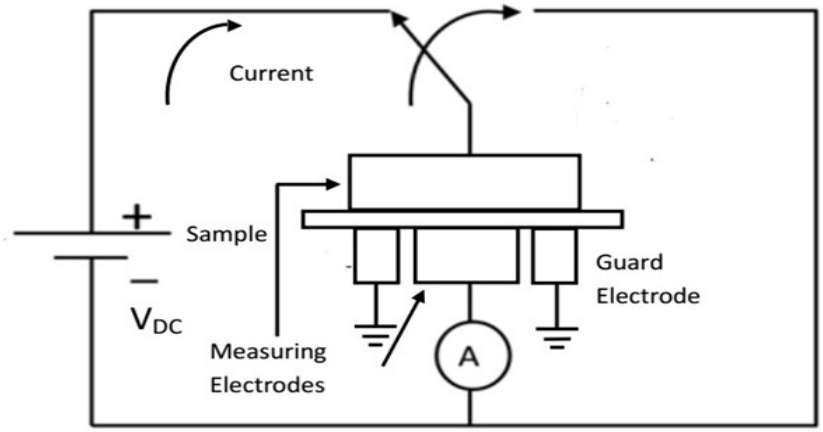

Figure 4.4: Schematic of the experimental set-up for charging-discharging current measurements.

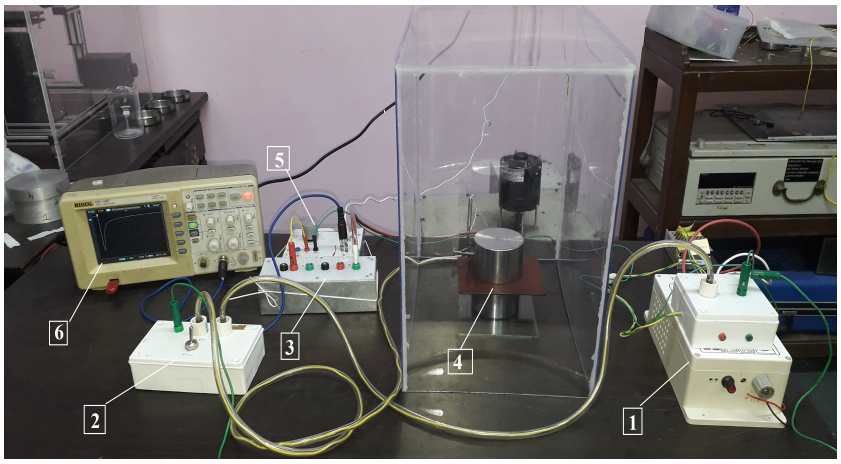

Figure 4.5: Photograph of the overall experimental set-up developed : 1.High Voltage DC Supply 2.Switch 3.Protective Resistance 4.Sample under test 5.Amplifier 6.Data Acquisition.

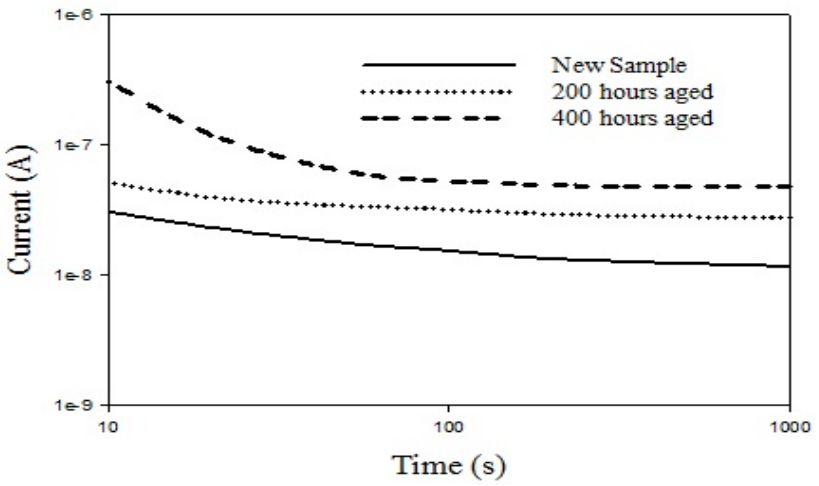

Figure 4.6: Effect of aging on charging currents at 1kV/mm electric field.

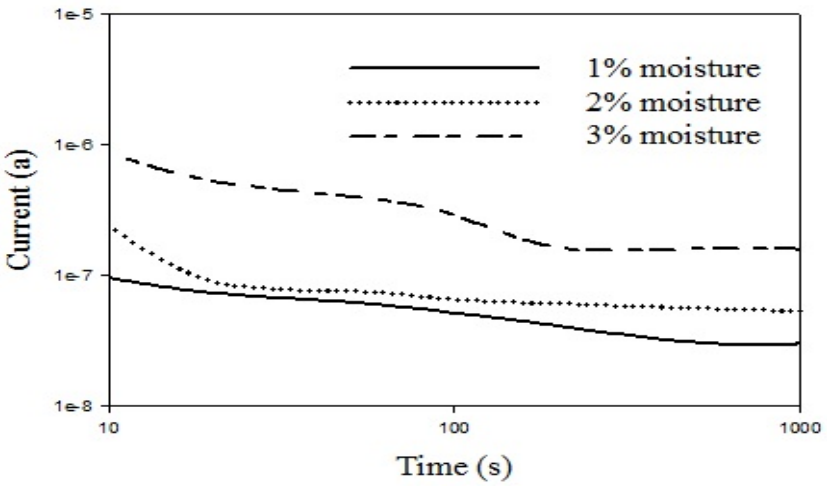

Figure 4.7: Effect of moisture on charging currents at 1 kV/mm electric field.

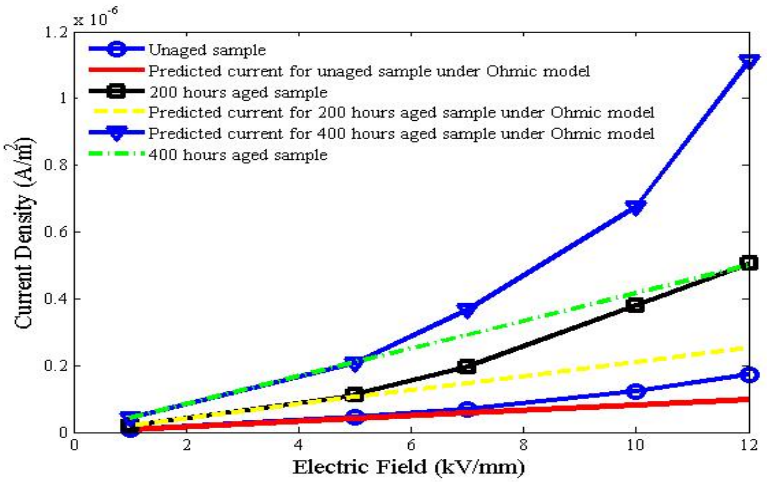

Figure 4.8: Effect of aging on conduction current density in pressboard.

Table 4.1: Effect of aging on conduction current density

Aging Duration	Electric Field (kV/mm)	Current Density (A/m^2)	Current Density under Ohmic Conduction (A/m^2)	Difference(%)
No aging	1	8.12E-9	——	——
	5	4.64E-8	4.11E-8	-13.6
	7	6.92E-8	5.68E-8	-21.8
	10	1.22E-7	8.12E-8	-50.7
	12	1.74E-7	9.74E-8	-77.8
200 hours	1	2.12E-8	——	——
	5	1.10E-7	1.06E-7	-3.8
	7	1.97E-7	1.48E-7	-32.7
	10	3.8E-7	2.12E-7	-79.2
	12	5.05E-7	2.54E-7	-98.8
400 hours	1	4.16E-8	——-	——
	5	2.06E-7	2.08E-7	-1
	7	3.67e-7	2.91E-7	-26.1
	10	6.74E-7	4.16E-7	-62
	12	1.11E-06	4.992E-7	-122.4

Table 4.2: Effect of moisture on conduction current density

Moisture Content (%)	Electric Field (kV/mm)	Current Density (A/m^2)	Current Density under Ohmic Conduction (A/m^2)	Difference(%)
1	1	2.21E-8	—	—
	5	1.04E-7	1.10E-7	5
	7	6.92E-8	1.54E-7	9.1
	10	2.55E-7	2.21E-7	-15
	12	4.93E-7	2.65E-7	-86
2	1	5.58E-8	——	—
	5	2.85E-7	2.79E-7	-2.1
	7	4.16E-7	3.90E-7	-6.6
	10	6.67E-7	5.58E-7	-19.5
	12	9.18E-7	6.67E-7	-37.6
3	1	4.16E-8	——-	—
	5	2.2E-6	2.15E-6	- 2.2
	7	3.16E-6	3.01E-6	-4.9
	10	4.6E-6	4.31E-6	-6.7
	12	5.68E-6	5.17E-6	-9.8

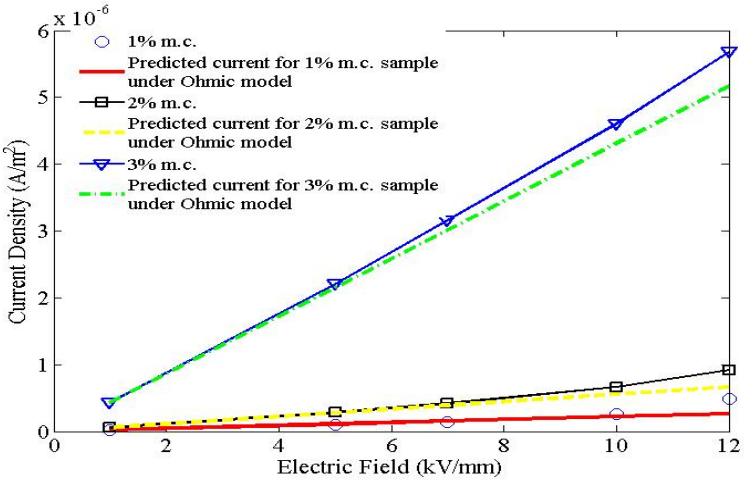

Figure 4.9: Effect of moisture on conduction current density in pressboard.

it can be observed, the conduction current density increases with aging at all electric fields. The current density of the fresh new sample at 1 kV/mm was $8.12 \times 10^{-9} A/m^2$, which increased to $4.16 \times 10^{-8} A/m^2$ after 400 hours aging. Upto 5 kV/mm electric stress, all samples with different aging conditions behaved uniformly. As the electric field was further increased, the non-linear effects on conduction became pronounced. This was evidenced by the growing difference between measured current density and predicted current density under Ohmic conduction model. This difference at high electric fields showed a clear correlation with the aging stage of the sample. For the new sample, the difference at 12kV/mm was -77.8% , whereas for the sample after 400 hours accelerated thermal aging, the difference increased upto 122.4%. This implies that the non-linear effects in conduction process of oil-impregnated pressboard increase with aging.

Similar to table 4.1, the non linearity in conduction process was also observed in samples with different moisture content. At 12 kV/mm electric field the current density was $4.93 \times 10^{-7} A/m^2$, for the sample with 1% moisture content. For 3% moisture content, the current density observed at 12 kV/mm was $5.68 \times 10^{-6} A/m^2$. One major dif-

ference between the observations of Table 4.1 and Table 4.2 was that the non-linearity in conduction current in moisture ingressed samples was observed in comparatively higher electric fields. In other words, the effect of aging on non-linearity was more pronounced when compared to moisture.

From Tables 4.1 and 4.2, it was clear that linear ohmic conduction model fails to explain the conduction current density-electric field characteristics particularly at stress levels higher than 5 kV/mm. To explain the deviation from Ohmic model of conduction, in the following sections, two non-linear conduction models namely Space Charge Limited Conduction (SCLC) and Hopping Conduction model are studied to understand their applicability in the context of oil-pressboard insulation.

4.3.2 SCLC Model

A brief idea regarding Space Charge Limited Conduction (SCLC) Model has already been provided in ***Chapter 1***. In this conduction mechanism, at low electric fields, the conduction current is Ohmic in nature, i.e. current density is proportional to the applied voltage. At high electric fields, there is accumulation of space charge near the electrodes. This happens because the mobility of the space charge is low. For example, if the negative electrode (cathode) emits more electrons, than the ability of the dielectric to transport electrons from one electrode to another per unit time, a negative space charge will be produced near the negative electrode. This will create a field to reduce the electron emission from the cathode.Thus, the current is controlled not only by the electron injecting electrode, but also by the charge carrier mobility in the space inside the dielectric. As a result, after a threshold electrical field, the conduction current will not be simply proportional to the applied voltage.

The generation of space charge is inherently related to the trapping characteristics of the dielectric. In the case of oil impregnated pressboard, the trap distribution will not be uniform across trap depth. Depending upon the trap distribution, the conduction current-applied voltage characteristics will change in the following ways:

The dielectric is trap free-ideal case

This is an ideal case.In this case, above the threshold voltage of ohmic conduction V_Ω the current density is given by the following equation, [110]

$$J = \frac{9}{8}\varepsilon\mu\frac{V^2}{d^3} \tag{4.2}$$

where J is current density, ε is permittivity of the dielectric, μ is mobility of charge carrier, V is applied voltage and d is the thickness of the insulator. It can be observed from equation that the current density (J) is proportional to the square of the applied voltage (V^2).

Traps confined in single or multiple discrete energy levels

If the traps are confined to a particular energy level or multiple discrete energy levels, then the conduction current density above V_Ω is given by, [110]

$$J = \frac{9}{8}\varepsilon\mu\theta\frac{V^2}{d^3} \tag{4.3}$$

where θ is the ratio of free carrier density to total (free and trapped) carrier density. Other terms are defined as above. For trap free case θ is 1. In the presence of traps, θ is always less than unity and can be as small as 10^{-7}.

Traps Distributed Exponentially within the Forbidden energy gap

In this case,the distribution function of trap density is an exponential function of trap energy. The density of shallow traps are much higher than the density of deep traps. In such case, the conduction current density above V_Ω is given by,[110]

$$J = q^{1-l}\mu N_c(\frac{2l+1}{l+1})(\frac{l}{l+1}\frac{\varepsilon}{H_b})^l \times \frac{V^{l+1}}{d^{2l+1}} \tag{4.4}$$

where q is the charge amount of an individual carrier, N_c is the carrier density in conduction band, H_b is the density of traps and l is

a parameter, whose value will depend on the distribution characteristic and should be always greater than 1. Therefore $l+1$ should be always greater than 2.

4.3.3 Hopping Conduction

The transport of a charged carrier in a dielectric can be performed through "hopping" of the carrier "from a molecule (or atom) to an unoccupied state of a neighboring molecule if it acquires the energy necessary to overcome the potential barrier" [110]. The probability of hopping depends on two things,-(i), the required energy, which is obtained by the carrier mainly through thermal excitation and (ii)the distance between two hopping sites. Hopping transport has been used to explain charge transport in many disordered and amorphous materials. A brief idea of hopping conduction has already been given in ***Chapter 1***. In this section, the basics of hopping conduction are revisited with little more detail. The hopping probability can be given by the following equation, [110]

$$W_H = \nu exp(-\Delta E_H/kT) \tag{4.5}$$

where, W_H is the hopping probability, ν is the attempt to escape frequency of the carrier (in 10^{13} Hz), ΔE_H is the height of the potential barrier involved in hopping process.It can be observed from equation 4.5, that if the barrier height is less, the probability of hopping increases. In a dielectric containing trap sites, the potential barrier height can be thought to be same as the trap energy, required by trapped charge carriers to escape from the trap. Application of external electric field modifies the potential barrier or required energy for hopping. If the externally applied electric field is E_0, and the distance between two trapping sites is a, then the energy required to hop in the direction of field is reduced by an amount of QE_0a, and is increased in the direction against the applied field by the same amount. The hopping probability is then the sum of the probabilities in both direction, given by,

$$W_H(E_0) = \nu exp(E_t/kT)[exp(\frac{QE_0a}{2kT}) - exp(\frac{QE_0a}{2kT})] \tag{4.6}$$

which can also be written as,

$$W_H(E_0) = W_{H0}(2sinh(\frac{QE_0a}{2kT})) \tag{4.7}$$

The mobility μ related to hopping can be given as,

$$\mu = \frac{2\nu a}{lE_0}exp(\frac{-E_{mt}}{kT})sinh(\frac{QE_0a}{2kT}) \tag{4.8}$$

Where, l is the number of equivalent neighboring sites to which the carrier is allowed to jump. This corresponds to the co-ordination number of lattice.
The conductivity of a material σ can be given through the following equation,

$$\sigma = N_c q\mu \tag{4.9}$$

where, N_c is the charge carrier density and q is the amount of charge of an individual carrier. Combining equations 4.8 and 4.9, the hopping conductivity can be given as,

$$\sigma_H = N_{charge}q\frac{\nu a}{3E_0}exp(\frac{-E_{mt}}{kT})sinh(\frac{qE_0a}{2kT}) \tag{4.10}$$

The hopping conduction current density at electric field Ecan be given as,

$$J_H = \sigma_H E \tag{4.11}$$

At high electric fields, $sinh(\frac{qE_0a}{2kT}) \approx exp(\frac{qE_0a}{2kt})$
Therefore, from equation 4.7 and 4.8, it can be written,

$$J_H = N_{charge}q\frac{\nu a}{3E_0}exp(\frac{-E_{mt}}{kT})exp(\frac{qE_0a}{2kT}) \tag{4.12}$$

Table 4.3: SCLC fitting parameters

Aging Condition	p	Correlation Coefficient
Unaged	1.36	0.98
200 hours aging	1.74	0.99
400 hours aging	1.78	0.98
1% moisture content (Unaged)	1.31	0.98
2% moisture content (Unaged)	1.22	0.98
3% moisture content (Unaged)	1.05	0.99

4.3.4 Application of SCLC model and Hopping Conduction model for analysing non linearity in oil-pressboard insulation

It has been already discussed in section 4.3.2 that in SCLC model, the current density $J\alpha V^p$, where V is the applied voltage and p is a parameter whose value depends on the trapping characteristics of the material.If the material is trap free, then the value of p becomes 2 (equation 4.1). The same holds true if the traps are confined to single or discrete levels. If the traps are exponentially distributed the value of p is greater than 2. To investigate whether the SCLC model is applicable to oil-impregnated insulation or not, the conduction current density obtained with all samples with different aging conditions and moisture contents are fitted with $J\alpha V^p$ form in the electric field 5-12kV/mm range. This range was chosen primarily because the non-linear affect was negligible below 5 kV/mm stress. The fitting results for samples with different aging conditions and different moisture contents are shown in Figure 4.10 and Figure 4.11 respectively. The values of p and fitting accuracy (Correlation Coefficient)of all samples are tabulated in Table 4.3.

It was observed from Table 4.3 that for all specimens, the values of p lie between 1 and 2. This observation rules out the applicability of SCLC model for oil-impregnated insulation in the investigated electric field range. Therefore, the focus was shifted to Hopping Conduction model.

As discussed in section 4.3.3, for hopping conduction model the current density J_H is proportional to $exp(\frac{qE_0a}{2kt})$, where E_0 is the

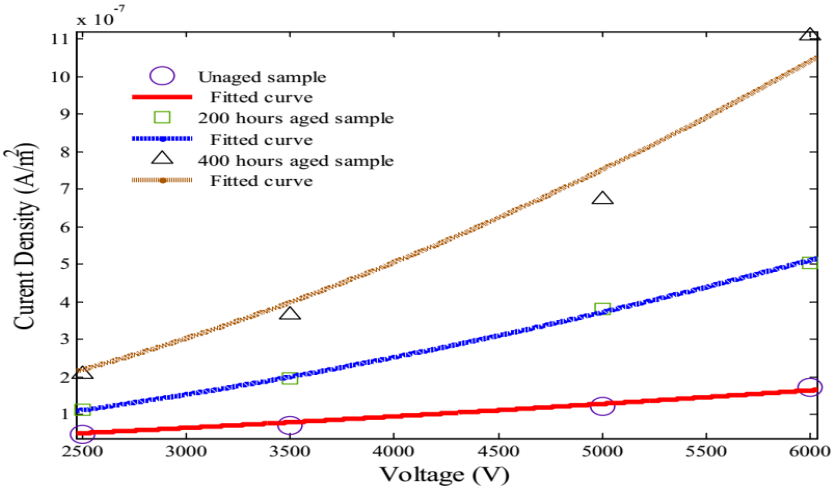

Figure 4.10: Fitting of current density of unaged and aged samples through SCLC model .

applied electric field. At very low electric fields,

$$exp(\frac{qE_0a}{2kt}) \approx \frac{qE_0a}{2kt} \tag{4.13}$$

Therefore, at low electric fields, the current density simply becomes proportional to the externally applied electric field. This resembles the linear Ohmic conduction, where the current is proportional to the applied stress. This observation is similar to what is obtained in the current density-electric field characteristics of all oil-pressboard specimens in the electric field range 1-5kV/mm (Tables 4.1 and 4.2)

However, the simplified relationship (equation 4.13) between current density and applied electric stress does not hold true when higher electric fields are considered. At higher electric fields, the application of equation 4.12 becomes necessary. A close look on equation 4.12 reveals that, if the logarithmic values of current density are plotted with respect to applied electric field E_0, the characteristics would resemble a straight line. Keeping this in mind, the $lnJ - E$ characteristics of samples with different aging conditions and moisture contents are plotted in

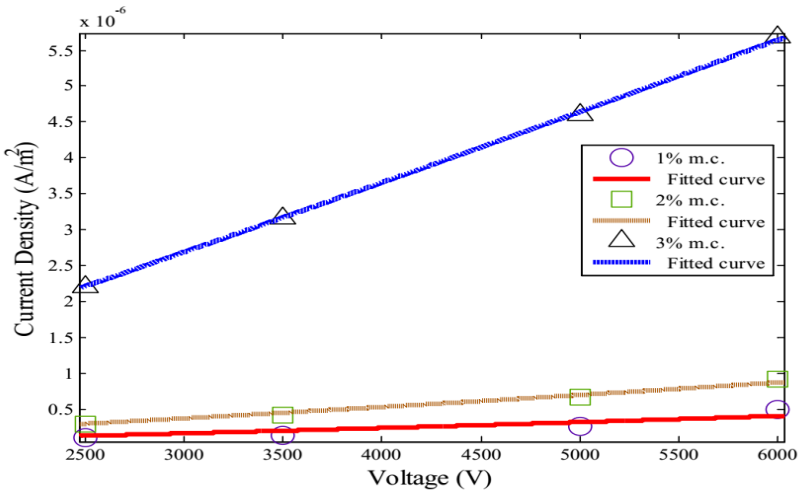

Figure 4.11: Fitting of current density of samples having different moisture content through SCLC model, m.c. refers to moisture content

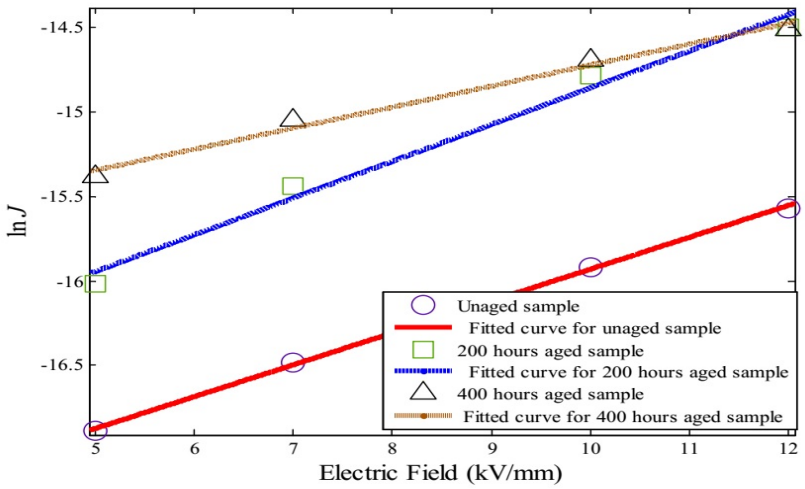

Figure 4.12: Effect of aging on $lnJ - E$ charcteristics of oil impregnated pressboard.

Figure 4.12 and Figure 4.13 respectively. It was observed, that for all the samples the $lnJ - E$ characteristics were very close to a straight line. This is a strong evidence of Hopping Conduction model being the dominant conduction mechanism in the 5-12 kV/mm electric field levels.

From the above discussion, the following conclusions can be drawn,

(i)The non-linearity in conduction processes is strongly dependent on the applied external electric field. Upto 5kV/mm field, the conduction process is Ohmic in nature.At higher fields, non-linearity and deviation from Ohmic behavior become significant. The influence of aging on non-linear conduction is more significant, when compared to that of moisture content.

(ii) SCLC model fails to explain the non linearity in the conductivity of oil-pressboard insulation in the 5-12kV/mm electric field range.

(iii) The Hopping conduction model satisfactorily explains the linear conduction behavior at low electric fields and the non-linear behavior at 5-12 kV/mm electric field range. This holds true for nearly all insulation specimens having different aging conditions and moisture con-

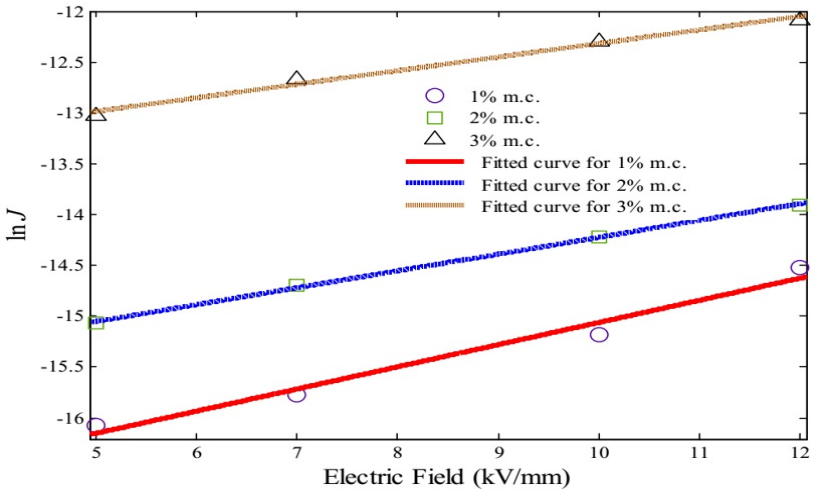

Figure 4.13: Effect of moisture on $lnJ - E$ characteristics of oil impregnated pressboard, m.c. refers to moisture content.

tents.It should be mentioned here that Hopping conduction has been proven to be the dominant conduction mechanism in many disordered and non-crystalline polymers [110]-[112]. It has been speculated in,[113] that protonic (H^+) ion hoping is responsible for electrical conduction in moist cellulosic materials. In present investigation, the nature of the carriers involved in charge conduction in oil-pressboard insulation has not been investigated. More experiments involving a greater range of electric fields as well as temperatures are needed to obtain detailed information regarding the Hopping conduction process in oil-pressboard insulation.

4.3.5 Discharge Current Measurements

As discussed in section 4.2, for understanding the effect of moisture and aging, a set of samples having different aging conditions (Unaged, 200 hours thermally aged and 400 hours thermally aged) and moisture content (1%, 2% and 3%) were prepared. These samples were first stressed at 10 kV/mm for around 1000s and then discharged. The measured discharging currents are depicted in Figure 4.14 and Figure 4.15, respectively. Figure 4.14 shows measured discharging current of samples having different aging conditions and Figure 4.15 shows discharging currents of samples having different moisture contents.

From Figure 4.14, it can be seen that with aging depolarization current increases. Similarly, moisture ingression also increases the depolarization current (Figure 4.15). However, after 400 hours of aging the initial value of depolarization current was observed to be much higher compared to that of depolarization current of the specimen having 3 % moisture content. Therefore, the impact of aging was more than moisture in the initial part of depolarization currents. On the other hand, the effect of moisture was stronger on the final values of depolarization current. Another important observation is that for the specimen containing 3% moisture content, depolarization current showed little variation beyond 2000s, where as depolarization current steeply declined with time for all aged samples. These observations indicated that moisture and aging do not impact oil-pressboard under HVDC conditions in the same way.

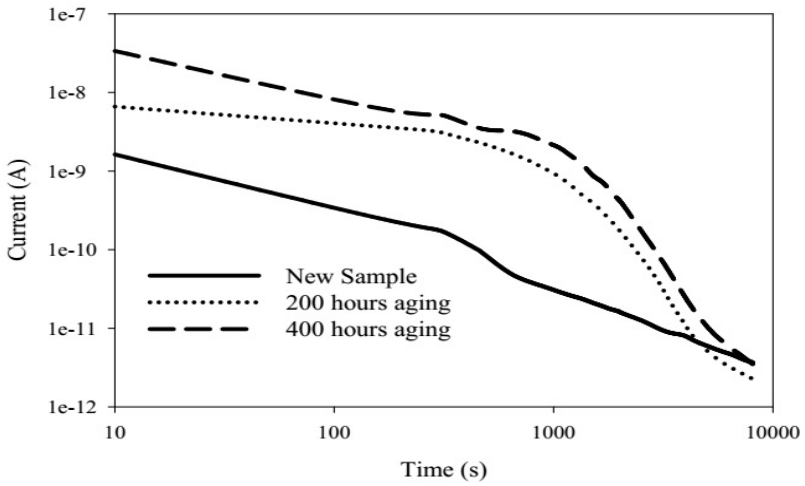

Figure 4.14: Effect of aging on discharging current of oil-impregnated pressboard.

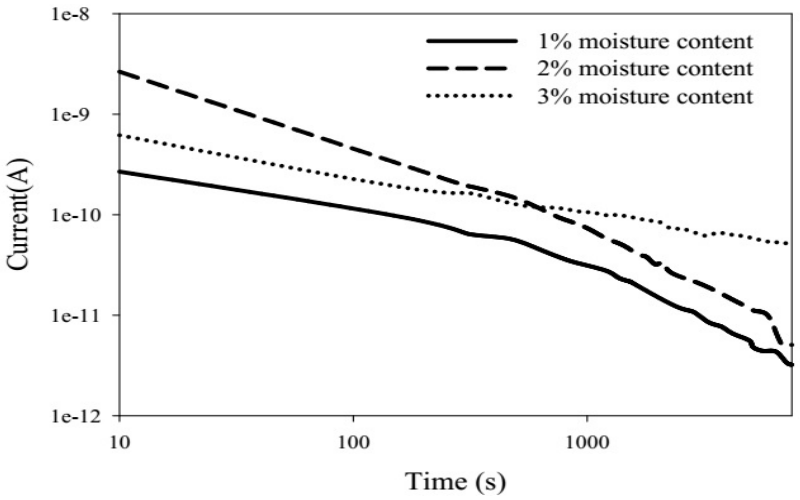

Figure 4.15: Effect of moisture on discharging current of oil-impregnated pressboard.

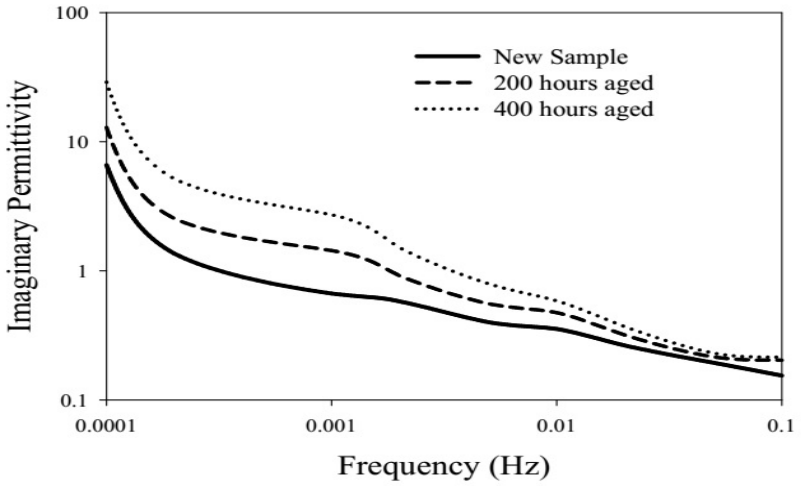

Figure 4.16: Effect of aging on imaginary component of permittivity of oil-impregnated pressboard.

4.3.6 Extraction of de-trapping current from measured discharge currents

A mathematical model to extract the charge de-trapping component from discharge current has already been discussed in the previous chapter. In that methodology, frequency domain data was converted to time domain for separating charge de-trapping component from dipolar polarization. The methodology of identifying the charge-detrapping component from discharge current measurements using FDS measurements is outlined through the following steps,
(i)Frequency Domain Spectroscopy (FDS) measurements were performed on the dielectric specimen at very low fields (100V/mm) to obtain ϵ'' characteristics. The effect of aging and moisture on the imaginary component of permittivity (ϵ'') characteristics of oil impregnated pressboard specimens are shown in Figure 4.16 and Figure 4.17, respectively.

(ii)Discharging current measurements were performed at the same set of samples, which were now pre-stressed at 10kV/mm fields. Oil-pressboard insulation is a composite dielectric, which contains both po-

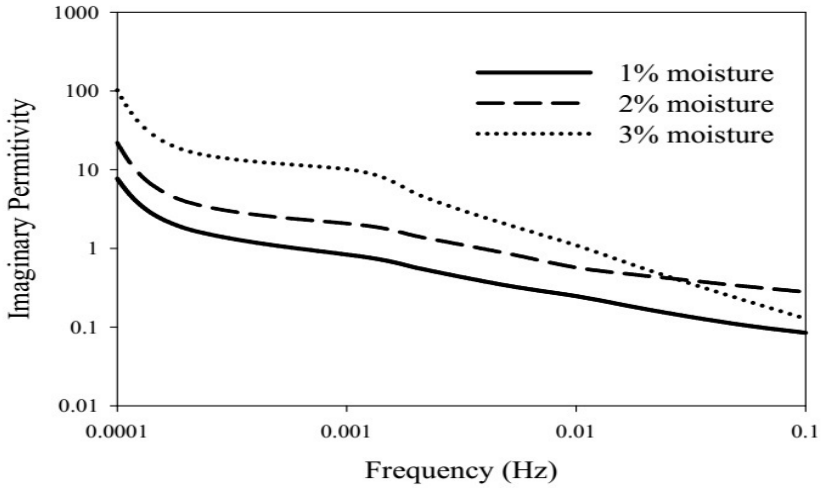

Figure 4.17: Effect of moisture on imaginary component of permittivity of oil-impregnated pressboard.

lar and nonpolar compounds. As a result, the discharge current will also be highly affected by dipolar relaxation. Therefore, the net discharge current can now be considered as a combination of two different currents, one due to charge de-trapping and the other due to dipolar relaxation. The net discharge current can now be expressed as

$$i_{dis} = i_d + i_{de-trap} \tag{4.14}$$

(iii)As FDS measurements are normally performed at very low fields (typically 10V/mm), charge injection can be safely ignored [114]. Therefore the FDS measurements are solely due to dipolar orientation and dc conduction. Recalling Chapter 3, the values of imaginary permittivity can be given through the following equation.

$$\varepsilon''(\omega) = \frac{\sigma_0}{\epsilon_0 \omega} + \chi''(\omega) or \varepsilon''(\omega) \approx \frac{G_{dc}}{\omega} where G_{dc} = \frac{\sigma_0}{\epsilon_0} \tag{4.15}$$

In equation 4.15 dipolar relaxation process is represented by the term

Table 4.4: DC conductivity

Aging Condition	DC Conductivity (pS/m)
Unaged	8.12E-15
200 hours aging	2.12E-14
400 hours aging	4.16E-14
1% moisture content (Unaged)	2.21 E-14
2% moisture content (Unaged)	5.58E-14
3% moisture content (Unaged)	4.31E-13

$\chi''(\omega)$.

The values of DC conductivity σ_0 can be easily obtained from the charging measurements performed on the identical samples used in charging current measurements. It has been already shown that at low electrical fields, the conductivity values of oil-pressboard insulation can be treated as constant. Hence, the conductivity values of the prepared samples at 1kV/mm are taken as σ_0 values. The values of dc conductivity were calculated using the equation,[110]

$$\sigma_0 = \frac{i}{ES} \tag{4.16}$$

where i, E and S are measured current, applied electric stress and surface area of the electrode, respectively.
The values of DC conductivities are given in the following Table 4.4.

(iv)From DC conductivity, the value of G_{dc} can be calculated. Once G_{dc} is estimated, the contribution of dc conductivity at any frequency can be estimated by $\frac{G_{dc}}{\omega}$. This DC contribution is subtracted from the $\varepsilon^{"}(\omega)$ characteristics, thereby giving the contribution of dipoles in $\varepsilon^{"}(\omega)$. From the remaining part of imaginary permittivity, current due to dipolar polarization at 10 kV/mm field is calculated through Hamon approximation, using the following equation,

$$\varepsilon''(\omega) \approx \frac{\sigma_0}{\varepsilon_0 \omega} + \frac{-i_d(\frac{0.1}{f}))}{\omega C_0 U_0} \tag{4.17}$$

Table 4.5: Variation of A_c and n with aging

Aging Condition	A_c	n
New sample	2.05E-8	0.85
200 hours aging	3.31E-8	0.93
400 hours aging	3.09E-7	1.18

Table 4.6: Variation of A_c and n with moisture.

Moisture Content (% by weight)	A_c	n
1%	5.25E-9	0.51
2%	9.31E-8	0.87
3%	3.14E-07	0.62

where, ω is the frequency, i_d is the dipolar polarization current,ε_0 is the permittivity of free space, C_0 is geometric capacitance and U_0 is the applied voltage. Here, U_0 will refer to the voltage used for stressing the oil-pressboard specimens prior to discharging.

(v)It should be remembered here, as ε" values are obtained at discrete frequencies, the value of dipolar relaxation current i_d will also be obtained at discrete time instants. Hence, it is represented as $i_d(t)$. The calculated $i_d(t)$ is fitted in Curie Von Schneidler form of $A_c t^{-n}$ .The calculated values of A_c and n for pressboard specimens having different aging conditions and moisture contents are depicted in Table 4.5 and 4.6 respectively.

The function At^{-n} is nothing but the dielectric response function of the specimen. Using this expression, the values of i_d over a continuous time span can be obtained. This i_d is subtracted from measured discharge current i_{dis} to obtain the de-trapping current $i_{de-trap}$. This process is performed for every specimen.

The separated de-trapping currents for samples with different aging conditions are depicted in Figure 4.18. It can be observed from Figure 4.18 that the magnitude of de-trapping current increases with aging. The largest difference was observed between the de-trapping current of the fresh sample and sample after 200 hours accelerated aging. This can be explained by the formation of new trapping sites. With aging, the long molecular chains break and the broken bonds produce new

trapping sites. This allowed more charge getting trapped. A comparison of dipolar relaxation current and de-trapping current of the new sample and 400 hours aged sample is shown in Figure 4.19. It can be seen from Figure 4.19 that for the new sample, the de-trapping current magnitude was lower than the dipole current magnitude throughout most parts of the measurement. For 400 hours aged specimen, it was the opposite. In this case, for most of the measurement time, the de-trapping current was higher than the dipole current.
Once the de-trapping current is separated, the normalized trap distribution along trap depth was calculated using the procedure discussed in ***Chapter 2***. The value of time interval (Δt), after which each time extracted charge was calculated, was kept at 1s. In this way a continuous trapped charge-trap depth distribution form was obtained from separated de-trapping current. The variation in normalized trap distribution with aging is shown in Figure 4.20. It was observed that with aging, the trapped charge in 0.96-1.02 eV trap region showed high increase. However, very little increase in trapped charge was noticed in 1.02-1.08 eV region. This indicated that the new traps produced by aging were comparatively shallower.

The calculated de-trapping currents for moisture ingressed samples are depicted in Figure 4.21. With the increase in moisture content, the de-trapping current increased. However, the largest increase was observed when moisture content increased from 2% (by weight) to 3% (by weight). A comparison of de-trapping current and dipole current at 1% and 3% moisture content is presented in Figure 4.22. It was observed, at 3% moisture content, the magnitude of de-trapping current was higher than dipole current. The normalized trapped charge distributions for moisture ingressed specimens are depicted in Figure 4.23. The trap distribution was almost same at 1% and 2% moisture contents. However, at 3% moisture content, there was a higher presence of trapped at charge at 1.04-1.10 eV region when compared to 1% and 2% levels.

A comparison of Figure 4.20 and Figure 4.23 reveals that in all observations the trapped charge density decreased almost linearly in the trap depth region 0.94eV-1.00eV. Therefore, in oil-pressboard insulation, the density of shallow traps is much higher compared to deep traps. However, due to both aging and moisture ingress, the proportion of deep traps becomes significant. Presence of deep trap signifies slow decay of trapped space charge, which can trigger insulation degradation at an alarming rate shortening insulation life [61].

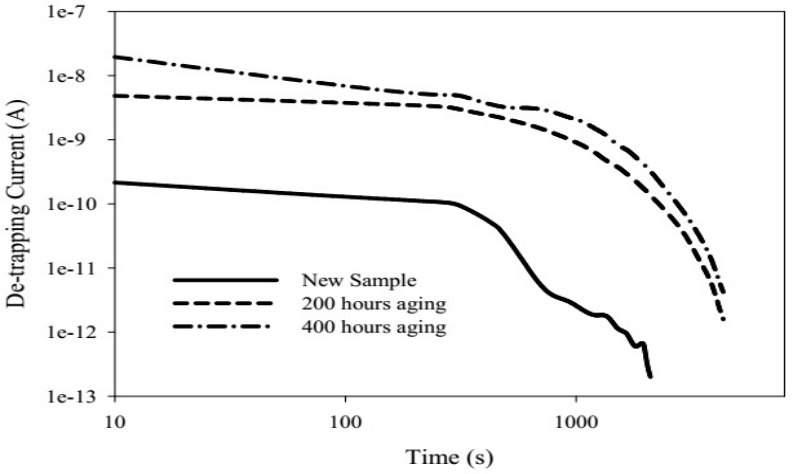

Figure 4.18: Effect of aging on de-trapping current of oil-impregnated pressboard.

4.4 Discussions

The present chapter is aimed at understanding the effect of moisture and aging on oil-pressboard insulation under HVDC environment. Two aspects of insulation behavior has been analyzed, one the conduction properties of oil-pressboard under HVDC stress and the other, charge trapping and de-trapping properties of oil-pressboard. At first, the major findings regarding the conduction properties are studied. From the electric field dependence on conductivity, it was observed that above 5kV/mm electric fields, the conduction process in oil-impregnated pressboard deviates from Ohmic conduction. The non-lineraity in conduction process is strongly affected by aging. It was found that Hopping Conduction model can explain the electric field dependence of oil-pressboard insulation satisfactorily.

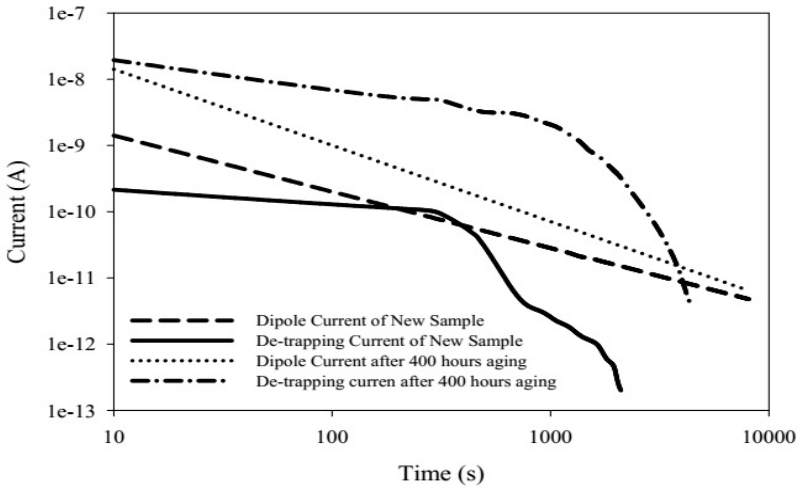

Figure 4.19: Comparison of dipole current and de-trapping current of new sample and 400 hour aged sample.

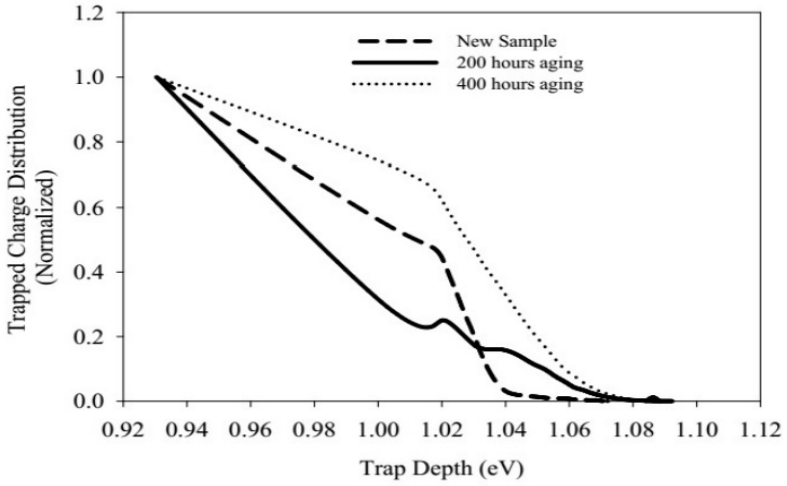

Figure 4.20: Normalized Trapped charge distribution of samples with different aging condition.

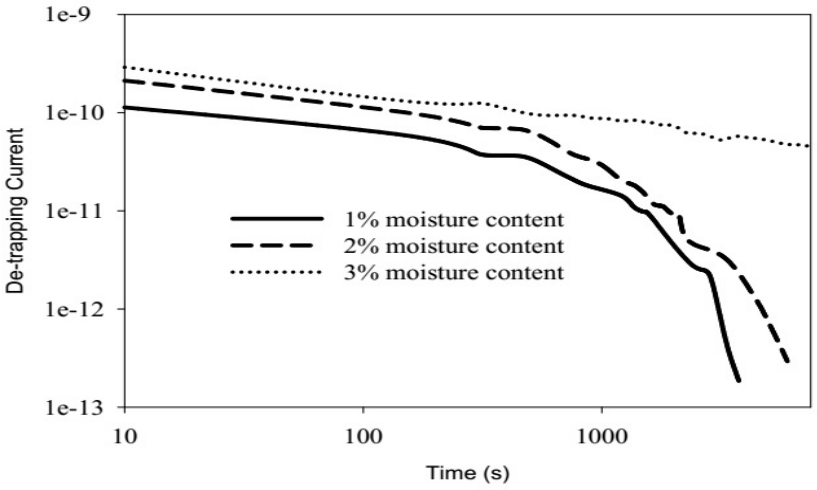

Figure 4.21: Effect of moisture on De-trapping current.

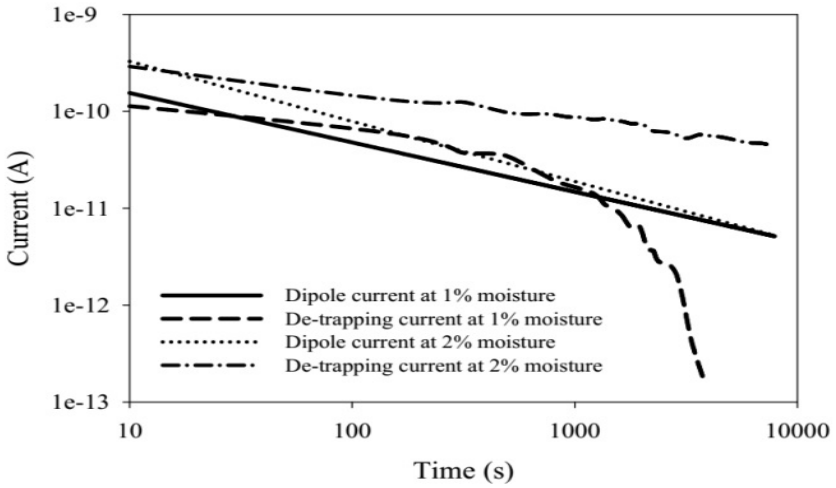

Figure 4.22: Comparison of dipole current and de-trapping current for 1% and 2% moisture content (by weight).

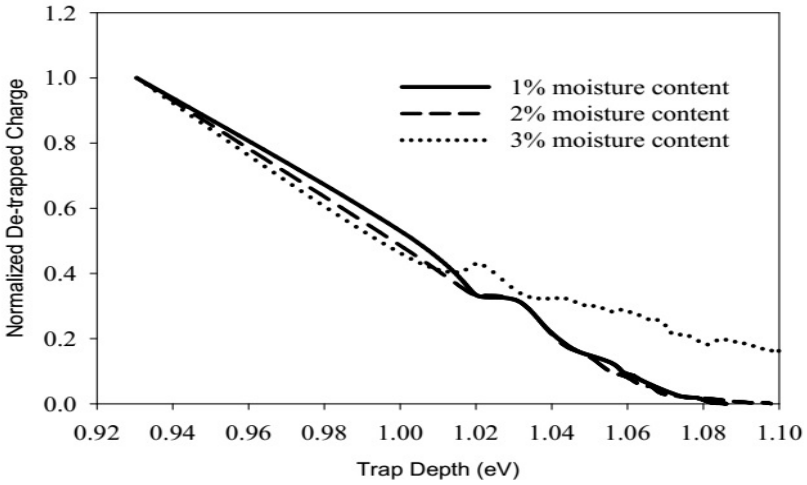

Figure 4.23: Normalized trapped charge distribution of samples with different moisture content.

To investigate charge trapping parameters in oil-pressboard insulation, the methodology developed in chapter 3 is applied. Using that methodology, the dipolar relaxation current and charge de-trapping current are separated from the total discharge current. The effect of aging and moisture on both of the current components was studied. The major observations of the study are discussed in brief below,
(i) For the fresh sample with low moisture content, the de-trapping current is less compared to the dipole relaxation current. However, with the increase in aging and moisture content, de-trapping current increases and exceeds the dipolar relaxation current component. For highly aged and moisture contained oil-pressboard insulation, the depolarization current after the insulation is stressed at high electric field (10 kV/mm in this work) is highly influenced by charge de-trapping.
(ii) For fresh insulation having low moisture content, the presence of very deep traps (traps having trap depth more than 1.00eV) is negligible. However, with increase in aging and moisture content, the proportion of these very deep traps increases. This leads to slow decay of accumulated space charge under HVDC conditions, eventually triggering insulation degradation.

The method presented in this work facilitates direct estimation of trap distribution from dielectric response measurements. Results presented have shown that trap depth characteristics are highly impacted by aging and moisture content. Therefore, the method can be useful for insulation diagnosis of HVDC equipment.

Chapter 5

Conclusions

In this dissertation, efforts have been made to understand various aspects of charge trapping and de-trapping commonly encountered in HVDC insulation systems through charging and discharging current measurements. The methodology and investigation approach used throughout this thesis work is quite straightforward, simple and does not require complicated signal processing tools. Moreover, as charging-discharging current measurements can be performed on any insulation geometry, the methodology developed in this thesis is applicable to real life high voltage insulations also. In this dissertation work, three common materials were subjected to charge trapping and de-trapping investigations, viz. LDPE, epoxy resin and oil impregnated pressboard.

Polyethylene based materials have been a popular choice for HVDC applications for quite some time. In the second chapter of this thesis, the de-trapping behavior of LDPE, a nonpolar dielectric was studied. To obtain charge trapping parameters directly from discharge current, a model was developed. Using this model, from discharging current measurements performed on thin LDPE specimens, the normalized trapped charge values across different trap depths were evaluated. Furthermore, the effect of temperature on charge de-trapping was also investigated. It was observed that as temperature increases, primarily due to material expansion new traps are formed in the insulation. The trap depth also increases with temperature, i.e. charges trapped at the higher temperature will also require higher energy to get released. This observation was quite significant, as it demonstrated that in practical

scenarios, i.e. HVDC cables where high temperature fluctuations are common, the combined effect of high temperature and high electric field can be quite severe.

Epoxy resin is another dielectric widely used in high voltage insulation. Unlike LDPE, epoxy resin is electrically polar. Therefore to understand charge trapping behavior in epoxy resin from charging-discharging current measurements, it is important to identify the current due to dipolar polarization. In ***Chapter 3***, a method was proposed to separate the dipolar polarization component and charge de-trapping component from discharge currents of a previously stressed epoxy resin specimen. The presented method incorporates the observation from frequency domain spectroscopy measurements to the previously developed model. Once the de-trapping current is identified, using the mathematical model developed in ***Chapter 2***, charge trapping parameters can be calculated. It was seen that charge trapping becomes significant above 10 kV/mm stress. Below this stress level, the discharge current was primarily due to dipolar relaxation. The effect of temperature was also studied. It was observed that as the temperature of epoxy resin approaches glass transition temperature, charge injection and charge trapping increases severely. Therefore, at higher temperatures, the charge de-trapping current component becomes comparable with the dipolar relaxation component.

Compared to polymeric insulations (i.e.LDPE,HDPE,XLPE) there has been significantly less amount of research on space charge investigations in oil-paper insulation. Oil-paper insulation, which is widely used in HVDC cables and converter transformers, degrades under the combined effect of moisture and aging. Therefore, it is important to understand the effect of moisture and charge trapping and de-trapping in oil-paper insulation. The final chapter in this dissertation addresses this issue. For this purpose, experimental studies were performed on oil-impregnated pressboard specimens, which revealed that moisture and aging impact charge de-trapping in different ways. In addition to it, the effect of moisture and aging on charge transport in oil-pressboard insulation was also studied. It was concluded that charge transport in oil-pressboard insulation is performed primarily through ionic hopping.From discharging current measurements, it was observed that both dipolar relaxation current and charge de-trapping current are highly in-

fluenced by aging and moisture. For higher moisture content and poor aging condition, the charge de-trapping current is significantly larger than the dipolar polarization current. The findings of ***Chapter 4*** can be helpful in insulation diagnoses of converter transformers, as traditional dielectric response methods fail to provide sufficient information regarding charge trapping.

5.1 Scope of Future Works

Future works can be directed in many different directions. Some of the possible works are mentioned below.

The effect of aging on trapped charge behavior of polyethylene based materials has not been investigated in the present thesis work. Aging is a complicated process and is affected by different thermal, electrical and environmental factors. Understanding the effect of these factors on charge trapping will be highly beneficial to the power engineering community. In this thesis work, the trapping parameters are normalized trapped charge and trap depth. In future, it can be tried to evaluate more parameters, e.g. trap density, trap cross-section etc, from charging and discharging currents. Besides this, there is not much information regarding the relation between charge trapping and tree inception in polymeric insulators. Therefore the relation between different trapping parameters and various aging processes can be explored in future.

Finally, it is worthwhile to mention that this dissertation has presented certain mathematical approaches, which can b e used for future investigations on trapping behavior in different polar and non-polar dielectrics from charging-discharging currents.

References

[1] A. Cavallini, D. Fabiani, G. Mazzanti and G. C. Montanari, "Life model based on space-charge quantities for HVDC polymeric cables subjected to voltage-polarity inversions" , IEEE Trans. Dielectr. Electr. Insul., Vol. 9, No. 4, pp. 514-523,2002.

[2] G. Mazzanti and G. Montanari, "Electrical aging and life models: the role of space charge", IEEE Trans. Dielectr. Electr. Insul., Vol. 12, No. 5, pp. 876-890,2005.

[3] G. C. Montanari,"Bringing an insulation to failure: the role of space charge", IEEE Trans. Dielectr. Electr. Insul., Vol. 18, No. 2, pp. 339-364, 2011.

[4] G. Chen, M. Fu, X. Z. Liu and L. S. Zhong,"AC aging and space-charge characteristics in low-density polyethylene polymeric insulation", J. Appl. Phys., Vol. 97, No. 8, pp. 0837113, 2005.

[5] M. P. Bahrman, HVDC Transmission Overview, 978-1-4244-1904-3/08 IEEE.

[6] C. Kim, V. K. Sood, G. Jang, S. Lim, and S. Lee, HVDC Transmission: Power Conversion Applications in Power Systems. Upper Saddle River, NJ: Wiley-IEEE Press, Apr. 2009.

[7] J. Arrillaga, High Voltage Direct Current Transmission, 2nd ed., (IEE Power and Energy Series 29) London, U.K., 1998.

[8] W. Long and S. Nilsson, "HVDC transmission yesterday and today", IEEE Power and Energy Magazine, Vol. 5, No. 2, pp. 22-31, Mar./Apr., 2007.

[9] R. Bodega, "Space Charge Accumulation in Polymeric High Voltage DC Cable Systems", Ph.D. dissertation, Delft University of Technology, 2006.

[10] J.O. Bostrom, A. Campus, R. N. Hampton and U. H. Nilsson,"Evaluation of the material reliability for polymeric direct current cables", CIGRE 2002,2002.

[11] T. L. Hanley, R. P. Burford, R. J. Fleming and K. W. Barber, "A General Review of Polymeric Insulation for Use in HVDC Cables", IEEE Electr. Insul. Mag., Vol. 19, No.1, pp. 13-24, 2003.

[12] D.A. Bolon, "Epoxy chemistry for electrical insulation", IEEE Electr. Insul. Mag., Vol. 11,No.4, pp. 10-18, 1995.

[13] Niels Bohr, "On the Constitution of Atoms and Molecules, Part III Systems containing several nuclei", Philosophical Magazine, Vol. 6, pp. 857-875, 1913.

[14] M. Meunier, N. Quirke, and A. Aslanides,"Molecular modeling of electron traps in polymer insulators: chemical defects and impurities", J. Chem. Phys., Vol. 115, No. 6, pp. 2876-2881,2001.

[15] M. Meunier and N. Quirke, "Molecular modeling of electron trapping in polymer insulators", J. Chem. Phys., Vol. 113, No. 1, pp. 369-376,2000.

[16] J. A. Anta, G. Marcelli, M. Meunier, and N. Quirke,"Models of electron trapping and transport in polyethylene: Current-voltage characteristics", J. Appl. Phys., Vol. 92, No.2, pp. 1002-1008, 2002.

[17] C.K. Williams,"Kinetics of trapping, detrapping, and trap generation",J. Electronic Materials, Vol. 21, No. 7, pp. 711-720, 1992.

[18] T. Zhou,G. Chen, R. Liao and Z. Xu,"Charge trapping and detrapping in polymeric materials: Trapping parameters", J. Appl. Phys., Vol. 110, No. 4, pp. 043724(1-6), 2011.

[19] D. R. Lamb, Electrical Conduction Mechanisms in Thin Insulating Films, Methuen, London, UK, 1967

[20] K. C. Kao and W. Hwang, Electrical Transport in Solids, Pergamon Press, New York, NY, USA, 1981.

[21] F.C. Chiu,"A review on conduction mechanisms in dielectric films", Advances in Materials Science and Engineering, Vol. 2014, Article ID 578168, pp. 1-18, 2014.

[22] J. G. Simmons,"Richardson-Schottky effect in solids", Physical Review Letters, Vol. 15, No. 25, pp. 967-968, 1965.

[23] R. H. Fowler and L. Nordheim,"Electron emission in intense electric fields", Proc. Roy. Soc. London,vol.119,No. 7811, pp 173-181,1928.

[24] D. K. Schroder, Semiconductor Material and Device Characterization, 2nd ed. Wiley, New York, 1998, p. 392.

[25] S. M. Sze, Physics of Semiconductor Devices, 2nd ed. Wiley, New York, 1981.

[26] J. G. Simmons,"Poole-Frenkel effect and Schottky effect in metal-insulator-metal systems", Phys. Rev., Vol.155, No. 3, pp 657-660, 1967.

[27] S.D. Ganichev,E. Ziemenn, W. Prettl, I.N. Yessivich,A.A, Istratov and E.R. Weber,"Distinction between the Poole-Frenkel and tunneling models of electric-field-stimulated carrier emission from deep levels in semiconductors", Phys. Rev. B, Vol. 61, No. 15,pp. 10361-10365, 2000.

[28] N. F. Mott and E. A. Davis, Electronic Processes in Non-Crystalline Materials, Oxford University Press, Oxford, UK, 1979.

[29] J. Y. M. Lee, F. C. Chiu, and P. C. Juan,"The application of highdielectric-constant and ferroelectric thin flmsin integrated circuit technology", in Handbook of Nanoceramics and Teir Based Nanodevices, T. Y. Tseng and H. S. Nalwa, Eds., Vol. 4, American Scientifc Publishers, Stevenson Ranch, Calif, USA, 2009.

[30] F. C. Chiu, W. C. Shih, and J. J. Feng, "Conduction mechanism of resistive switching flms in MgO memory devices", Journal of Applied Physics, Vol. 111, No. 9, Article ID 094104, pp. 1-5, 2012.

[31] F.C. Chiu, C. Lee, and T.M. Pan, "Current conduction mechanisms in Pr2O3/oxynitride laminated gate dielectrics", Journal of Applied Physics, Vol. 105, No. 7, Article ID 074103,pp. 1-4, 2009.

[32] P. Mark and W. Helfrich, "Space-charge-limited currents in organic crystals", Jour. App. Phys., Vol. 33, No.1, pp. 205-215, 1962.

[33] M. A. Lampert and P. Mark, Current Injection in Solids, Academic, New York, 1970.

[34] M. A. Lampert,"Simplified theory of space-charge-limited currents in an insulator with traps",Physical Review, Vol. 103, No. 6, pp. 1648-1656, 1956.

[35] N. Ando and F. Numajiri,"Experimental investigation of Space Charge in XLPE Cable using Dust Figure Method", IEEE Trans. Electr. Insul., Vol 14, No.2, pp. 36-42, 1979.

[36] T. R. Foord, "Measurement of the Distribution of Surface Electric Charge by Use of a Capacitive Probe", J. Phys. E: Sci. Instrum., Vol. 2,No. 5, pp. 411- 413, 1969.

[37] R. E. Collins,"Analysis of spatial distribution of charges and dipoles in electrets by a transient heating technique", J. Appl. Phys., Vol. 47, No.11,pp. 4404-4408, 1976.

[38] P. Notingher, S. Angel and A. Tourielli,"Thermal step method for space charge measurements under applied dc field", IEEE Trans. Dielectr. Electr. Insul., Vol. 8, No. 6, pp. 985-994,2001.

[39] S. B. Lang and D. K. Dasgupta,"Laser-intensity-modulation method: a technique for determination of spatial distributions of polarization and space charge in polymer electrets", Jour. App. Phys., Vol. 59, No. 6, pp. 2151-2160, 1986.

[40] T. Takada,"Acoustic and optical methods for measuring electric charge distributions in dielectrics", IEEE Trans. Dielectr. Electr. Insul., Vol. 6, No. 5, pp. 519-547, 1999.

[41] R. Gerhard-Multhaupt,"Analysis of pressure-wave methods for the nondestructive determination of spatial charge or field distributions in dielectrics", Phys. Rev. B, Vol. 27, No. 4, pp. 2494-2503, 1983.

[42] T. Ditchi, C. Alqui and J.Lewiner,"Broadband determination of ultrasonic attenuation and phase velocity in insulating materials", Journal of the Acoustical Society of America, Vol. 94, No.6, pp. 3061-66, 1993.

[43] G. M. Sessler, J. E. West and G. Gerhard,"High-resolution laser-pulse method for measuring charge distributions in dielectrics", Phys. Rev. Lett., Vol. 48, No. 8, pp. 563-566, 1982.

[44] W. Eisenmenger and M. Haardt,"Observation of charge compensated polarization zones in polyvinylidenefluoride (PVDF) films by piezoelectric acoustic stepwave response", Solid State Commun., Vol. 41, No 12, pp. 917-920, 1982.

[45] J. M. Alison, "The pulsed electro-acoustic method for the measurement of the dynamic space charge profile within insulators", in Space charge in solid dielectric, edited by J. C. Fothergill and L. A. Dissado, ISBN 0-9533538-0-X, pp. 93-121, 1998.

[46] J. B. Bernstein,"Improvements to the electrically stimulated acoustic-wave method for analysing bulk space charge", IEEE Trans. Electr. Insul., Vol. 27,No.1, pp. 152-161, 1992.

[47] K. Fukunaga,"Innovative PEA space charge measurement systems for industrial applications", IEEE Electr. Insul. Mag., Vol. 20, No. 2, pp. 18-26, 2004.

[48] G. Chen, T. Y. G. Tay, Davies, A. E. Davis, Y.Tanaka and T.Takada,"Electrodes and charge injection in low-density polyethylene using the pulsed electroacoustic technique", IEEE Trans. Dielectr. Electr. Insul., vol 8, no.6, pp. 867-873, 2001.

[49] T. Maeno, T. Futami, H. Kushibe, T. Takada and C. M. Cooke,"Measurement of spatial charge distribution in thick dielectrics using the pulsed electroacoustic method", IEEE Trans. Dielectr. Electr. Insul., Vol. 23, No. 3, pp 433-439, 1988.

[50] A. Migliori and J.D. Thompson,"A non-destructive acoustic electric field probe", Jour. App. Phys., Vol. 51, No. 1, pp. 479 485, 1980.

[51] T. Takada, Y. Tanaka, N. Adachi and X. Qin,"Comparison between the PEA method and the PWP method for space charge measurements in solid dielectrcs", IEEE Trans. Dielectr. Electr. Insul., Vol. 5, No. 6, pp. 944-950, 1998.

[52] P. K. Watson,"The transport and trapping of electrons in polymers", IEEE Trans. Dielectr. Electr. Insul., Vol 2, No. 5, pp. 915-924, 1995.

[53] J.G. Simmons and M. C. Tam., "Theory of isothermal currents and the direct determination of trap parameters in semiconductors and insulators containing arbitrary trap distributions", Phys. Rev. B, Vol. 7, No. 8, pp. 3706-3713, 1973.

[54] J. Li,F. Zhou,D. Min,S. Li and R. Xia,"The energy distribution of trapped charges in polymers based on isothermal surface potential decay model", IEEE Trans. Dielectr. Electr. Insul, Vol. 23, No. 2, pp. 1723-1732, 2015.

[55] F. Zhou, J. Li, M. Liu, D. Min, S. Li and R. Xia,"Characterizing Traps Distribution in LDPE and HDPE through Isothermal Surface Potential Decay Method", IEEE Trans. Dielectr. Electr. Insul, Vol. 23, No.6, pp. 1174-1182, 2016.

[56] J. Lindmayer ,"Current transients in insulators",Jour. Appl. Phys., Vol. 36, No.1,pp. 196-201, 1965.

[57] J.G. Simmons and M. C. Tam,"Theory of isothermal currents and the direct determination of trap parameters in semiconductors and insulators containing arbitrary trap distributions", Phys. Rev. B, Vol. 7, No. 8, pp. 3706-3713, 1973.

[58] E.R. Neagu and J. N. Marat-Mendes,"Charge injection/ejection and trapping in low-density polyethylene at low and medium fields". Appl. Phys. Letters , Vol. 83, No. 1, pp. 75-77, 2003.

[59] M. Fu, G. Chen, A.E. Davies and J.G. Head,"Space charge measurements in power cables using PEA system", Proceedings of Eighth International Conference on Dielectric Materials, Measurements and Applications,Edinburgh, UK, 2000.

[60] T. Muronaka, Y. Tanaka, T. Takada,S. Maruyama and H. Mutou,"Measurement of space charge distribution in XLPE cable using PEA system with flat electrode", Proceedings of IEEE 1996 Annual Report of the Conference on Electrical Insulation and Dielectric Phenomena, San Francisco, USA, 1996.

[61] T W Dakin,"Electrical Insulation Deterioration Treated as a Chemical Rate Phenomenon", AlEE Transactions, Vol. 67, No. 1,pp. 113-122, 1948.

[62] L. A. Dissado, G. Mazzanti and G. C Montanari,"The Role of Trapped Space Charges in the Electrical Aging of Insulating Materials", IEEE Trans. Dielectr. Electr. Insul, Vol 4, pp. 496-506, 1997.

[63] S. Glasstone, K. J. Laidler and H. Eyring, The Theory of Rate Processes, New York:McGraw Hill,1941

[64] T. Tanaka and A. Greenwood, "Effects of Charge Injection and Extraction on Tree Initiation in Polyethylene", IEEE Trans. on PAS, Vol. 97, pp. 1749-1759, 1978.

[65] L. A. Dissado, G. Mazzanti and G.C. Montenary,"The incorporation of space charge degradation in the life model for electrical insulating materials",IEEE Trans. Dielectr. Electr. Insul.,Vol. 2. No. 6,pp. 1147-58, 1995.

[66] L. A. Dissado, G. Mazzanti and G.C. Montanary,"Elemental strain and trapped space charge in thermoelectrical aging of insulating materials. Part 1: elemental strain under thermo-electrical-mechanical stress",IEEE Trans. Dielectr. Electr. Insul., Vol. 8, No. 6,pp. 959-965, 2001.

[67] D. Das Gupta and R. S. Brockley, "A study of absorption currents in low-density polyethylene", J. Phys. D: Appl. Phys., Vol. 11,No.6, pp. 955-961, 1978.

[68] W.S. Zaengl, "Dielectric spectroscopy in time and frequency domain for HV power equipment. I. Theoretical considerations",IEEE Electr. Insul. Magazine,Vol. 19, No. 5,pp. 5-19, 2003.

[69] D.K. Dasgupta, K. Doughty, and R. S. Brockley, "Charging and discharging currents in polyvinylidene fluoride", J. Phys. D: Appl. Phys, Vol. 13, No. 11, pp. 2101-2114, 1980.

[70] C Guillermin, P Rain and SW Rowe,"Transient and steady-state currents in epoxy resin", J. Phys. D: Appl. Phys, Vol. 39, No. 3, pp. 515-524, 2006.

[71] R. Lovell, "Decaying and steady currents in an epoxy polymer at high electric fields", J. Phys. D: Appl. Phys, Vol. 7, No. 11, pp. 1518-1530, 1974.

[72] M. Farahani, H. Borsi, and E. Gockenbach, "Dielectric Response Studies on Insulating Systems of Rotating Machines", IEEE Trans. Dielectr. Electr. Insul., Vol. 13, No. 2, pp. 383-393, 2006.

[73] A. Bouacha, I. Fofana, M. Farzaneh, A. Seytashmehr, H. Borsi, E. Gockenbach, A. Broual and N. T. Aka, "On the Usability of Dielectric Spectroscopy Techniques as Quality Control Tool", Proceedings of IEEE Electr. Insul. Mag., Vol. 25, No. 1, pp. 6-14, 2009.

[74] T Maeno, and K. Fukunaga, "High-resolution PEA charge d istribution measurement system", IEEE Trans Dielectr. Electr. Insul., Vol 3,No.6, pp. 754-757,1994.

[75] M. Arnaout. Ir. Baudoin.L. Berquez and D. Payan, "Study of signal treatment for a pulsed electro-acoustic measurement cell: a way of improving the transfer matrix condition number",Journal of Physics D: Applied Physics, Vol 40, No. 44,pp.4050403(1-9),2011.

[76] G.C. Montanari., G. Mazzanti, F. Palmieri, A. Motori, G. Perego and S.Serro, "Space-charge trapping and conduction in LDPE, HDPE and XLPE",Journal of Physics D: Applied Physics, Vol 34, No. 18,pp.2901-2911,2001.

[77] N. L. Dao, P. L. Lewin, I. L. Hosier and S. G. Swingler, "A Comparison Between LDPE and HDPE Cable Insulation Properties Following Lightning Impulse Ageing", International Conference On Solid Dielectrics, Potsdam, Germany, 4-9 July, 2010.

[78] A. Amin,A.K.R. Dantuluguri and A.K. Bansal,"Investigating the effect of humidity on the α-relaxations of low-density polyethylene using dielectric spectroscopy", International Journal of Pharmaceutics, Vol. 422, No.1-2, pp. 302-309, 2012.

[79] G. Mazzanti, G.C. Montanari and J.M. Alison, "A space-charge based method for the estimation of apparent mobility and trap depth as markers for insulation degradation. Theoretical basis and experimental validation", IEEE Trans. Dielectr. Electr. Insul, Vol. 10, No. 2, pp. 187-197, 2003.

[80] G. Mazzanti, G. C. Montanari, F. Palmieri, and J. Alison, "Apparent trap-controlled mobility evaluation in insulating polymers through depolarization characteristics derived by space charge measurements". J. Appl. Phys., Vol. 94, No.9,pp. 5997-6004, 2005.

[81] F. Rogti and M. Ferhat, "Effect of temperature on trap depth formation in multi-layer insulation: Low density polyethylene and fluorinated ethylene propylene", Appl. Phys. Letters, Vol. 104, No. 3, pp. 031605(1-4), 2015.

[82] T. W. Daikin,"Application of epoxy resins in electrical apparatus", IEEE Trans. Electr. Insul., Vol. EI-9, No.4,pp. 121-128, 1974.

[83] O Gallot-Lavallee, G Teyssedre, C Laurent and S Rowe, "Space charge behaviour in an epoxy resin: the influence of fillers, temperature and electrode material", J. Phys. D: Appl. Phys, Vol. 38, No. 12, pp. 2017-2025, 2005.

[84] C Guillermin, P Rain and SW Rowe, "Transient and steady-state currents in epoxy resin", J. Phys. D: Appl. Phys, Vol. 39, No. 3, pp. 515-524, 2006.

[85] R. Lovell, "Decaying and steady currents in an epoxy polymer at high electric fields", J. Phys. D: Appl. Phys, Vol. 7, No. 11, pp. 1518-1530, 1974.

[86] A.K.Jonscher, "Dielectric Relaxation in solids", Chelsea Dielectric Press, 1983.

[87] M. Farahani, H. Borsi, and E. Gockenbach, "Dielectric Response Studies on Insulating Systems of Rotating Machines", IEEE Trans. Dielectr. Electr. Insul., Vol. 13, No. 2, pp. 383-393, 2006.

[88] V. Der Houhanessian, "Measurement and Analysis of Dielectric Response in Oil-Paper Insulation System", PhD thesis, Swiss Federal Institute of Technology, ETH, No. 12832, Zurich, 1998.

[89] B. V. Hamon, "An Approximation Method for Deducting Dielectric Loss Factor from Direct-Current Measurements", Proc. Inst. Elec. Eng. (IEE), Vol. 99, No. 27, pp. 151-155, 1952.

[90] E. David and L. Lamarre, "Low-Frequency Dielectric response of Epoxy-Mica Insulated Generator Bars During Multi-Stress Aging", IEEE Trans. Dielectr. Electr. Insul., Vol. 14, pp. 212-226, 2007.

[91] N. Liu, C. Zhou, G. Chen, and L. Zhong, "Determination of threshold electric field for charge injection in polymeric materials",Appl. Phys. Lett., Vol.106, No.19, pp.-192901, 2015.

[92] V. Griseri, "The Effects of High Electric Fields on an Epoxy Resin", PhD thesis, University of Leicester,2000.

[93] F. Rogti and M. Ferhat, "Effect of temperature on trap depth formation in multi-layer insulation: Low density polyethylene and fluorinated ethylene propylene", Appl. Phys. Letters, Vol. 104, No. 3, pp. 031605, 2015.

[94] M. Kazikazi, H. Nakayami, H Tanaka and T Hideshima, "Dielectric Relaxations in Poly (γ-n-alkyl L-glutamate) s I. Study of the Relaxations above Room Temperature Using the Direct-Current Technique", Polymer Journal -Nature Publishing Group, Vol. 17, No. 11, pp 1179-1188, 1985.

[95] T. V. Oommen and T. A. Prevost, "Cellulose insulation in oil-filled power transformers: part II maintaining insulation integrity and life", IEEE Electr. Insul. Mag., Vol. 22, No. 2, pp. 5-14, 2006.

[96] A. M. Emsley and G. C. Stevens, "Kinetics and mechanisms of the lowtemperature degradation of cellulose", Cellulose, Vol. 1, No. 1, pp. 26- 56, 1994.

[97] R. J. Heywood, A. M. Emsley and M. Ali,"Degradation of cellulosic insulation in power transformers. Part 1: Factors affecting the measurement of the average viscometric degree of polymerization of new and aged electrical papers", IEE Proceedings of Science, Measurement and Technology, Vol. 147, No. 2, pp. 86-90, 2000.

[98] F.M. Clark, "Factors Affecting the Mechanical Deterioration of Cellulose Insulation", AIEE Transactions, Vol. 61, pp. 742-749, 1942.

[99] T.W. Dakin, "Electrical Insulation Deterioration Treated as a Chemical Rate Phenomenon", AIEE Transactions, Vol. 67, pp. 113-122, 1948.

[100] F. Vahidi, S. Tenbohlen, M. Rosner and T. Stirl, "The influence of moisture during the electrical conductivity measurement on the high density impregnated pressboard" Proceedings of 19th International Symposium on High Voltage Engineering, Pilsen, Czech Republic, 2015.

[101] M. Bo, D. Min, J. Ru, S. Pan, H. Yin, Y. Zhu and S. Li, "Investigating the Influuence of Temperature and DC Electric Field on the

Electric Conduction of Oil Impregnated Paper Insulation", Proceedings of IEEE International Conference on Condition Monitoring and Diagnosys, pp. 514-517, Xi'an, China,2016.

[102] P. Zhukowski, T.N. Koltunowicz, K. Kierczynski, J. Subocz, M. Szrot and M. Gutten, "Assessment of water content in an impregnated pressboard based on DC conductivity measurements. Theoretical assumptions", IEEE Trans. Dielectr. Electr. Insul., Vol. 21, no. 3, pp. 1268-1275, 2014.

[103] P. Morshuis and M. Jeroense, "Space charge measurements on impregnated paper: a review of the PEA method and a discussion of results", IEEE Electr.Insul. Mag., Vol. 13, No. 3, pp. 26-35, 2003.

[104] R. Ciobanu, C. Schreiner, W. Pfeiffer and B. Baraboi, "Space charge evolution in oil-paper insulation for DC cables application", IEEE 14th Intern. Conf. Dielectr. Liquids (ICDL), Massachusetts, USA, pp. 321-324, 2002.

[105] R. Liu and A. Jaksts, "Moisture and space charge in oil-impregnated pressboard under HVDC", IEEE Intl. Conf. Conduction and Breakdown in Solid Dielectr., Vasteras, Sweden , pp. 17-22, 1998.

[106] J. Hao, G. Chen, R. Liao, L. Yang and C. Tang, "Influence of moisture on space charge dynamics in multilayer oil-paper insulation", IEEE Trans. Dielectr. Electr. Insul., vol. 19, No. 4, pp. 1456-1464, 2012.

[107] S. Wang, G. Zhang, H. Mu, D. Wang, M. Lei Suwamo, Y. Tanaka and T. Takada, "Effects of paper-aged state on space charge characteristics in oil-impregnated paper insulation", IEEE Trans. Dielectr. Electr. Insul, Vol. 19, No. 6, pp. 1871-1878, 2012

[108] S. Wang, G. Zhang, J. Wei, S. Yang, M. Dong and X. Huang, "Investigation on dielectric response characteristics of thermally aged insulating pressboard in vacuum and oil-impregnated ambient", IEEE Trans. Dielectr. Electr. Insul., Vol. 17, No.6,pp. 1853-1862, 2010.

[109] A. K. Pradhan, B. Chatterjee and S. Chakravorti, "Effect of Temperature on Frequency Dependent Dielectric Parameters of Oil-Paper Insulation Under Non-sinusoidal Excitation", IEEE Trans. Dielectr. Electr. Insul., Vol. 21, No. 2, pp. 653-661, 2014.

[110] K.C. Kao, "Dielectric Phenomena in solids", Academic Press,2004.

[111] M. Kosaki , K. Sugiyama and M. Ieda " Ionic jump distance and glass transition in polyvinyl chloride" J. Appl. Phys., Vol. 42,No.9, pp. 3388-92, 1971.

[112] L.E. Amborski, "Structural dependence of the electrical conductivity of polyethylene terephthalate", J. Polym. Sci. Vol. 62, No. 174,pp.331-46, 1962.

[113] J. H. Christie, S. R. Sylvander, I. M. Woodhead and K. Irie, "The dielectric properties of humid cellulose", J. Non-Crystalline Solids, Vol. 341,No.1-3, pp. 115-123, 2004.

[114] A. Seytashmehr, I. Fofana, C. Eichler, A. Akbari, H. Borsi and E. Gockenbach, "Dielectric spectroscopic measurements on transformer oil-paper insulation under controlled laboratory conditions", IEEE Trans. Dielectr. Electr. Insul., vol. 15, No. 4, pp. 1100-1111, 2008.